R-09-28

Compilation and analyses of results from cross-hole tracer tests with conservative tracers

Calle Hjerne, Rune Nordqvist, Johan Harrström
Geosigma AB

September 2010

Svensk Kärnbränslehantering AB
Swedish Nuclear Fuel
and Waste Management Co

Box 250, SE-101 24 Stockholm
Phone +46 8 459 84 00

SKB

ISSN 1402-3091
SKB R-09-28

Compilation and analyses of results from cross-hole tracer tests with conservative tracers

Calle Hjerne, Rune Nordqvist, Johan Harrström
Geosigma AB

September 2010

Keywords: Tracer test, Aperture, Transmissivity, Hydraulic diffusivity, Storativity, Dispersivity, Peclet number.

Abstract

Radionuclide transport in hydrogeological formations is one of the key factors for the safety analysis of a future repository of nuclear waste. Tracer tests have therefore been an important field method within the SKB investigation programmes at several sites since the late 1970´s.

This report presents a compilation and analyses of results from cross-hole tracer tests with conservative tracers performed within various SKB investigations. The objectives of the study are to facilitate, improve and reduce uncertainties in predictive tracer modelling and to provide supporting information for SKB's safety assessment of a final repository of nuclear waste. More specifically, the focus of the report is the relationship between the tracer mean residence time and fracture hydraulic parameters, i.e. the relationship between mass balance aperture and fracture transmissivity, hydraulic diffusivity and apparent storativity.

For 74 different combinations of pumping and injection section at six different test sites (Studsvik, Stripa, Finnsjön, Äspö, Forsmark, Laxemar), estimates of mass balance aperture from cross-hole tracer tests as well as transmissivity were extracted from reports or in the SKB database Sicada. For 28 of these combinations of pumping and injection section, estimates of hydraulic diffusivity and apparent storativity from hydraulic interference tests were also found.

An empirical relationship between mass balance aperture and transmissivity was estimated, although some uncertainties for individual data exist. The empirical relationship between mass balance aperture and transmissivity presented in this study deviates considerably from other previously suggested relationships, such as the cubic law and transport aperture as suggested by /Dershowitz and Klise 2002/, /Dershowitz et al. 2002/ and /Dershowitz et al. 2003/, which also is discussed in this report.

No clear and direct empirical relationship between mass balance aperture and hydraulic diffusivity was found. However, indications of a relationship between mass balance aperture and apparent storativity from hydraulic interference tests as well as between mean residence time and pressure response time were found. This may indicate that there exists an indirect relationship between mass balance aperture and hydraulic diffusivity.

Estimates of dispersivity in terms of Peclet numbers (Pe) from the tracer tests were also viewed in the report. However, no clear relationship between Pe and transmissivity or travel distance was found.

Sammanfattning

Transport av radionuklider i hydrogeologiska formationer är en av nyckelfaktorerna i SKB:s säkerhetsanalys av ett framtida slutförvar av kärnbränsle. Spårförsök har därför varit en viktig fältundersökningsmetod inom SKB:s olika undersökningsprogram sedan sent 1970-tal.

Denna rapport presenterar en sammanställning och analyser av resultat från mellanhålsspårförsök med konservativa spårämnen som utförts inom SKB:s olika undersökningar. Syftena med studien är att underlätta, förbättra och minska osäkerheterna av prediktiv spårämnesmodellering och att ta fram stödjande information för SKB:s säkerhetsanalys av ett slutförvar av kärnbränsle. Mer specifikt, rapportens fokus är samband mellan spårämnens uppehållstid och hydrauliska parametrar, med andra ord samband mellan massbalansapertur och transmissivitet, hydraulisk diffusivitet och storativitet.

För 74 olika kombinationer av pumpsektioner och injiceringssektioner från sex olika undersökningsområden (Studsvik, Stripa, Finnsjön, Äspö, Forsmark, Laxemar) sammanställdes massbalansapertur utvärderat från mellanhålsspårförsök och transmissivitet. För 28 av dessa kombinationer sammanställdes också rapporterade värden för hydraulisk diffusivitet och magasinskoefficient från hydrauliska interferenstester.

Ett empiriskt samband mellan massbalansapertur och transmissivitet hittades, trots en del osäkerheter för enskilda data. Sambandet avviker avsevärt från tidigare föreslagna samband såsom kubiska lagen och transportapertur som tidigare rapporterats av /Dershowitz and Klise 2002/, /Dershowitz et al. 2002/ och /Dershowitz et al. 2003/. Denna diskrepans är diskuterad i denna rapport.

Inget klart och direkt empiriskt samband mellan massbalansapertur och hydraulisk diffusivitet kunde hittas. Dock finns indikationer på empiriskt samband mellan massbalansapertur och magasinskoefficient från hydraulisk interferenstester samt mellan uppehållstid och tryckresponstid. Det kan tyda på att det finns ett indirekt samband mellan massbalansapertur och hydraulisk diffusivitet.

Dispersivitet i termer av Peclet-tal (Pe) analyserades också i denna rapport. Man kunde inte finna något tydligt samband mellan Pe och transmissivitet eller transportsträcka.

Contents

1 Introduction

Transport of trace elements in hydrogeological formations is one of the key factors in the safety analysis of a future repository of nuclear waste performed by SKB. One of the difficulties in this process is to determine what values for transport parameters pertinent to groundwater advective velocity, sorption, diffusion and dispersion. This is also the major challenge in predictive modelling and scoping calculations, made prior to in situ tracer tests (in order to optimize the test by aspects of e.g. test time and test procedure).

For a single fracture with a width normal to the flow direction, the groundwater advective velocity should be the groundwater flux divided by the width and the fracture's wall separation, or aperture. Many different concepts of aperture with different names are present in the literature. In the present report, *transport aperture* will be used as a general term for the aperture available for advective transport of groundwater. Different concepts of aperture will be further discussed in Chapter 3 of this report.

In scoping calculations prior to a tracer test, a first estimate of the mean residence time of a conservative (non-sorbing) tracer may be based on an assumed aperture (i.e. mean aperture available for flow) and experimental flow rates. Experimental flow rates are more or less known while the knowledge of transport aperture is very uncertain. The available data useful for the scoping calculations prior to a tracer test often only consists of transmissivity and sometimes hydraulic diffusivity, pressure and flow responses from hydraulic tests.

The transport aperture may be estimated using transmissivity values together with the so called *cubic law* or other suggested relationship between aperture and transmissivity. However, it is known from experience that the cubic law underestimates the transport aperture considerably and the cubic law aperture is of often used as a minimum estimate of the transport aperture. Other suggested relationships between transport aperture and transmissivity are also associated with uncertainties. Hence, the uncertainty about the mean residence time for conservative tracers is considerable in scoping calculations prior to in situ tracer tests. Consequently, predictions for sorbing tracers will also be uncertain since the water mean residence time also affects these. In addition, uncertainty about parameters for other transport processes such as sorption, diffusion and dispersion also contribute to the total uncertainty in predictive tracer modelling.

SKB has since the late 1970's performed in situ tracer tests at several locations in Sweden. The tracer tests performed between 1977 and 2007 are described and discussed with focus on possibilities and limitation of tracer tests by /Löfgren et al. 2007/. The description of the tracer test in the report is primarily qualitative with focus on experiences from the tracer tests. /Löfgren et al. 2007/ does not publish any comprehensive compilation of transport parameter values from the tracer tests.

In order to reduce the uncertainties of predictive tracer modelling, the results from SKB's numerous tracer test were compiled and analysed. The analysed results will also provide supporting information for SKB's ongoing safety analysis of a repository for nuclear waste.

2 Objective and scope

The objective of this report is to facilitate, improve and reduce uncertainties in predictive tracer modelling and provide supporting information for SKB's safety assessment of a final repository of nuclear waste.

As mentioned in the introduction, values of hydraulic parameters usually compose the only useful data available prior to predictive tracer modelling. At the sites investigated by SKB, the amount of hydraulic data is generally very extensive. The focus of this study is therefore on the relationship between hydraulic parameters and tracer transport parameters. More specifically, the transport parameter that is expected to be closest related to hydraulic parameters is the mean residence time, i.e. base for calculation of mass balance aperture which therefore will be the primary focus of the study.

The mass balance aperture is in this report evaluated, from conservative tracers used in cross-hole tracer tests.

The scope of the study is to:

- Collect and compile data of tracer transport parameters and hydraulic data from cross-hole tracer tests performed with conservative tracer.
- Analyse the transport parameters and their correlation to relevant hydraulic parameters.

3 Background

The tests considered in this study were carried out in crystalline bedrock, which likely is very heterogeneous in terms of transmissivity in the fractures. Accordingly, the flow distribution in the fractures during the various tests was probably also very heterogeneous. However, basic evaluation of the tracer and hydraulic tests often assumes homogeneous conditions. This discrepancy between the true and assumed flow distribution should be kept in mind when viewing and discussing the results.

3.1 Tracer tests

Tracer tests may be performed as cross-hole tests or single-hole tests. The focus of this study is the relationship between hydraulic parameters and mass balance aperture. Hence, only cross-hole tracer tests are discussed further on in this report since single-hole tracer tests, such as SWIW test /Nordqvist 2008/ and LTDE-SD /Byegård et al. 2010/, does not in itself give sufficient data for evaluation of mass balance aperture.

There are two major types of tracer test configurations that describe the flow situation in cross-hole tests: radial flow and dipole flow.

The radial flow is in a majority of the cases created by pumping in a borehole section while no other disturbances of the flow field occur. This type of test is called a radially converging tracer test. Radial flow may also be created by injection and is then known as a radially diverging tracer test. Among the tracer tests performed within the SKB programmes the converging test is much more common than the diverging.

The dipole flow situation is created by injecting water in a borehole section while pumping another borehole section. The test is called a dipole tracer test. If the flow rate of the injection section is equal to the flow rate in the pumping section, the test is known as an equal dipole tracer test. Dipole flow may also be created with a lower injection flow rate than pumping flow rate. In this case it is known as a weak dipole tracer test or an unequal dipole tracer test. A special case of a dipole test is when several borehole sections are used for pumping and/or injection. In this case the tracer test is known as multipolar.

In practise, it is very difficult to avoid small disturbances when injecting tracer in a radially converging test. The radially converging test may then more resemble a weak dipole test. In the same way it is difficult to inject with the exact same flow rate as the pumping in equal dipole test. Additionally, some tests may be carried out as a weak dipole during the actual injection period by using a small excess injection pressure and as a radially converging tracer test during a later phase of the test. It is therefore somewhat difficult to establish an exact distinction between the different types of cross-hole tracer tests.

For evaluation purposes it is common to assume approximate radially flow for weak dipole test so that these tests are evaluated in the same manner as radially converging tests.

3.2 Hydraulic tests

There are several methods for evaluation of hydraulic parameters in the field. These methods may be divided into different categories based on borehole configuration and test principle. Either a single borehole or multiple boreholes are used for the hydraulic test. The latter is also known as an interference test.

Several hydraulic parameters may be evaluated from the tests. In this study the transmissivity, T, is of primary interest; this parameter is often also the main objective of the hydraulic tests. In addition, other hydraulic parameters such as hydraulic diffusivity, storativity, pressure response time and flow rate response from interference tests may also be of interest.

3.2.1 Single hole hydraulic tests

Single borehole hydraulic tests are used, as implied, to evaluate hydraulic parameters for a single borehole. The main methods are injection, pumping and flow logging tests. All three of them are commonly used within the SKB investigations. Depending on the method and the hydraulic conditions the tests may reflect the properties of the hydraulic features from very close to the borehole to properties far away from the borehole. There are several test methods available for evaluation of transmissivity for a single borehole or borehole section.

The basic principles for injection and pumping tests, respectively are similar. For both methods, water is injected or pumped water into or from a borehole section and observations are made of the pressure change and water flow rate. For evaluation purposes it is common to keep either the pressure constant and let the water flow rate vary over time, or vice versa, i.e. keep the water flow constant and let the pressure vary. In tunnels, where the pressure in the hydraulic feature is higher than in the tunnel itself, no pump is needed to withdraw water from a borehole section. This is also known as an outflow test or packer flow logging in some reports. However, the principle is still the same as for a pumping test. Both pumping and injection tests may be evaluated for transient conditions and approximate stationary condition. In order to obtain a more detailed description of the transmissivity distribution along the borehole, packers are commonly used to divide the borehole into shorter sections.

The basic principle for borehole flow logging is to disturb the flow in the borehole by pumping and simultaneously measure how the flow rate varies along the borehole. The flow rate is typically measured when approximate stationary conditions prevail. One method to measure the flow rate along the borehole is to use a flow logging impeller (basically a propeller). This principle is used in percussion drilled borehole within the SKB site investigations in Forsmark and Oskarshamn. Another principle to measure the flow rate along the borehole is to add a known amount of energy at one point and measure the increase in water temperature in another point nearby and calculate the flow passing the sensor. This principle is used in the difference flow logging method (Posiva Flow Logg, PFL), which was used for core-drilled boreholes within SKB site investigations.

3.2.2 Interference hydraulic tests

The basic principle for hydraulic interference tests is to withdraw water from a borehole or borehole section and to measure the pressure response in observations sections in the vicinity. Interference tests have been used in both boreholes drilled from tunnels and boreholes from the surface. The tests may be evaluated during both the transient period and the approximate stationary condition. When evaluating the transient period it is possible to obtain, besides transmissivity, hydraulic diffusivity, storativity and time lag (time to first observed pressure response) in an observation section, which can be of interest.

Most evaluation method used for the data discussed in this report assumes radial flow. To evaluate the transmissivity for each observation section, T_o, the standard method for transient evaluation assumes that the drawdown around the pumping section is uniform, implying homogeneous conditions. This is of course not true for fractured rock, especially when the system includes several fracture zones with different strike and dip and over long distances and the properties may also vary spatially significantly within each zone and (as mean values) between the zones. The T_o-values often tends to be rather uniform, and the main reason is that the same pumping flow rate is used in the evaluation of all observation points and this flow rate may only be corrected for the pumped borehole section. Structural information may provide convincing arguments that the observation point is within the same structure as the pumped section and that approximately radial flow can be assumed. This can then provide reason to assume that the pumping flow rate is approximately correct for the evaluation of the observation section.

Storativity for each observation section, S_o, is also obtained as a result from the transient evaluation. However, S_o evaluated from interference test is often regarded as a rather suspect parameter since it actually is the transmissivity, T_o, divided by hydraulic diffusivity, T_o/S_o, and both parameters may be uncertain due to reasons mentioned in previous paragraph. Hence, it is probably better to consider S_o as an apparent storativity rather than a true storativity for the tested system.

Instead, it is commonly accepted that a more reliable value from observation sections in a hydraulic interference test is time lag which is controlled by the hydraulic diffusivity. Hydraulic diffusivity may be evaluated by transient analysis of the pressure response in the observation borehole and the pumping flow rate. It may also be estimated directly from the pressure response time according to /Streltsova 1988/, assuming radial flow:

$$\frac{T}{S} = \frac{r^2}{4 \cdot dt_L \cdot \left(1 + \frac{dt_L}{t_p}\right) \cdot \ln\left(1 + \frac{t_p}{dt_L}\right)}$$ Equation 3-1

T/S = hydraulic diffusivity (m^2/s)
r = geometric (3D) distance between the pumping borehole (section) and observation section (m)
dt_L = response (lag) time for observation section (s)
t_p = duration of flow period (s)

For further information about performance and standard evaluation of hydraulic interference tests see e.g. /Lindquist et al. 2008a/ or /Ludvigson et al. 2010/.

3.3 Concept of aperture

The aperture of a single fracture is a measurement of the fracture wall separation. However, the aperture of a single fracture may be very different if it is considered in terms of advective transport, hydraulic or true physical aspects. It should also be noted that the true physical aperture of a single fracture in reality probably varies considerably. Nevertheless, the aperture of a single fracture is often described by a single value that is considered to describe the effective or mean aperture in some sense.

For single fractures, it may be reasonable to use the concept of transport aperture for describing the water-flowing portion of the fractures involved in advective transport. For large fracture zones, the conceptual understanding is often that the fracture zone is made up of several interconnected smaller fractures. In such cases, an alternative is to discuss the portion of the fractures involved in advective transport in terms *of kinematic porosity* (also known as effective and flow porosity in literature) together with a specified thickness. However, in order to make a comparison, in the present report, of the various tracer tests performed, a single value representing the total transport aperture is used for both single fractures as well as fracture zones.

Several definitions of aperture are used in connection with hydraulic and tracer tests. /Tsang 1992/ presents a discussion of definitions, notations and usage of the term “equivalent aperture” in connection with hydraulic and tracer tests. Mainly, Tsang identified three definitions of equivalent aperture that are called *mass balance aperture*, *frictional loss aperture* and *cubic law aperture*. Basically, the same terminology will be used in this report. However, in this report the term mass balance aperture is only used in the context of tracer test evaluations assuming certain boundary conditions and geometries, cf Section 3.3.1. This is a slightly more restricted use of mass balance aperture than in /Tsang 1992/. For describing the aperture available for advective transport of groundwater in a more general sense, the term *transport aperture* is used in this report. Mass balance aperture is then, in this report, a special case of transport aperture.

For evaluation of the three definitions of equivalent aperture, δ, (mass balance, frictional loss and cubic law aperture) different measurable quantities are required. Besides, geometrical assumptions are needed for calculation of the three apertures as shown in Figure 3-1. In the linear case, length, l, and width, w, of the fracture are required while the radial distance, r, between two points is needed in the radial case. The flow direction is displayed with blue arrows in Figure 3-1, while the tracer injection and pumping points are shown in pink and red, respectively.

Mass balance aperture, δ_m, is defined so that it together with the geometrical assumptions makes a volume that equals mean residence time in the fracture, t_m, multiplied with the flow rate of the fracture, Q.

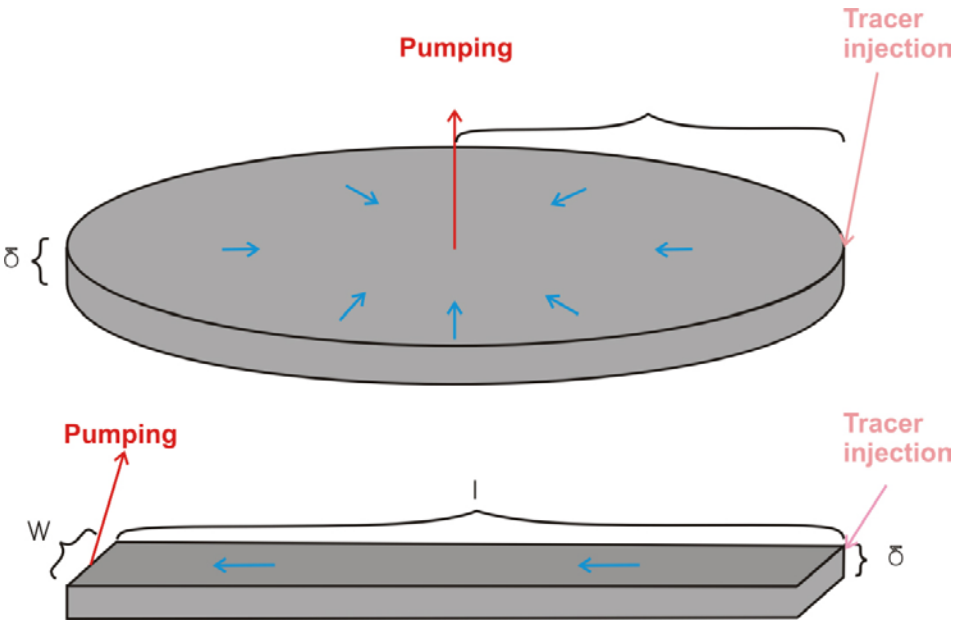

Figure 3-1. *Illustration of radial (top) and linear (bottom) geometries for evaluation of aperture.*

The definition of cubic law aperture, δ_c, assumes that permeability between a pair of parallel plates is proportional to the square of a constant aperture between the plates. It is then possible, with the use of the Darcy law, to evaluate the aperture required to have a certain flow rate, Q, for a given pressure drop, ΔH. Alternatively, one may use other estimates of transmissivity, T, from for example hydraulic tests.

The frictional loss aperture, δ_l, describes the fracture width required to give a certain water velocity for a given distance and pressure drop. The water velocity is given by tracer test results while the pressure drop is a result from hydraulic testing. Furthermore, the frictional loss aperture also assumes that the permeability between a pair of parallel plates is proportional to the square of a constant aperture, as assumed when evaluating the cubic law aperture.

It may be shown theoretically that /Tsang 1992/:

$$\delta_c^3 = \delta_l^2 \delta_m \qquad \text{Equation 3-2}$$

For a parallel plate fracture, all three apertures would be equally large /Dickson and Thomson 2003/. However, for realistic, heterogeneous fractures the relative magnitudes are /Tsang 1992/:

$$\delta_m \geq \delta_c \geq \delta_l \qquad \text{Equation 3-3}$$

Cubic law aperture and frictional loss aperture is smaller than mass balance aperture since the former includes pressure drop, which is very sensitive for local heterogeneities, such as fracture constrictions, so that they will be weighted towards the smaller apertures in the system while mass balance aperture is not /Tsang 1992/. /Zheng et al. 2008/ showed with laboratory experiments that mass balance aperture should be used, rather than the other two apertures, to describe tracer transport in a single variable fracture and that mass balance aperture is a good approximation of the arithmetic mean aperture of the fracture.

If a single plane-parallel single fracture and the same geometrical assumption are considered for all three apertures when estimating aperture from actual field experiments, the total flow rate in the single fracture needed to explain the frictional loss aperture is usually lower than the actual flow rate due to Equation 3-3. Hence, in order to achieve the same total flow rate, Q, as used in evaluation of δ_m and δ_c, several fractures with flow rate Q_{fr} are required when using δ_l so that the sum of all Q_{fr} equals Q /Abelin et al. 1985/.

In Sections 3.3.1 to 3.3.2 equations for calculation of the three different types of aperture are given for homogeneous radial flow. For a more thorough and general derivation of the aperture equations refer to /Tsang 1992/.

In addition to the three definitions of aperture discussed in /Tsang 1992/, other definitions have been used in the context of relationship between transmissivity and aperture. These definitions are discussed in Section 3.3.4. As in /Tsang 1992/, the symbol δ is used in this report for aperture in combination with an index in order to distinguish between the different definitions of aperture. In other reports, other symbols for aperture has been used, e.g. /Dershowitz et al. 2003/ used the symbol *e*.

3.3.1 Mass balance aperture

The mass balance aperture, δ_m [L], describes the average volume of a fracture, given certain boundary conditions and geometrical assumptions. It is derived by using the mean residence time for conservative tracer transport, t_m [T], and the pumping flow rate, Q [L^3/T]. Assuming a homogenous feature with volume V [L^3], the mean residence time from one end of the volume to the other with a steady-state flow rate Q, is given by:

$$t_m = \frac{V}{Q} \qquad \text{Equation 3-4}$$

For a radially converging steady-state flow field in a homogenous plane-parallel fracture with aperture δ_m, the mean residence time, t_m, for conservative tracer transport from a distance r to a pumping hole with radius r_w [L] is:

$$t_m = \frac{\delta_m \pi (r^2 - r_w^{\,2})}{Q} \qquad \text{Equation 3-5}$$

A simple rearrangement of Equation 3-5 results in the equation for mass balance aperture according to:

$$\delta_m = \frac{Q t_m}{\pi (r^2 - r_w^2)} \qquad \text{Equation 3-6}$$

In some cases, e.g. flow into tunnel, with radius, r_w, it is more appropriate to calculate δ_m for a part of the radially converging flow field. In such cases the collection length, B [L], of the homogeneous fracture into the tunnel must be known. The flow into a part of the tunnel, Q_p [L^3/T], may then be expressed:

$$Q_p = Q \frac{B}{2\pi r_w} \qquad \text{Equation 3-7}$$

Re-arranging and inserting Equation 3-7 into Equation 3-6 results in:

$$\delta_m = 2 \frac{Q_p t_m}{B(\frac{r^2}{r_w} - r_w)} \qquad \text{Equation 3-8}$$

Several other notations and names are used for the mass balance aperture, e.g. volume-balance aperture, fracture aperture and aperture from tracer experiment. In this report, only the term mass balance aperture will be used from now on for the aperture calculated directly from tracer experiments with Equation 3-6 or Equation 3-8. The only exception to this is a few cases of equal dipole tests where the equations are not applicable but mass balance aperture still is reported. In these cases, the mass balance aperture has been evaluated by other means, such as 2D homogeneous models.

The distinction between the more specific term mass balance aperture and the more general term transport aperture in this report is therefore that the latter may be calculated in a number of ways, for example with numerical modelling with a discrete fracture network of a tracer experiment, while mass balance aperture only is calculated from Equation 3-6 or Equation 3-8, expect for a few cases of equal dipole tests. In practise, however, transport aperture and mass balance aperture may be the same, assuming the same boundary condition and geometry are applied.

3.3.2 Cubic law aperture

The second kind of aperture discussed in /Tsang 1992/, cubic law aperture, uses only hydraulic parameters and not any results from tracer tests. It defines the aperture required to have a certain flow rate Q for a given pressure drop. The cubic law relates the fracture transmissivity, T_{fr}, to fracture aperture, b, in a parallel-plate fracture with smooth laminar flow by:

$$T_{fr} = \frac{\rho g}{12\mu} b^3 \qquad \text{Equation 3-9}$$

where r is the water density [M/L^3], m is the dynamic viscosity [$ML^{-1}T^{-1}$] and g is the gravitational acceleration [L/T^2]. The cubic law aperture may be simply stated by re-arranging Equation 3-9 and renaming the aperture as δ_c [L]:

$$\delta_c = \left(\frac{12 T_{fr} \mu}{\rho g} \right)^{1/3} \qquad \text{Equation 3-10}$$

where T_{fr} may be obtained from hydraulic test.

Cubic law aperture is in literature also sometimes referred to as hydraulic aperture. However, in this report it will only be referred to as the cubic law aperture in order to separate it from other relationships between transmissivity and aperture.

3.3.3 Frictional loss aperture

Frictional loss aperture δ_l [L], is estimated by using mean residence time and observed heads in contrast to evaluation of mass balance aperture where only information from the tracer transport is used.

For stationary conditions and radial flow in an individual fracture, Thiems equation (Equation 3-11) gives:

$$h - h_w = \frac{Q_{fr}}{2\pi T_{fr}} \ln \frac{r}{r_w} \qquad \text{Equation 3-11}$$

where T_{fr} is the fracture transmissivity [L^2/T], Q_{fr} is the fracture pumping flow rate, h and h_w are the heads [L] at the distances r and r_w, respectively.

The transmissivity of a homogenous fracture is given by:

$$T_{fr} = K_{fr}\, b \qquad \text{Equation 3-12}$$

where K_{fr} is the thickness-weighted mean hydraulic conductivity [L/T] of the fracture and b is the total thickness [L] of the fracture. If it assumed the fracture in mind is a single plane-parallel fracture with kinematic porosity equal to 1.0, the thickness b becomes an aperture. By considering the mass balance for the fracture (Equation 3-6 with Q_{fr}) and Equation 3-11 and Equation 3-12 the following equation is obtained for the hydraulic conductivity for the fracture, K_{fr}:

$$K_{fr} = \frac{(r^2 - r_w^{\,2})}{2 t_m (h - h_w)} \ln \frac{r}{r_w} \qquad \text{Equation 3-13}$$

Furthermore, the so called cubic law is invoked in the calculation of the frictional loss aperture according to Equation 3-9. If one assumes that Equation 3-12 is valid and b in Equation 3-9 is replaced by the frictional loss aperture δ_l then:

$$\delta_l = \left(\frac{K_{fr} 12 \mu}{\rho g} \right)^{1/2} \qquad \text{Equation 3-14}$$

3.3.4 Previous works on the relationship between aperture and transmissivity

Different relationships between aperture and transmissivity have been proposed and used in the general form of:

$$\delta_x = a_x \cdot T^{b_x} \qquad \text{Equation 3-15}$$

where δ_x is the aperture for definition x and a_x and b_x are constants.

First, may the cubic law aperture according to Equation 3-10 may be used as a relationship between transmissivity and aperture. If the following values are used for the constants in the equation:

ρ = 1,000 *kg/m³*
g = 9.81 *m/s²*
μ = 1.3 · 10–3 *kg/m/s* (*at* 10°C)

then the constants for the cubic law in Equation 3-15 would be:

$a_c = 0.0117$
$b_c = 1/3$

In several studies involving numerical modelling of tracer tests performed within the SKB investigation programmes, relationships between aperture and transmissivity have been used. According to the definition of the term transport aperture and the distinction of mass balance aperture in this report, as given above, the aperture in these cases of numerical modelling of tracer tests will be referred to as transport aperture, δ_t, further on.

Another type of aperture sometimes used in context of modelling is *hydraulic aperture*, δ_h. Hydraulic aperture is in these cases based on measurements of flux and friction loss, in contrast to transport aperture, which is based on velocity as measured with tracer test / Doe T 2010, pers. comm./. Due to this, it is more natural to compare mass balance aperture as defined in Section 3.3.1 to transport aperture than to hydraulic aperture. Hydraulic aperture is instead closely related to the cubic law aperture since they both are based strictly on hydraulic parameters. Besides, as mentioned above, cubic law aperture is sometimes referred to as hydraulic aperture in literature. The distinction between the two terms in this report is that cubic law aperture only is based on the physical constants given above and evaluated transmissivity while hydraulic aperture is based on measurement of flux and friction loss from real experiments and modelling.

In modelling of the large-scale pumping and tracer test LPT-2 at Äspö the general form of the relationship between transport aperture and transmissivity according to Equation 3-14 was used /Uchida et al. 1994/. A value of 0.5 for the constant b_t was suggested based on a theoretical discussion of the relationship between transmissivity and storativity while values of a_t were varied /Uchida et al. 1994/.

In Äspö Tack Force Task 6c /Dershowitz et al. 2003/, the general relationship in Equation 3-14 was also used. They also used the hydraulic aperture δ_h (e_h in /Dershowitz et al. 2003/) so that:

$$\delta_h = a_h T^{b_h} \qquad \text{Equation 3-16}$$

$$\delta_t = a_t \delta_h \qquad \text{Equation 3-17}$$

where a_h, a_t and b_h are constants. In accordance with /Uchida et al. 1994/, b_h was set to 0.5. The definition of δ_h in /Dershowitz et al. 2003/ is not given explicitly but is, according to the report estimated empirically using hydraulic experiments in TRUE Block Scale at Äspö to a_h= 0.46. /Dershowitz et al. 2003/ also gives a potential range of values between 0.25 and 0.60 for a_h. The details of the estimation process of a_h is not given in /Dershowitz et al. 2003/. However, according to personal communication /Aaron Fox, 2009/, a simplified description of the methodology is:

1. A channel network model was devised based on a deterministic deformation zone model combined with a stochastic background fracture model. The channel network represents a network of one-dimensional pipes created between fracture intersections. Each channel has a certain width (calculated as a function of the length of the fracture intersections), transmissivity and hydraulic aperture.

2. Values of T were assigned to deterministic structures based on difference flow logging or other hydraulic tests. For background fractures, values of T were assigned based on stochastic distributions calculated using available hydraulic data (tracer dilution, difference flow logging or interference testing) when possible.
3. Observed heads were used for estimation of model boundary conditions. Channel network simulations used a constant-head boundary condition on the exterior walls of the simulation volume, and generally used constant head or constant flux boundary conditions at injection and pumping wells, respectively.
4. The hydraulic calibration of the model was performed by changing the hydraulic aperture and comparing the observed flux from dilution tests with the flux in the model. The relationship between hydraulic aperture and flow rate Q is controlled by the Darcy law according to:

$$Q = -A \cdot K \frac{\Delta h}{\Delta l} = -w \cdot \delta_h \cdot K \frac{\Delta h}{\Delta l} \qquad \text{Equation 3-18}$$

where w [L] is the width of the channel.

5. After the hydraulic calibration, the channel network model was calibrated for tracer transport by changing the transport aperture and other parameters, such as dispersion length, matrix porosity, fracture infill thickness and tortuosity, so that tracer test simulations fits observed tracer breakthrough curves at the site.

In /Dershowitz et al. 2003/, the constant a_t is given a value of 0.125 with reference to /Dershowitz and Klise 2002/. However, in /Dershowitz and Klise 2002/ it was only possible to find the value of 0.3 for the constant a_t. In addition, the constant a_h is set to 2 in /Dershowitz and Klise 2002/, making the relationship of δ_t and T differ considerably between /Dershowitz and Klise 2002/ and /Dershowitz et al. 2003/. According to / Fox A 2009, pers. comm./ the value of 0.125 probably origins from simulations of the tests PT1–PT4 in the TRUE Block Scale experiments. In these simulations a value of 2 was assumed for a_h. In /Dershowitz et al. 2002/, a_h was set to 2 while a_t was calibrated to the range of 0.135–0.3. In /Dershowitz and Klise 2002/ and /Dershowitz et al. 2002/ the terms flow aperture and pipe aperture are analogous to hydraulic aperture in /Dershowitz et al. 2003/.

Note that /Dershowitz et al. 2002, 2003/ and /Dershowitz and Klise 2002/ estimate the constants empirically with a channel model and not a planar discrete fracture network model. The use of a channel model implies a significant difference from the geometry assumed for calculation of mass balance aperture according to Section 3.3.1. However, one may conclude that there exist some uncertainties about the constants presented in /Dershowitz et al. 2003/ regarding hydraulic and transport aperture. Additionally, alternative values of the constants are presented in /Dershowitz and Klise 2002/ and /Dershowitz et al. 2002/. It may not be possible, or would require a great effort, to review the work in /Dershowitz et al. 2003/, /Dershowitz and Klise 2002/ and /Dershowitz et al. 2002/ in order to evaluate which of these values that is the most robust and best supported. This study is therefore restricted to present the different values and not make any judgement of them.

In /Rhén et al. 1997/ an empirical relationship between aperture and transmissivity in the general form of Equation 3-15 is presented. In the report the aperture is called transport aperture, e_T. However, according to the presented equations in /Rhén et al. 1997/ it is identical with mass balance aperture according to the terminology used in the present study. The data used for the relationship in /Rhén et al. 1997/ is partly the same as in this study (Äspö and Stripa) but also some data from Canada was used (URL and Chalk River). The constants in /Rhén et al. 1997/ are $a_m = 1.428$ and $b_m=0.523$.

Within the work of developing a new flow and transport model for the Äspö laboratory, a relationship between aperture and transmissivity was used in the models /Svensson U et al. 2008/. This relationship was actually divided in two segments, one for fracture lengths of more than 100 m and one for fracture lengths < 100 m. The same segments were also used for the relationship between transmissivity and fracture length. The minimum value of T for fracture length > 100 m was set according to the relationship in /Svensson U et al. 2008/ to $5 \cdot 10^{-7}$ m^2/s where $\delta_t = 1.62 \cdot T^{0.53}$. The corresponding maximum value of T for fracture length <100 m was $5 \cdot 10^{-8}$ m^2/s where $\delta_t = 960 \cdot T^{0.82}$. Accordingly, in this study, the relationship between aperture and transmissivity from /Svensson et al. 2008/ are presented for two intervals of T, one for $T > 5 \cdot 10^{-7}$ m^2/s and one for $T < 5 \cdot 10^{-8}$ m^2/s. In /Svensson U et al. 2008/ it was not given any relationship between aperture and T for the interval of T between $5 \cdot 10^{-8}$ m^2/s and $5 \cdot 10^{-7}$ m^2/s.

Within the work of a site descriptive model for Laxemar (SDM-Site Laxemar), the relationship $\delta_m=0.705 \cdot T^{0.404}$ was used /Rhén et al. 2008, 2009/. This relationship was based on data from tracer tests in Äspö, Finnsjön and Stripa compiled in Table 5-18 in /Gustafsson and Nordqvist 1993/. However, the data for NE-1 at Äspö was considered as an outlier and not included in the data used for the relationship. As mentioned later in the present report, the mass balance aperture for NE-1 was not correctly calculated originally, which explain its deviation from the other data compiled in Table 5-18 in /Gustafsson and Nordqvist 1993/.

In order to separate apertures collected from different references, δ from /Dershowitz et al. 2003/, /Dershowitz and Klise 2002/ and /Dershowitz et al. 2002/ will from now on also be indicated with D as in Dershowitz. Likewise, δ from /Svensson U et al. 2008/ and /Rhén et al. 1997/ will from on also be indicated with S and R, respectively. Finally, δ from /Rhén et al. 2008, 2009/ will be indicated with L, as in Laxemar.

A compilation of proposed relationships between transmissivity and aperture that are used in this report is given below:

$\delta_c = a_c T^{bc} = 0.0117 \cdot T^{1/3}$ Cubic law aperture

$\delta_{h,D1} = a_h T^{bh} = 0.46 \cdot T^{0.5}$ Hydraulic aperture /Dershowitz et al. 2003/

$\delta_{h,D2} = a_h T^{bh} = 2 \cdot T^{0.5}$ Hydraulic aperture /Dershowitz and Klise 2002/ and /Dershowitz et al. 2002/

$\delta_{t,D1} = a_t \delta_{h,D} = 0.125 \cdot 0.46 \cdot T^{0.5} = 0.0575 \cdot T^{0.5}$ Transport aperture /Dershowitz et al. 2003/

$\delta_{t,D2} = a_t \delta_{h,D} = 0.135 \cdot 2 \cdot T^{0.5} = 0.27 \cdot T^{0.5}$ Transport aperture /Dershowitz et al. 2002/

$\delta_{t,D3} = a_t \delta_{h,D} = 0.125 \cdot 2 \cdot T^{0.5} = 0.25 \cdot T^{0.5}$ Transport aperture /Simulations of PT1–PT4/

$\delta_{t,D4} = a_t \delta_{h,D} = 0.3 \cdot 2 \cdot T^{0.5} = 0.6 \cdot T^{0.5}$ Transport aperture /Dershowitz and Klise 2002/

$\delta_{m,R} = 1.428 \cdot T^{0.523}$ Mass balance aperture /Rhén et al. 1997/

$\delta_{t,S} = 1.62 \cdot T^{0.53}$ $T > 5 \cdot 10^{-7}$ Transport aperture /Svensson U et al. 2008/

$\delta_{t,S} = 960 \cdot T^{0.82}$ $T < 5 \cdot 10^{-8}$ Transport aperture /Svensson U et al. 2008/

$\delta_{m,L} = 0.705 \cdot T^{0.404}$ Mass balance aperture /Rhén et al. 2008, 2009/

To summarise, a_h is between 0.46 and 2 while $a_t \delta_h$ is between 0.0575 and 0.6 for /Dershowitz et al. 2003/, /Dershowitz and Klise 2002/ and /Dershowitz et al. 2002/.

3.4 Tracer test evaluation

3.4.1 Models

Tracer tests may be evaluated in a number of ways with different models and methods, from simple one-dimensional analytical solutions to complex three dimensional numerical models.

For the evaluation of SKB's tracer tests, the dominating method has been to use a one-dimensional advection-dispersion (1-D AD) model in order to determine the equivalent mean residence time and dispersivity, where the velocity along the flow path is assumed to be constant. The use of a 1-D model for estimating mean residence time may be seen as conceptually incorrect if the following estimation of mass balance aperture is carried out by using a radial (2-D) concept as shown in Section 3.3.1. The assumption of constant velocity along the flow path is a simplification of the perhaps more realistic assumption of varying velocity with distance, as would be the case for a radial flow field (velocity inversely proportional to the distance from the pumping well). Another simplification is that transverse dispersion is neglected. It should be noted that in the absence of transverse dispersion, the basic advection-dispersion equations for homogenous linear and radial flow, respectively, are both in a sense one-dimensional (i.e. only one spatial coordinate) and the only difference is how the velocity varies with distance. However, it has been demonstrated /Sauty 1980/ that a linear flow field solution gives rather similar results as a radial model as long as the Peclet number is not too low. The difference between a linear flow field solution and a radial model depends not only on the Peclet number but also on other factors such as tracer input function and type of solution. It is therefore difficult to establish a definitive limit where the Peclet number becomes too low for a good agreement between the 1-D and 2-D models. However, for most cases the models give rather similar results when Peclet number > 3 /Sauty 1980/. Hence, mean residence time for the 2-D radial case is assumed to be approximately the same as the mean residence time from the 1-D model and then used for calculation of mass balance aperture for a radial case as shown in Section 3.3.1.

Considering a tracer test performed in a 2-D radial flow field, it is clear by a visual inspection of figures in /Sauty 1980/ that the true mean residence time may be both shorter or longer than the evaluated mean residence time with a 1-D model depending on several factors such Peclet number, tracer input function, boundary conditions and diverging or converging flow field. Another reason for the historic wide use of 1-D models assuming constant velocity for interpretation of radially converging tracer tests is the availability of simple analytical solutions, (e.g. /van Genuchten and Alves 1982/ and /Javandel et al. 1984/).

Sometimes one-dimensional advection-dispersion-diffusion (1-D ADD) models have been used as a complement to the 1-D AD models. It is also possible to use several separate pathways when using the 1-D models where the transport parameters are evaluated for each separate pathway. For equal dipole tests a two-dimensional homogenous advection-dispersion (2-D AD) model has been used.

In practise, the evaluation is performed by fitting a simulated tracer breakthrough curve to the observed tracer breakthrough curve from the test. This may either be done manually by trial-and-error or automatically with a parameter estimation method. Automatic parameter estimation methods have been employed on a regular basis in most of the tracer experiments performed by SKB.

It is often found, when evaluating the SKB tracer tests, that the 1-D AD models for one pathway fits the observed breakthrough curve fairly well. In such cases it is difficult to use models with a higher degree of freedom, e.g. 1-D AD with several pathways or 1-D ADD, in the evaluation without getting parameters closely correlated to each other. Therefore, the evaluation using the 1-D AD model is often regarded as the most easy to defend.

3.4.2 Other derived parameters from tracer tests

Besides mass balance aperture and mean residence time, other closely parameters are often reported from SKB crosshole tracer test. Kinematic porosity, ε_f [–], is defined as the volume involved in the flow driven transport divided by the total volume. Kinematic porosity is either estimated for a packed-off section (often pumping section) or an assumed feature such as a fracture zone. For a packed-off section of length L [L] (or feature thickness L), the kinematic porosity is generally assumed to be:

$$\varepsilon_f = \frac{\delta}{L} \qquad \text{Equation 3-19}$$

The transmissivity of the packed-off section may be defined with the section length L and hydraulic conductivity of the test section K_L or with the aperture δ and the hydraulic fracture conductivity K_{fr} as:

$$T_{fr} = K_{fr}\,\delta \approx K_L\,L \qquad \text{Equation 3-20}$$

The kinematic porosity may then be expressed as:

$$\varepsilon_f = \frac{K_L}{K_{fr}} \qquad \text{Equation 3-21}$$

which also is the definition used in many of the tracer tests reviewed in this study. Furthermore, for most SKB tracer tests Moye´s formula for steady state evaluation of pumping test have been used for estimating K_L:

$$K = \left(\frac{Q}{2 \cdot \pi \cdot \Delta h \cdot L}\right)\left(1 + \ln\left(\frac{L}{2r_w}\right)\right) \qquad \text{Equation 3-22}$$

where Δh [L] is the pressure drawdown during the pumping test. However, it is not clear that all tracer tests have used Equation 3-22 for evaluation of K_L but alternative methods, such as Theim's equation (Equation 3-11) or transient evaluation methods may have been used. Still, this possible deviation between different tracer tests is considered to only have a minor effect on the result.

Another parameter often reported from tracer test evaluations is the Peclet number, Pe [–]. In one-dimensional transport, the Peclet number may be defined as:

$$Pe = \frac{v \cdot x}{D_L} = \frac{x}{\alpha_L} \qquad \text{Equation 3-23}$$

where v [L/T] is the average linear groundwater velocity, over the travel distance x [L], D_L [L^2/T] is the average longitudinal dispersion coefficient and α_L [L] is the longitudinal dispersivity.

4 Tracer tests included in study

As described in the introduction, SKB has performed many tracer tests through the years at a number of locations in Sweden as shown in Figure 4-1 /Löfgren et al. 2007/. In the present study the primary interest is the transport parameters that may be derived from cross-hole tracer test and their relationship to other parameters, such as transmissivity. The summary of tracer tests by /Löfgren et al. 2007/ was used as a basis for tracer tests included in this study. However, some tests were excluded early in the process such as SWIW tests and LTDE-SD since they are single hole tracer tests. Additionally, since the focus in this study is an aperture and its relation to transmissivity, no search for data of sorbing tracers were performed.

This section of the report is only a brief summary of the cross-hole tracer tests from which data were collected. For a more comprehensive description of the tests, for example test methods and geological formation, refer to /Löfgren et al. 2007/ or the specific references given herein. Furthermore, to make it easier for the reader, the headlines in this section are as much as possible similar to the headlines in /Löfgren et al. 2007/.

The tests included in the study are carried out in crystalline bedrock. The tracer tests cover a rather large distance scale from a few metres to hundreds of metres. Another important aspect, especially considering the assumptions made for evaluation of transport and hydraulic parameters, is the configuration of fractures and fracture zones and the position of the tracer injection sections relative the pumping section. Figure 4-2 illustrates a schematic tracer test with three major fractures (yellow, red and green planes), one pumping section (P), four injection section (I1–I4) and a number of arrows indicating probable flow direction. The evaluation of mass balance aperture according to Equation 3-3 assumes a *homogenous radially converging flow field* and includes the straight line distance from injection to pumping section. Basically the same assumptions are made for standard evaluation of hydraulic interference tests. These assumptions can be considered to be valid for I4 to P assuming a plane fracture since both are located in the same fracture (yellow) and no other fractures intercepts between them.

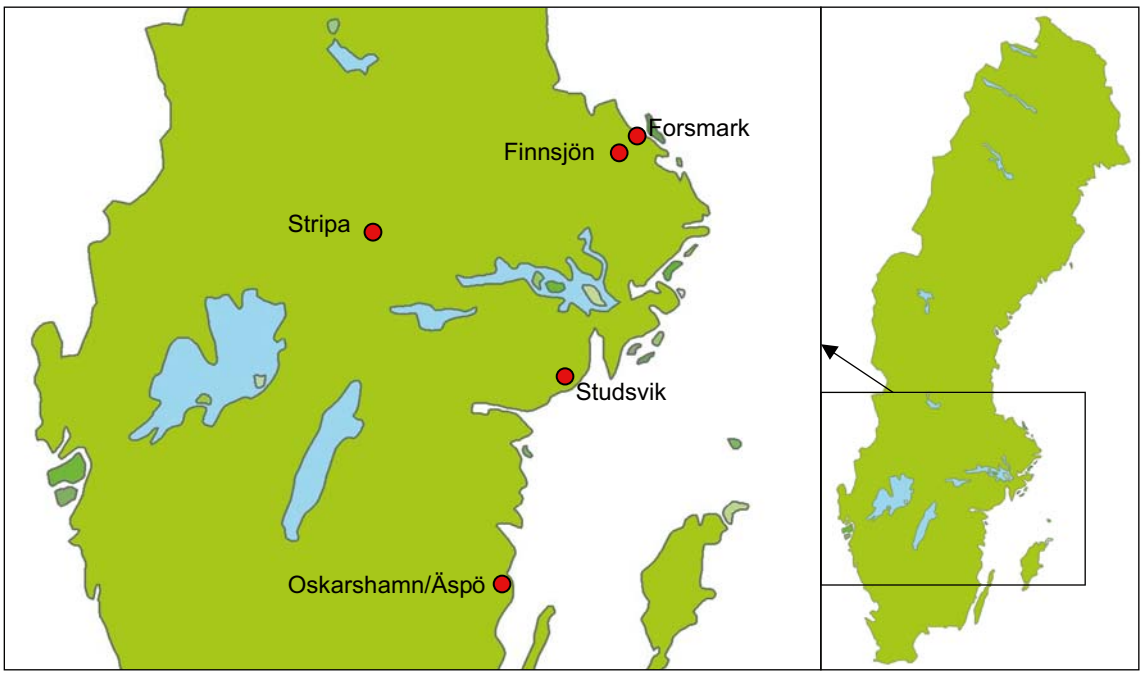

Figure 4-1. *Locations in Sweden where studied tracer tests was carried out.*

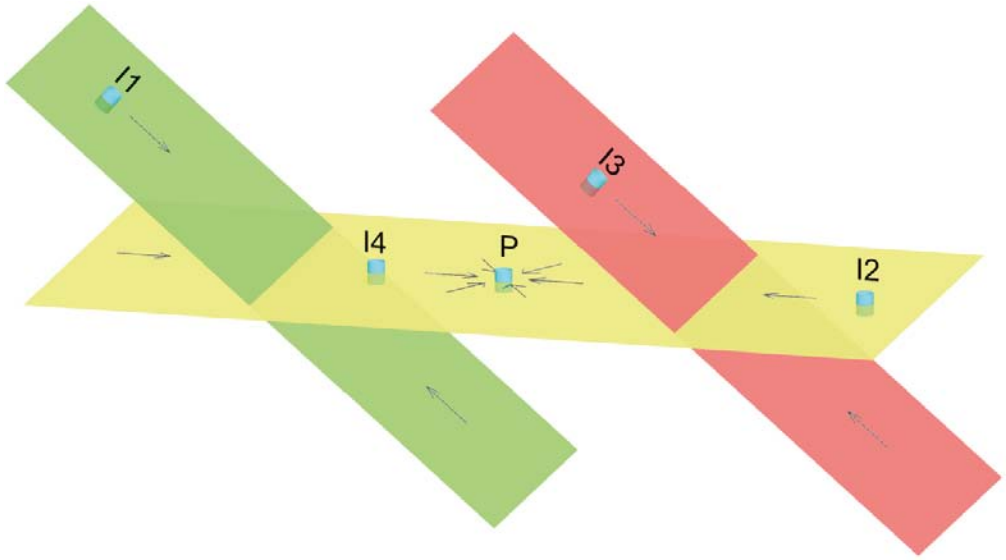

Figure 4-2. *Schematic illustration of a fracture system with pumping section P and injection section I1–I4.*

Due to the green and red fractures, the observations I1, I2 and I3 are located where 3D effects of the flow field are likely to affect the results, most probably delaying the responses. I1 and I3 are located in another fracture plane than P, making the straight line distance between the injection and pumping deviating considerably from the "true" distance of tracer transport. Due to the configuration of the system, this is especially true for I3. The fractures are probably also heterogeneous, creating a winding flow path longer than a straight line assumption within a fracture plane. Since the travel distance in the case of I3 will be underestimated with the assumptions used for calculations mass balance aperture according to Equation 3-6, the aperture estimate will be overestimated. The flow rate passing observations I1, I2 and I3 is also smaller (assuming same flow properties of all fractures) than if they were within one single fracture with distance between P and observations within the shown fractures in Figure 4-2, as crossing fractures creates 3D flow and affects the evaluated parameters.

As indicated above, it is important to consider the system of fracture used for the tracer tests when viewing the evaluated parameters from tracer and hydraulic tests. The exact configuration of fractures within the system is of course an unknown factor in these cases. However, most of the tested sites are rather well examined prior to the tests with other supporting methods. Besides, in order to achieve a good tracer recovery within the rather short time used for most experiments, the selection of injection and pumping sections were often made so that they would be in the same interpreted feature, rather close to each other and with a good connection in between. Hence, for many of the tracer tests included in the study, the assumptions of radial flow and straight line distance between injection and pumping section may be considered as rather reasonable.

The terminology used in this report to define parts of single fractures and fracture zones is illustrated in Figure 4-3. The terminology used may differ from some other reports. Figure 4-3 shows a system of three boreholes (black) including one pumping section, two tracer injection sections, A and B, and two major fractures, feature 1 and 2. Both single fractures and fracture zones are referred to as *features* in this report. With the setup illustrated in Figure 4-3, cross-hole tracer tests may be performed with two combinations of pumping and injection sections. The term *flow path* is used to define one specific combination of injection and pumping section, in this case is flow path A the part of feature 1 between injection section A and the pumping section. Flow path B consists of both feature 1 and 2 between injection section B and the pumping section. In reality, the tracer transport between the injection and pumping section is most likely divided into several branches, where each branch may be an entire fracture, as in Figure 4-3, or a separate channel within a single fracture. These branches are called *pathways* in this report as illustrated with pathway A1 and A2 for flow path A in Figure 4-3.

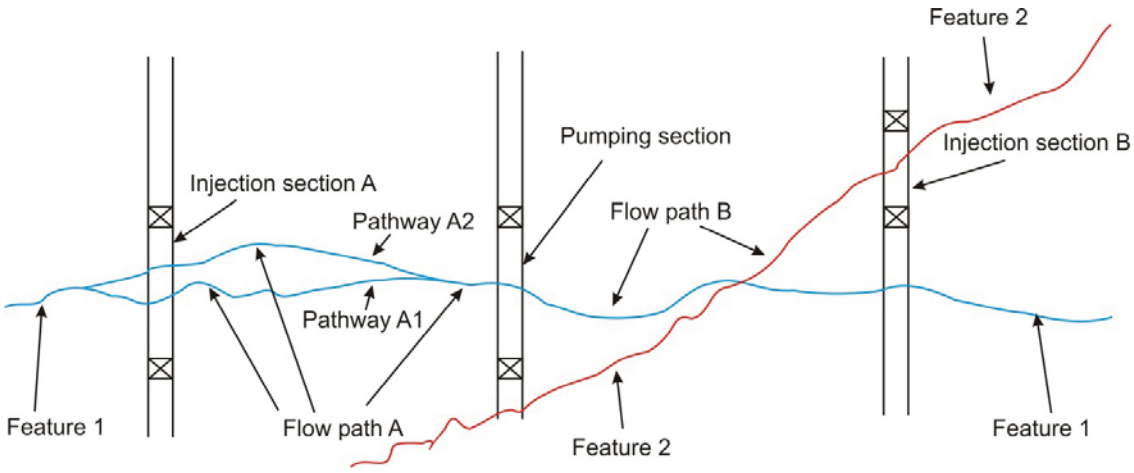

Figure 4-3. *Schematic illustration of terminology used for defining different parts of single fractures and fracture zones in this report.*

4.1 Studsvik research centre area

Two different campaigns of cross-hole tracer test were performed at the Studsvik research centre area.

4.1.1 Cross-hole tracer test 1 at Studsvik

The first cross-hole tracer test at Studsvik is presented in /Landström et al. 1978/. The test was performed as a dipole tracer test using both sorbing and non-sorbing tracers with pumping in borehole B2 at a depth of 65 m and injection in borehole B8, Section 71.5–72.5 m. The distance between the borehole sections was 51 m. Breakthrough was observed and mean transit time and dispersion coefficient were evaluated. The aperture δ_m was not reported but possible to calculate according to Equation 3-3. However, from the information in the report it is not possible to establish the strength of the dipole. It is therefore questionable to use the calculated value of δ_m for further analysis. Hence, the first cross-hole tracer test at Studsvik was not included in the analyses in this report.

4.1.2 Cross-hole tracer test 2 at Studsvik

The second cross-hole tracer test at Studsvik was performed as a weak dipole with 0.01 l/min injection flow rate in boreholes B1N, B5N and B8N and 1.2 l/min pumping flow rate in borehole B6N. The distance from B6N to B1N, B5N and B8N is 11.8, 14.6 and 22.6 m, respectively. The test is reported in /Klockars et al. 1982/ and /Landström et al. 1983/. The parameters ε and K_{fr} were calculated according to Equation 3-20 and 3-8, respectively, for flow paths B1N–B6N and B5N–B6N. No evaluation was made for the flow path B8N–B6N. The aperture δ_m was not evaluated in the report.

Unfortunately, when reviewing /Klockars et al. 1982/ for collection of data, a suspected erroneous calculation for conductivity values was found in Table 4-2c of the report. In addition, data in later tables of the report were difficult to trace. Hence, there are some uncertainties about the conductivity values in the report. It was therefore decided to check and recalculate values during the collection of data for this report and use the new values further on in this report. Some values presented in this report do therefore not agree with values presented in /Klockars et al. 1982/ and /Landström et al. 1983/. In addition, δ_m was calculated by using Equation 3-6.

4.2 Finnsjön test area

Two different parts of the Finnsjön test area have been used for tracer tests at two different times.

4.2.1 Cross-hole tracer tests in Finnsjön

The first feature in Finnsjön used for cross-hole tracer tests was a fracture zone between boreholes G1, Section 100–102 m, and G2, Section 91–93 m, where G1 was used for pumping and G2 for tracer injection. The straight-line distance between the two sections was 30 m. A number of tests were performed during two campaigns reported in /Gustafsson and Klockars 1981/ and /Gustafsson and Klockars 1984/. The latter campaign focused on the migration of the sorbing tracers strontium and caesium and do not present any new values for conservative tracer transport or hydraulic properties. Hence, values presented in this report are collected from /Gustafsson and Klockars 1981/. A total of five tests were made with instantaneous or continuous injections in radially converging flow field. No significant differences in values from the evaluation for the two injection methods are shown.

4.2.2 The fracture zone project, phase 3

The other feature in Finnsjön used for cross-hole tracer tests is called Zone 2. This zone was used in phase 3 of the Fracture zone project. Phase 3 included three campaigns of tracer tests. Borehole BFI02 was used as a pumping hole and boreholes BFI01, KFI06 and KFI11 for tracer injections in all campaigns.

The first campaign within this phase was performed in the upper highly conductive part of Zone 2 as a radially converging test and is reported in /Andersson J-E et al. 1989/. Pumping section was BFI02, 193–217 m, while the three packed-off injection sections were BFI01, 239–250 m, KFI06, 202–227 m, and KFI11, 217–240 m. The tracers were injected as pulses in the sections and when the pressures had stabilized to natural conditions the pumping in BFI02 started. All three tracers had a breakthrough and were evaluated.

The second campaign was more extensive than the first, as three separate sections in each injection borehole were used for tracer injection resulting in a total of nine injection sections. Pumping was carried out in section BFI02, 193–288.7 m, creating a radially converging flow field. Breakthrough of tracers in BFI02 was registered for the entire section, but they were also separated for pathways to an upper and a lower level in the pumping section. Tracer breakthroughs were recorded from all nine of the injection points. The second campaign is reported in /Gustafsson and Nordqvist 1993/.

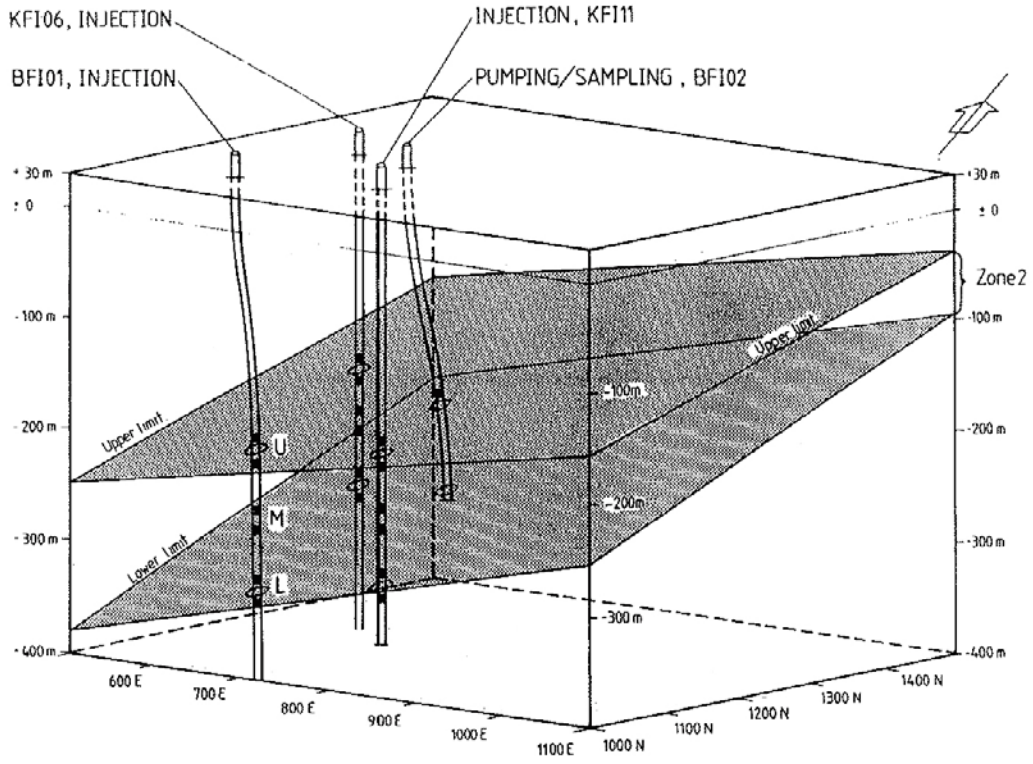

Figure 4-4. *Schematic overview of borehole configuration and the upper and lower limits of the fracture zone used in the second campaign of the fracture zone project, phase 3 (from /Gustafsson and Nordqvist 1993/).*

The third and final campaign was performed as a dipole tracer test in the upper part of Zone 2 with pumping in BFI02 and re-injection in BFI01 as reported by /Andersson et al. 1993/. BFI01 as well as KFI11 were used as tracer injection points while tracer observation was made in BFI02, KFI06 and KFI11. Evaluation was carried out for both 1-D and 2-D advection-dispersion-models. However, no value of δ_m was calculated in the report. This was not done when collecting data for this report either since the dipole flow field makes the assumption of radially converging flow field in Equation 3-5 invalid.

4.3 Stripa mine

Numerous tracer tests have been carried out in the Stripa mine with the potential to provide values for this study, i.e. cross-hole test or other types of tests with a tracer detection point separated from the tracer injection point. However, some of the tests were performed or evaluated in such a manner that parameters of interest for this study, i.e. δ_m and T, are not reported. Hence, some tracer tests are therefore missing in the data collection of this report. These tests are briefly described in Section 4.3.4.

4.3.1 Migration in single fracture

A number of tracer test was performed within the project Migration in a single fracture as reported in /Abelin et al. 1985/. Several single fractures were considered and tested within the project. Potentially useful parameters for the purpose of this study are presented for tracer tests performed in a fracture named Fracture 2. The tracers were injected in four boreholes, H1–H3 and H5, and a number of short sampling holes were used. No additional pumping was used in the sampling holes. Instead, the natural hydraulic gradient towards the drift was utilised for tracer transport. In order to keep the natural flow field unaffected the injection rates were low. Significant breakthrough of tracers were detected in sampling holes 2–6 and 2–8 originating from tracer injection holes H2 and H3. However, it seems like the injection in H2 was the only one used for calculations of tracer transport parameters. Equation 3-8 was used for calculating δ_m under the assumption of radial flow in /Abelin et al. 1985/ by using the assumption of 1 m collection length, B. It is not clear in /Abelin et al. 1985/ what basis there is for this assumption. B is directly proportional to δ_m, whereas this possible uncertainty about B also raises questions about the uncertainty in δ_m reported in /Abelin et al. 1985/.

4.3.2 Small-scale tracer tests at the SGAB tracer test drift

This tracer test was carried out with one central injection borehole surrounded by eight (odd numbers 1 to 15) tracer observation boreholes at an equal distance of 1.5 m to the central borehole. The injection flow rate was 27 ml/h while the combined pumping flow rate in the observation holes was only 2.4 ml/h. Since the withdrawal flow rate is so low compared to the injection flow rate this test is classified as a radially diverging test in this study. The test is reported in /Andersson and Klockars 1985/. Each observation borehole consisted of two sections, 11.5–15.8 and 15.8–20.0 m. Tracer breakthrough was registered and evaluated for six of the observation sections. The mass balance aperture, δ_m, is not reported in /Andersson and Klockars 1985/ but was calculated by using Equation 3-6 during the collection of data for this report.

The transmissivity in the central borehole was evaluated at three occasions, after drilling, before tracer test and after tracer test. Unfortunately, the transmissivity decreased over time, which was explained by a probable clogging of the fractures. Due to this change in hydraulic conditions during the tracer test, some uncertainties exist about the values of T for this test.

4.3.3 Monitoring of saline tracer transport with borehole radar

Two different tracer tests were performed with similar methods in the Stripa mine and was treated together in /Löfgren et al. 2007/. Consequently, they are so also here but in two separate sections.

Zone C

This tracer test was conducted in a fracture zone, called zone C as shown in Figure 4-5, in the Stripa mine and is reported in /Andersson P et al. 1989b/. It was carried out by a constant injection of tracer solution in borehole F3 with a flow rate of 800 ml/min while tracer breakthrough was monitored in surrounding boreholes E1, F1, F2, F4 and F5. The flow rates in the observation holes were in the range of 5.2 ml/min to 233 ml/min with a total of 540 ml/min. Since the total withdrawal rate is relatively high compared to the injection flow rate, it is classified as a multipolar tracer test in this study. Nevertheless, values for δ_m and K_{fr} were found in the report and used in the analyses in this study.

Zone H

The second of the two tracer tests was carried out in zone H and is reported in /Olsson et al. 1991/. Two tests were performed within zone H. In both, a saline tracer solution was injected with a constant flow rate in borehole C2 were it intersects zone H. In the first test, an array of boreholes were used for tracer breakthrough observations, while in the second, both boreholes and the tunnel drift were used by using plastic sheets for collection of water. Kinematic porosity was calculated for the entire zone H in the report. Together with an estimate of the zone thickness, δ_m could be calculated using Equation 3-19. Values of transmissivity and storativity were in the report given for several observation boreholes in the zone. In order to be able to compare the calculated δ_m for the zone with the hydraulic parameters, transmissivity and apparent storativity of the zone was calculated as the median value of the different estimates for zone H within this study. However, it was decided to not include this apparent storativity in further analysis in this report since it was evaluated in a different way than other values of apparent storativity in this study.

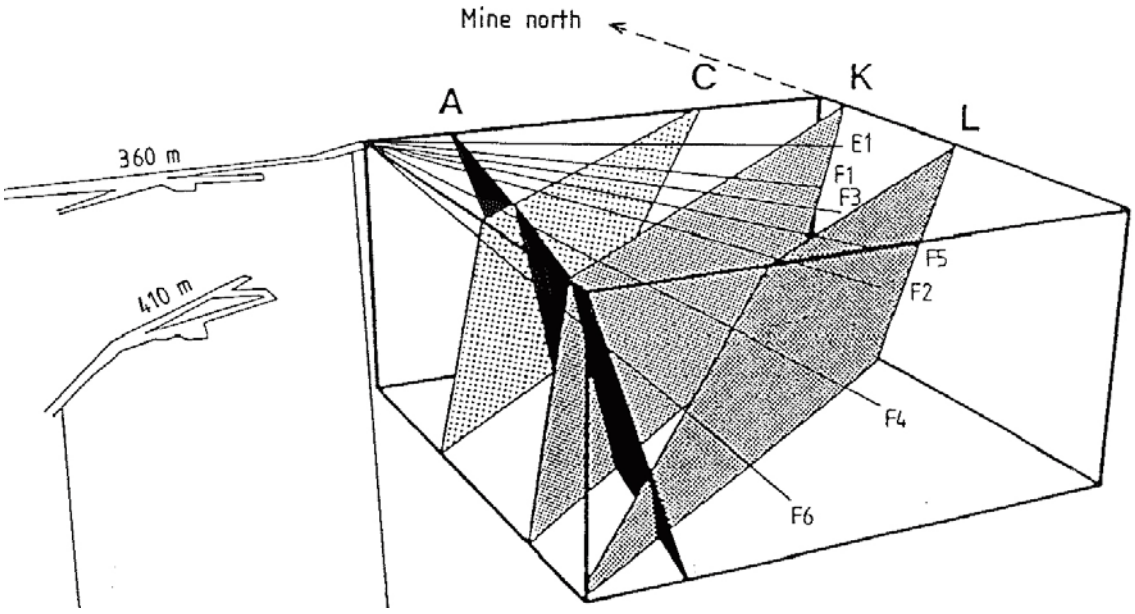

Figure 4-5. *Schematic overview of borehole configuration and fracture zones (A, K and L) in the vicinity of fracture zone C in Stripa (from /Andersson P et al. 1989b/).*

4.3.4 Tracer tests at Stripa not included in study

3-D migration experiment

The 3-D migration experiment is described in reports /Abelin and Birgersson 1987, Abelin et al. 1987a, b, c/. In principle, this experiment was carried out by injection of tracers in different section of three boreholes and observation of tracer breakthrough in the tunnel drift. The inside of the entire drift was covered in sections of plastic sheets and all the water seeping out through the walls was collected and analyzed for each section of the tunnel. This experiment setup makes it a potential candidate for providing values for this study. However, no relevant values of transmissivity for the injection boreholes or the tunnel drift was found in the reports and the 3-D migration experiment in Stripa was omitted from this study.

Channelling experiments

The channelling experiments in the Stripa mine was performed in two boreholes situated parallel to each other in the plane of a fracture. The distance between the boreholes was 1.95 m and the boreholes were approximately 2 m long. A so called multipede packer was used, making it possible to monitor the tracer breakthrough in 20 short sections in borehole 12. Five tracers were injected at five different locations in borehole 7. No values of δ_m calculated according to Equation 3-6 were found in the report. Nor was it possible to find information in the report to support any calculations of δ_m this study. Hence, this test was omitted from this study. For further information on this tracer test, see /Abelin et al. 1990/.

Tracer migration in the validation drift

The tracer migration test in the validation drift, as reported by /Birgersson et al. 1992/, was performed in a similar manner as the 3-D migration experiment, but in this case focused on zone H. Four boreholes and a total of nine sections were injected with a total of 12 tracers. The water entering the drift was collected with plastic sheets and ten boreholes at the bottom of the drift. No values of δ_m or data useful for calculation of δ_m could be found in the report. The test was therefore not included in the data analysed within this study.

4.4 Äspö Hard Rock Laboratory

4.4.1 Long term pumping and tracer test – LPT-2

Prior to the construction of the tunnel for Äspö Hard Rock Laboratory, a large-scale pumping test including tracers was performed. The tracer test was done by pumping in the open borehole of KAS06 creating a converging flow field and by sampling at several levels in the pumping hole. Non-sorbing tracers were injected in six other packed-off borehole sections. Tracer breakthrough was detected from three of the six injection points. The straight-line distance between points of injection to detection in the pumping hole ranged from 100–300 m. For further information about the tracer test, see /Rhén et al. 1992/.

Data regarding evaluated transport parameters was gathered from Appendix B and C in /Rhén et al. 1992/.

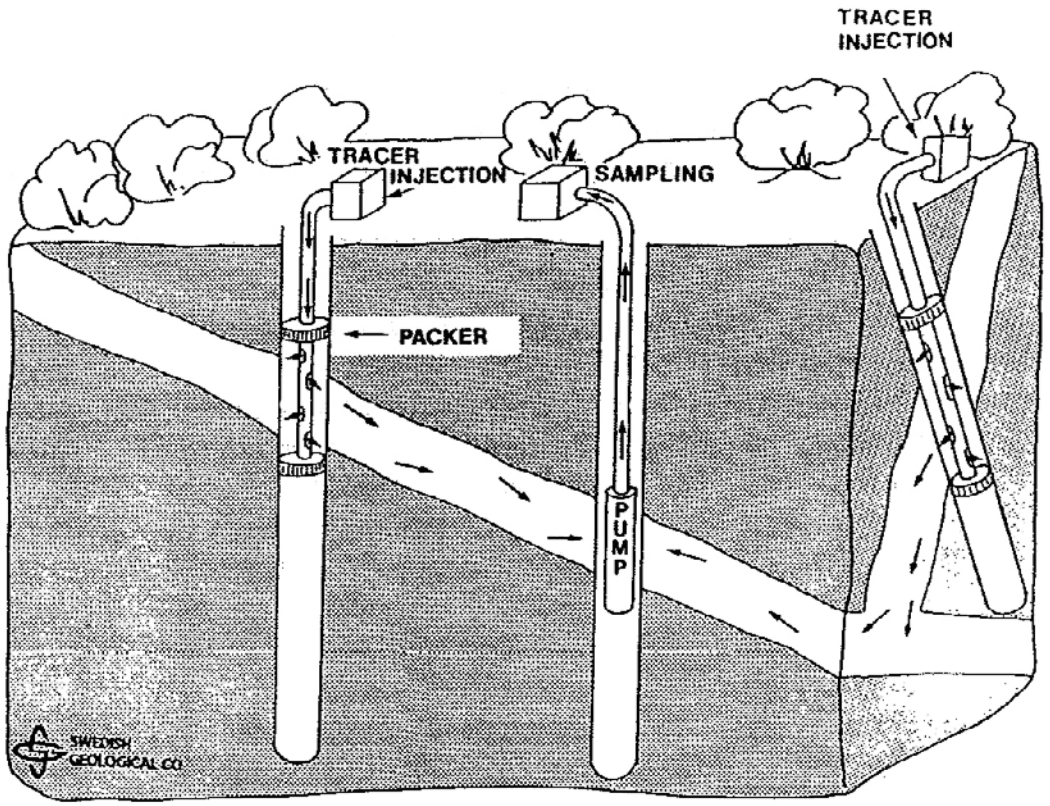

Figure 4-6. *Illustration of LPT-2 (from /Rhén et al. 1992/).*

4.4.2 Passage of NE-1

During the construction of the Äspö tunnel a tracer test was performed by injecting tracer in the surface boreholes KAS09 and KAS14 while pumping in the tunnel borehole KA1131B. The tracer transport was assumed to take place in the fracture zone called NE-1. Tracer breakthrough was only registered in KA1131B from the injection in KAS14. This tracer test is described in /SKB 1992/. Hydraulic data are available in the SKB data base Sicada.

During the collection of data from /SKB 1992/ it was discovered that π was forgotten when calculation δ_m. Hence, the values presented for δ_m in /SKB 1992/ do not agree with the value presented in this study.

4.4.3 Tracer Retention Understanding Experiments – TRUE

TRUE (Tracer Retention Understanding Experiments) is a series of project with the general objectives to /Winberg et al. 2000/:

- Develop the understanding of radionuclide migration and retention in fractured rock.
- Evaluate to what extent concepts used in models are based on realistic descriptions of fractured rock and if adequate data can be collected in site characterisation.
- Evaluate the usefulness and feasibility of different approaches to model radionuclide migration and retention.
- Provide in situ data on radionuclide migration and retention.

Within the TRUE project many different investigations were carried out. However, in this report the focus is on cross-hole tracer tests primarily and other aspects of the TRUE experiments are not included in this report. Generally, TRUE may be divided into two parts, TRUE-1 and TRUE Block Scale, based on the test site for the tracer tests.

TRUE-1

The main focus of the tracer tests performed within TRUE-1 was a single fracture called Feature A shown in Figure 4-7. A series of 19 tracer tests were performed investigating six different flow paths, primarily in Feature A but also in Feature B /Winberg et al. 2000, Andersson et al. 2002b/. Radially converging as well as dipole tracer tests were used with different strategies for tracer injections.

Most of the data from TRUE-1 presented in this report was extracted from Sicada. However, some data were missing in Sicada and had to be collected from /Winberg et al. 2000/ and /Andersson et al. 2002b/.

TRUE Block Scale

In general, the cross-hole tracer tests performed at TRUE Block Scale (TRUE-BS) were carried out in one or several inter-connected single fractures. For the purpose of this study, these tests are classified as single fracture tests, even though a more accurate description would be multiple single fractures.

In the first part of TRUE-BS, 14 tracer test campaigns were carried out including 32 tracer injections in 16 different flow paths with both conservative and sorbing tracers /Andersson et al. 2002a/. These tests were primarily performed in structures #13 and #20–23. In the second part of TRUE-BS (Continuation), three cross-hole tracer tests were performed with a total of nine tracer injections, investigating six different flow paths with the primary structure #19 /Andersson et al. 2004, 2007/. A total of 30 individual evaluations of tracer breakthrough, representing 18 different flow paths, were compiled from Sicada and reports regarding TRUE-BS. Figure 4-8 illustrates the boreholes and interpreted features at the TRUE-BS site.

Some hydraulic values cannot be found in reports or Sicada. For example, difference flow logging measurements were performed in boreholes KI0025F02, KA2563A, KA2511A and KI0025F03 /Rouhiainen and Heikkinen 1998, 1999a, b/ but tabulated results could not be found.

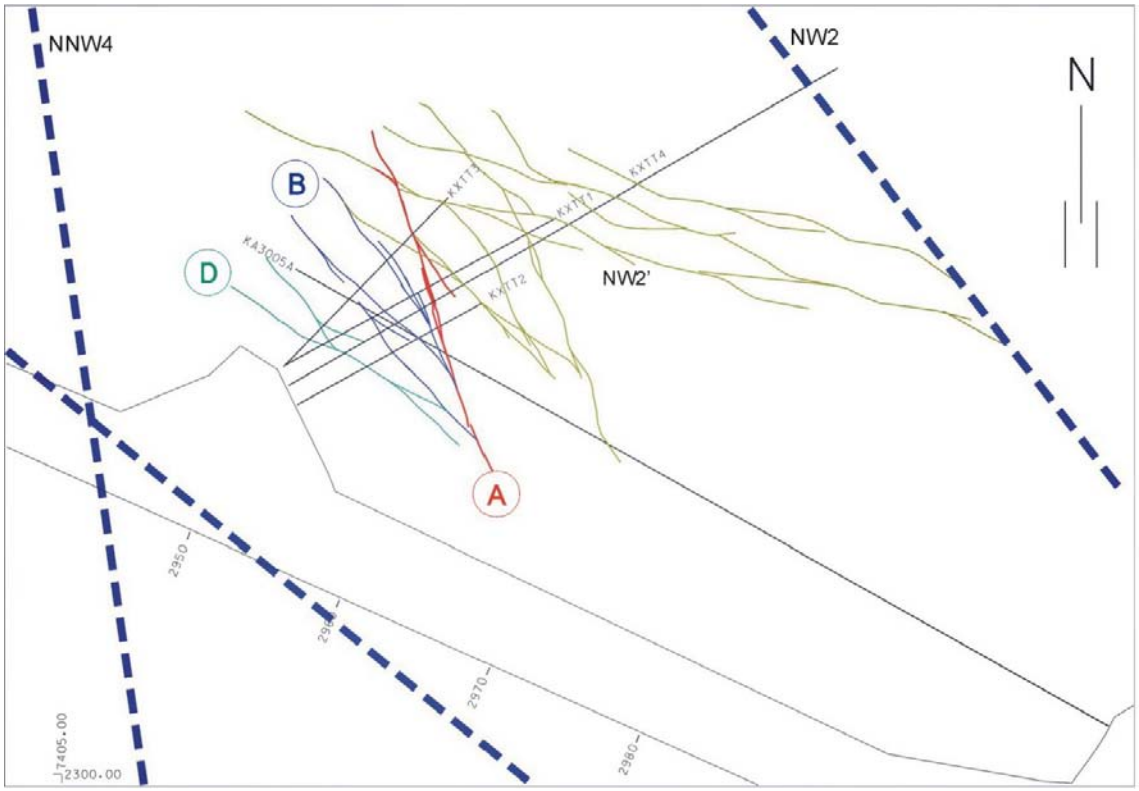

Figure 4-7. *Boreholes and interpreted features at the TRUE-1 site (from /Winberg et al. 2000/).*

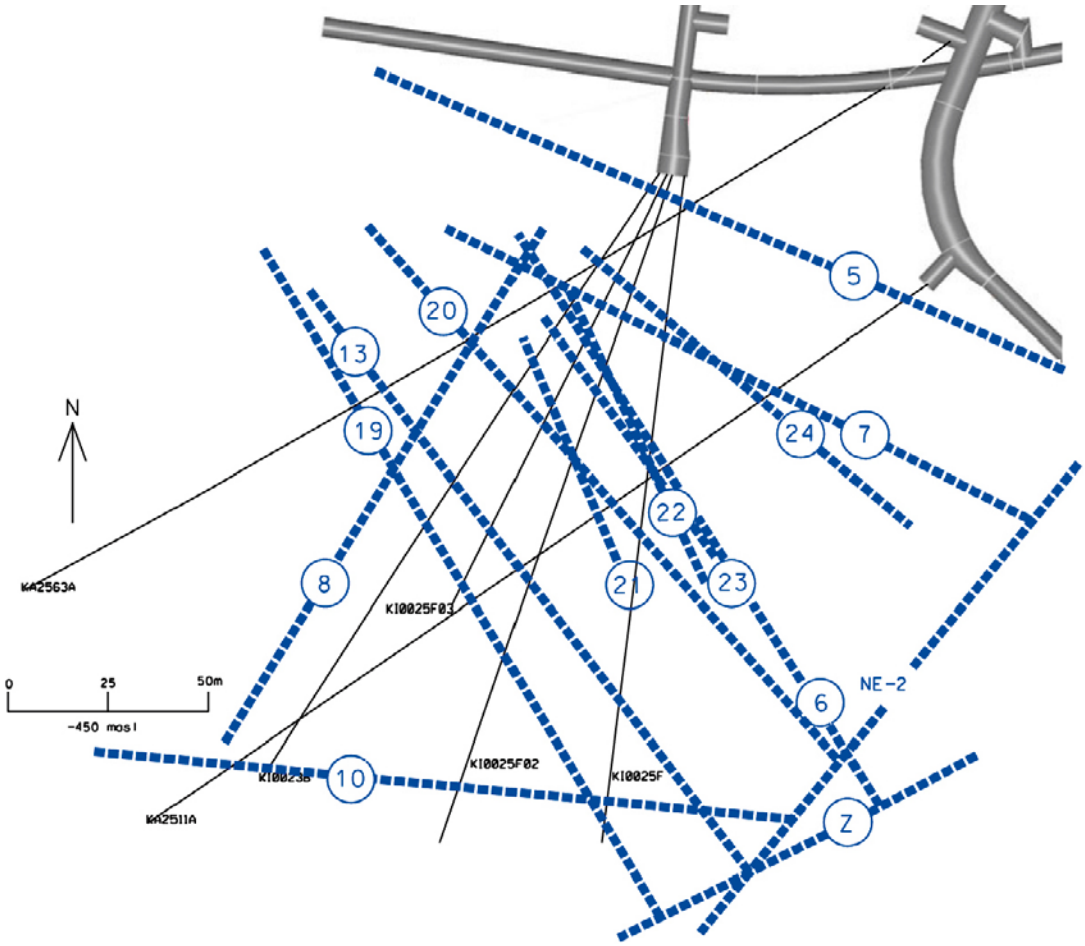

Figure 4-8. *Boreholes and interpreted features at the TRUE-BS site (from /Andersson et al. 2002a/).*

4.5 Forsmark site investigation

Data regarding the tracer tests within the Forsmark site investigation was collected from Sicada.

4.5.1 Large scale tracer test with pumping in HFM01

The first large scale tracer test at Forsmark was carried out by pumping in HFM01 while tracers were injected in HFM02, HFM15 and KFM01A as reported by /Wass and Andersson 2006/. The time for tracer transport in the test was rather short (c 400 h) due to a tight time schedule at the site investigation area. Tracer breakthrough in HFM01 was detected from the injection in HFM02. However, the recovery at pump stop was very low and evaluation of tracer transport parameters was considered as very uncertain and thus not reported. This test was therefore not included in this study.

4.5.2 Large scale tracer test with pumping in KFM02B

The second large scale tracer test at Forsmark was performed at drill site 2 and reported by /Lindquist et al. 2008a/. The test was carried out by pumping in KFM02B and tracer injection in KFM02A with a small excessive pressure. The test is therefore classified as a weak dipole experiment in this study. Both conservative and sorbing tracers were used and also observed in the pumping hole. The straight line distance between the two sections is 46 m. A schematic view of the test is shown in Figure 4-9.

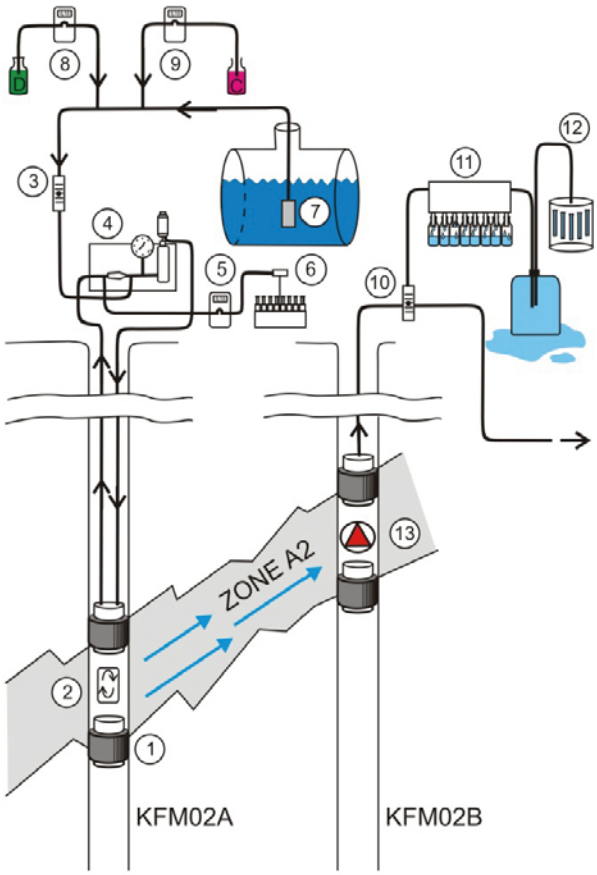

1. Packer
2. Circulation pump
3. Flow meter connected to logger
4. Circulation unit
5. Peristaltic pump for sample withdrawal
6. Fractional sampler
7. Tracer tank with injection pump
8. Peristaltic pump for sub flow D ($Fe(II)$)
9. Peristaltic pump for sub-flow C (HCO_3^-)
10. Flow meter connected to logger
11. Automatic sampler
12. Fractional sampler
13. Pump

Figure 4-9. *Schematic overview of the large scale tracer test with pumping in KFM02B (from /Lindquist et al. 2008a/).*

4.5.3 Large scale tracer test with pumping in HFM14

During the summer and autumn of 2007, a large scale tracer test was performed in Forsmark with pumping in HFM14 and injections of conservative tracers in HFM01, HFM13, HFM15, HFM19, HFM32 and KFM10A as illustrated in Figure 4-10. The test is reported in /Lindquist et al. 2008c/. The tracer injections were performed as exchange of section water and this test is classified as a radially converging test in this study. Additionally, an extra injection including both conservative and sorbing tracers was carried out in HFM15 after breakthrough of the first injection in HFM15. The second injection was performed with a small excess pressure and is classified as a weak dipole test. The straight line distance from the injection section to the pumping section was in the range of 72–510 m. Tracer breakthrough was observed and could be evaluated from all injection points except HFM32.

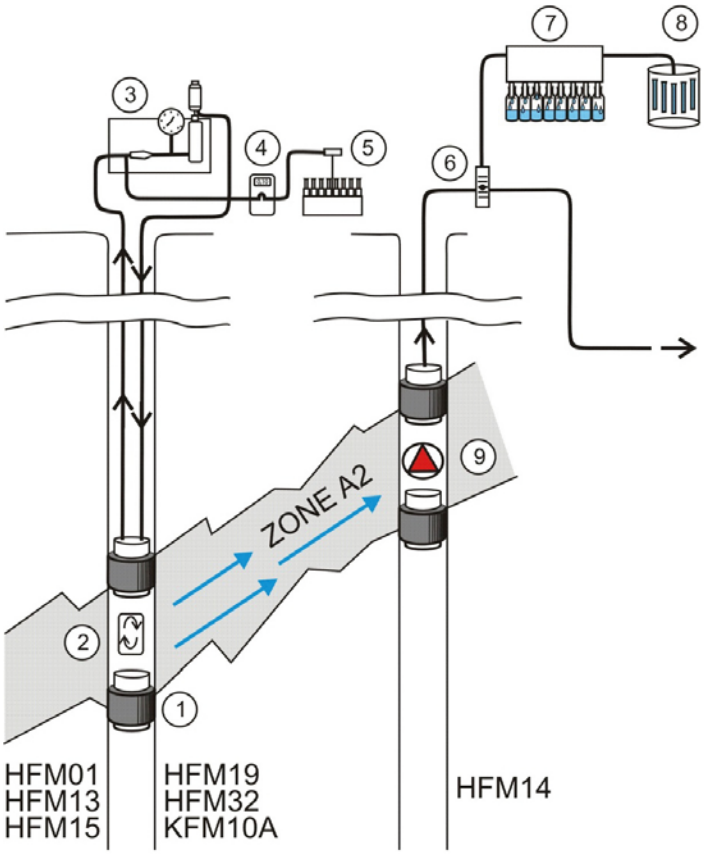

1. Packer
2. Circulation pump
3. Circulation unit
4. Peristaltic pump for sample withdrawal
5. Fractional sampler
6. Flow meter connected to logger
7. Automatic sampler
8. Automatic sampler
9. Pump

Figure 4-10. *Schematic overview of the large scale tracer test with pumping in HFM14 (from /Lindquist et al. 2008c/).*

4.6 Oskarshamn site investigation

Data regarding the tracer tests within the Oskarshamn site investigation was collected from Sicada except the test with pumping in HLX27 and HLX28 where the data was collected from the draft of the report.

4.6.1 Tracer test with pumping in HLX10

In this test, HLX10 was used for pumping and KLX02 for tracer injection /Gustafsson and Ludvigson 2005/. However, no tracer breakthrough was observed during the test and this test is not included in the data used for analysis in this study.

4.6.2 Tracer test with pumping in HLX35

In the spring of 2006 a tracer test was performed with injection in the soil boreholes SSM000222 and SSM000223 while pumping in HLX35 /Morosini and Wass 2007/. Tracer breakthrough was only detected from the injection in SSM000223. The recovery at pump stop was only 7%. No value of δ_m is available in Sicada, but other values needed for calculation of δ_m according to Equation 3-6 were, so δ_m was calculated during the collection of data for this study. However, since the recovery is so low, the value of δ_m is very uncertain which also is identified in /Morosini and Wass 2007/. It is reasonable to assume, based on the description in /Morosini and Wass 2007/, that the majority of the flow path from SSM000223 to HLX35 was situated in rock.

4.6.3 Tracer test with pumping in HLX33

A similar test as the test in HLX35 was carried out during the summer of 2006 but with pumping in HLX33 and injection in SSM000228 /Svensson T et al. 2008/. Also in this case δ_m was not reported in Sicada even though the evaluation seems to be more reliable in this case than for the test in HLX35. As in the case of HLX35, δ_m was calculated within this study using Equation 3-6. It is reasonable to assume, based on the description in /Svensson T et al. 2008/, that the majority of the flow path from SSM000228 to HLX33 was situated in rock.

4.6.4 Large scale tracer test with pumping in HLX27

A large scale tracer test with pumping in HLX27 and tracer injection in KLX15A was performed in Laxemar during the spring and summer of 2007. The test is similar to the test in Forsmark with pumping in KFM02B, i.e. performed with both conservative and sorbing tracers. However, an important difference between the two tests is that the Forsmark test was conducted with injection and pumping in the same interpreted feature while the injection in KLX15A was done in a different feature than the pumped feature in HLX27 according to the current site description of Laxemar /SKB 2009/. Figure 4-11 shows an interpretation of fracture zones possibly involved in the tracer transport. The test is reported by /Lindquist et al. 2008b/.

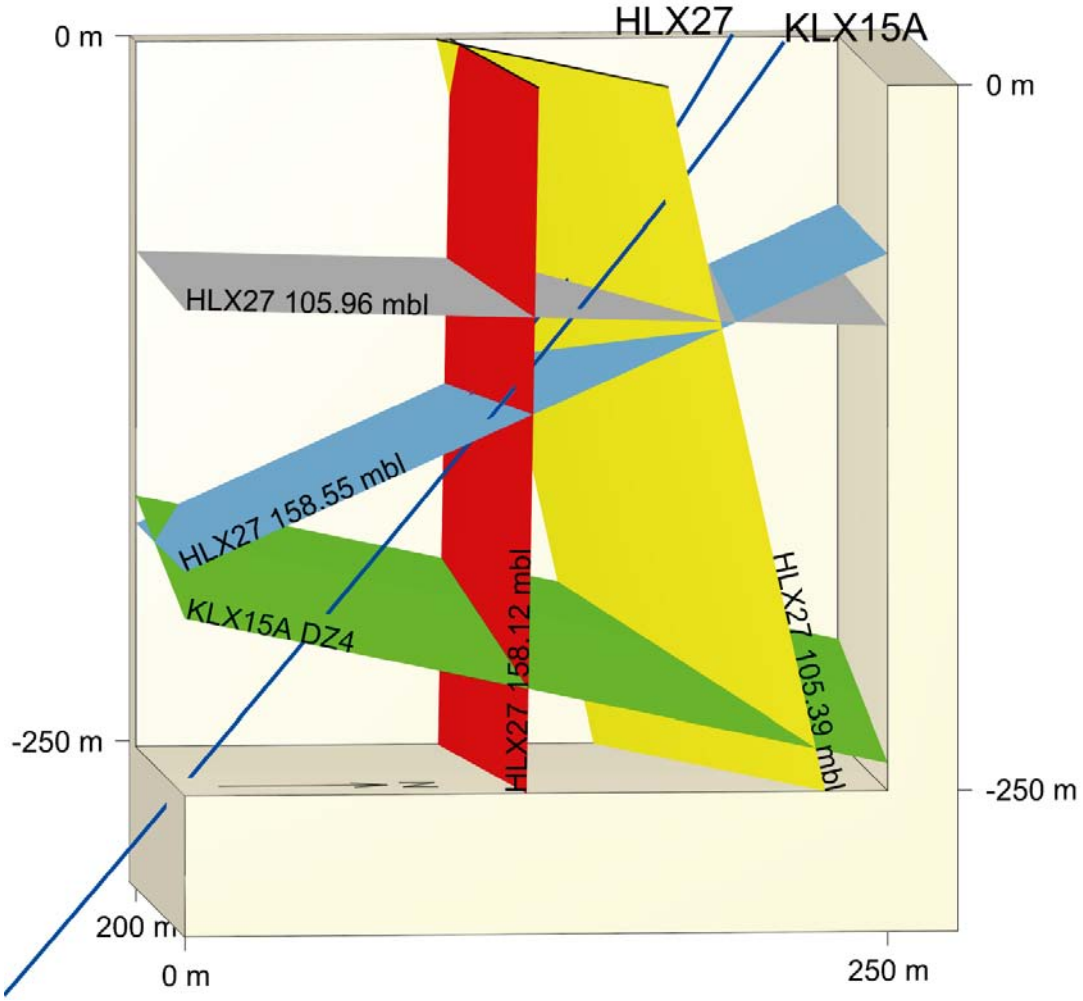

Figure 4-11. *Extrapolation of identified fractures possibly involved in the tracer transport from KLX15A:6 to HLX27 (from /Lindquist et al. 2008b/). The tracer injection point is located where the green plane intersects KLX15A. The entering point of tracer into HLX27 is located where the red or light-blue intersects HLX27 and/or where the yellow and grey plane intersects HLX27.*

4.6.5 Large scale tracer test with pumping in HLX28

During the first half of 2009 a large scale tracer test was performed in Laxemar with pumping in the open borehole HLX28 and injections of conservative tracers in packed-off sections in HLX32, HLX37, HLX38, KLX11A, KLX20A and KLX27A as reported in /Thur et al. 2010/. This test is an analogous to the large-scale tracer test with pumping in HFM14 in Forsmark in terms of test performance and setup. However, in contrast to the HFM14 test, which was performed with tracer injections in the same major structure as pumping, the injection points were considered to be in some other hydraulic feature than the pumping in HLX28. Tracer breakthrough could only be detected from the injections in HLX32, HLX37, HLX38 and possibly KLX27. However, the tracer breakthroughs from HLX38 and KLX27 were not sufficient to give an unambiguous evaluation regarding mean residence time and therefore also mass balance aperture.

5 Methods

5.1 Collection of data from literature and Sicada

Data from tracer tests as well as hydraulic test were collected from reports and the Sicada database. For a majority of the tests, data were not available in Sicada and the data had to be collected from reports. The exception to this was the tests performed more recently within the site investigations at Forsmark and Oskarshamn as well as some tests performed at the TRUE-1 and TRUE Block Scale sites at Äspö.

Data were only collected from tests where tracer breakthrough was observed. As discussed earlier in the report, the 1-D AD model has been used for evaluation of mean residence time for most tracer tests and often been regarded as the most easy to defend, due to a low correlation between fitting parameters with a good fit to data, if alternative models have been used. Consequently, the data in this report has been collected from the evaluation based on 1-D AD models if possible and nothing contrary has been found in the reports. The priority of results from 1-D AD models also reduces the subjectivity in the data collection and the risk of introducing additional deviations caused by the use of different evaluation concepts and models when comparing data from different tracer tests. Besides, as discussed in Section 3.4.1, 1-D and 2-D models give in most cases rather similar results regarding the mean residence time.

One challenge when collecting data was to match the tracer test data to relevant hydraulic data since the different types of data often relates to different test sections. However, after some consideration of the hydraulic feature tested it was often quite obvious which hydraulic test section that was relevant for the tracer test.

For some tracer tests, especially the older ones, the mass balance aperture was not calculated even if all necessary data was available. In such cases, when possible, the mass balance aperture was calculated during the collection of data within the present study. According to Section 3.3, the mass balance aperture may be calculated according to Equation 3-6 or Equation 3-19.

Observe that all data were collected from reports regarding the primary description of the tracer test and not other reports in which the data may have been re-interpreted. For example, the mass balance apertures used in this report are only from the primary evaluation of each tracer test. In some cases, results from tracer tests have been used for developing a descriptive model for the site. In these models the aperture may have been different from the evaluated mass balance aperture for some reason. In other cases, a fracture zone interpreted from the tracer test may have been modified or removed from the final version of the model. These later changes of data are not considered in this analysis since the objective of this study is to evaluate the transport parameters from cross-hole tracer tests.

5.2 Review of data

Prior to any analyses of the data collected from the tests described in Section 4 and according to the methods in Section 5.1, the data was reviewed in order to select useful tracer tests and representative values for the evaluated flow paths.

5.2.1 Selection of tracer tests

The amount of data available from various tracer tests varies substantially. In some cases, large amounts of data are reported that are useful in this study whereas other tests barely results in any useful data at all. As pointed out in Section 3.3, evaluations of tracer tests may be done by fitting a model with several pathways to a breakthrough curve. In such cases, tracer transport parameters are evaluated for each individual pathway. For some tests this was also performed, sometimes as an alternative interpretation to evaluations with one pathway but sometimes without an evaluation with one pathway.

Due to the differences in data available, the first step in the selection process was to consider which tracer tests and evaluations of tracer tests that should be included for further analysis. The primary analysis in this study is to compare the mass balance aperture to the transmissivity. Hence, evaluations of tracer tests where any of the two parameters are missing were therefore excluded from the data used for further analyses.

Transmissivity data is generally representative for entire test sections. These transmissivities are not easily distributed among sub-sections without supporting information. Even if this would be possible, it would not be possible to assign sub-section transmissivities to specific evaluations for an individual pathway if the evaluation was made with more than one pathway. Consequently, evaluations using more than one pathway were excluded from further analyses. Exceptions were made if the transport parameters for multiple pathway evaluations could be joined into a single value for a parameter.

5.2.2 Merging of tracer tests into flow path and features

In some flow paths, such as Feature A from KXTT4 to KXTT3 at the TRUE-1 site at Äspö, many tracer tests have been performed whereas in other flow paths, e.g. in NE-1 from KAS14 to KA1131B at Äspö, only one tracer test has been performed. If all tracer tests that was selected in Section 5.2.1 would be used in analyses this would result in an emphasis of the flow paths tested multiple times and consequently introduce a bias in the analyses. For this reason, multiple tracer tests in a flow path were merged into one. Feature A at the TRUE-1 site may be used as an example. Six evaluations were merged for the flow path Feature A, KXTT1–KXTT3 (tracer injection in KXTT1, withdrawal in KXTT3) while six other evaluations were merged for the flow path Feature A, KXTT4–KXTT3. In order to eliminate the effect of outliers when merging the tracer test parameters, the median value was considered to be representative for the flow path.

The values for individual flow paths in a feature may also be merged into a single value for the entire feature. This was performed by extracting the median values for tracer tests parameters and hydraulic parameters. Consequently, all values presented in Section 6 for flow paths and features are median values.

The analyses presented in Section 6 are primarily based on flow paths. In Section 6.2.1, the differences regarding the relationship between δ_m and T for tracer tests, flow paths as well as features are presented.

5.2.3 Selection of representative transmissivity

Many different field and evaluation methods are used for calculation of transmissivity values in a single or a pair of boreholes (c.f. Section 3.2). Furthermore, for each flow path used for tracer test, transmissivity values may be available for the tracer injection section, tracer withdrawal section and a combination of the two (hydraulic interference test). If the analyses would be limited to comparing tracer tests with transmissivity data evaluated with identical methods, only a few data points would be possible to use for each comparison. The transmissivity data available for comparison with tracer test parameters were divided into three categories for converging tracer tests according to:

T_I = Transmissivity for the tracer injection section, based on single-hole interpretation.

T_W = Transmissivity for the tracer withdrawal section, based on single-hole interpretation.

T_C = Transmissivity evaluated for an individual observation section in a hydraulic interference test.

Often T_C is referred to as T_o when evaluating with transient methods. However, a few transmissivity values from interference tests in this report were evaluated with stationary methods. Hence, T_C is used in this report for all transmissivity values originating from hydraulic interference tests.

For the one diverging tracer test in this study (c.f. Section 4.3.2), the definitions of T_W and T_I are the opposite, i.e. T_W represent the injection section and T_I the withdrawal section, so that the test would be more compatible with the converging tests in the data analysis.

In order to reduce the effect of single deviating transmissivity values and to reduce the subjectivity in the process, the median value within each category (T_C, T_W and T_I) and flow path was selected as a representative value for each category.

It was possible to find transmissivity values for all of the three categories above for 26 of the 74 flow paths included in the analysis. For 35 of 74 values T_C are available. The corresponding number for T_W and T_I are 63 and 62, respectively. Still, it would be desirable to make correlation analyses including all tracer flow paths. In order to do this, a fourth transmissivity category, T_S, in this study called selected transmissivity, was required.

The value selected for T_S was T_C at a first choice, T_W secondly and finally T_I. This implicates that if T_C existed for a flow path then $T_S = T_C$. If T_C was missing for the flow path, then $T_S = T_W$. If also T_W was missing then $T_S = T_I$. The reasons for this order of prioritising are further discussed in Section 7.1.1.

T_W was chosen as the second selection, in the choice between T_W and T_I, since earlier experiences show that T_C from interference tests often is closer to T_W than T_I, see e.g. /Lindquist et al. 2008a/. This is also supported by the results in Figure 5-1 where the three categories are compared pair-wise for each flow path. For example, Figure 5-1c shows T_W on the x-axis and T_I on the y-axis. Figure 5-1 indicates that the correlation is best between T_C and T_W (Figure 5-1a) since its corresponding fit (blue line) is situated closer to the unit slope line and has a higher value of R^2 than the other fits.

As seen in Figure 5-1b and Figure 5-1c, the transmissivity of the injection section, T_I, was generally lower than T_C and T_W. This is an effect of the choices made prior to the tracer test for practical reasons. It is often favourable to have a high pumping flow rate in the tracer test and by this, if it is possible, choosing the section with higher transmissivity for pumping and the section with lower transmissivity for injection.

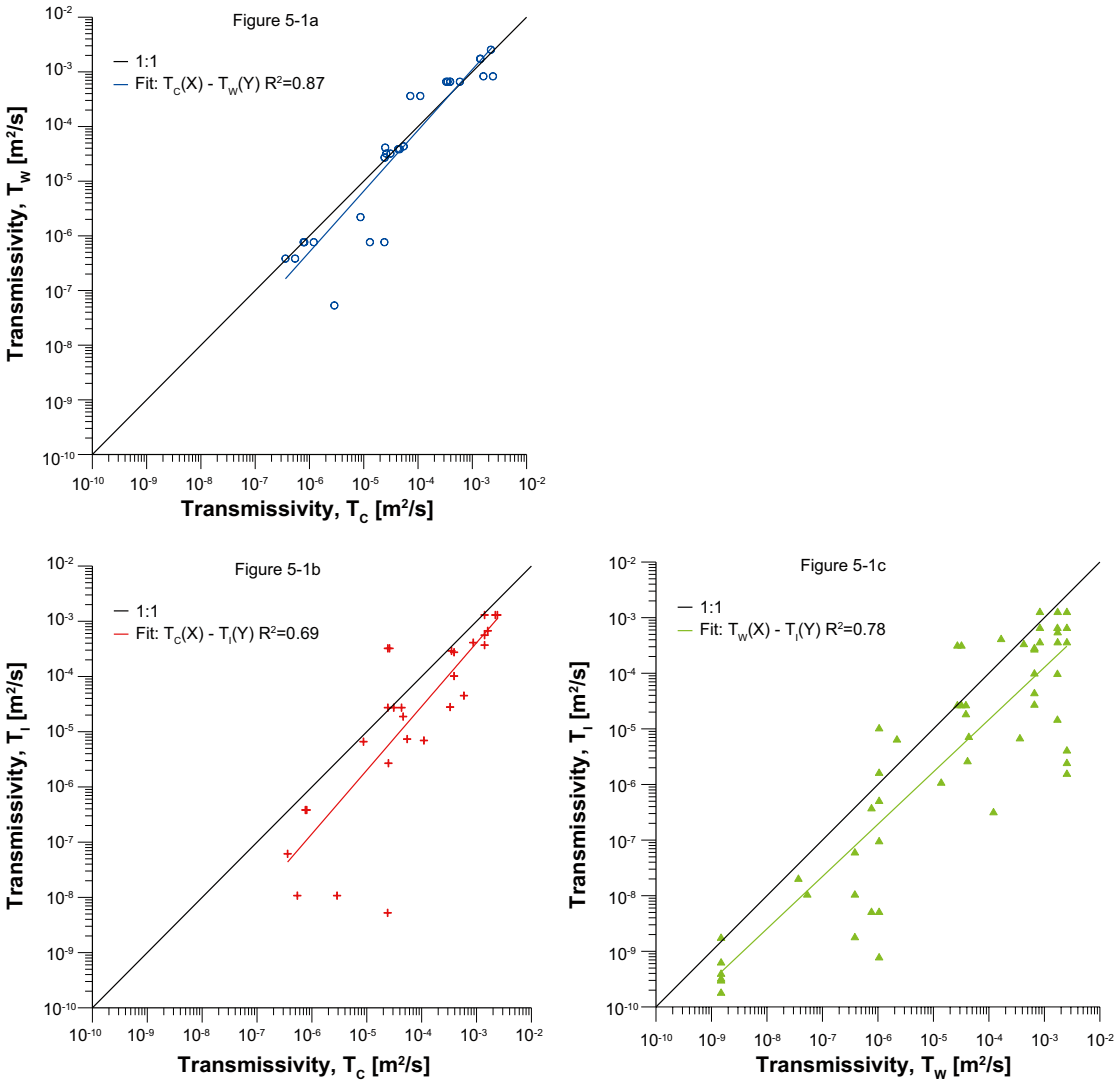

Figure 5-1 a–c. *Correlation between transmissivity (T) measured in the tracer observation section (T_W), tracer injection section (T_I) and cross-hole test between the two sections (T_C).*

5.3 Analyses

Analyses were primarily performed by plotting the collected values of different parameters with the Grapher software. The possible correlation between the parameters was evaluated by fitting equations with least square regression to the data.

6 Results

6.1 Data collected

The data collected from the various tracer tests and hydraulic tests are presented in Appendix 1.

6.2 Mass balance aperture – transmissivity

6.2.1 Tracer tests, flow paths and features

As stated in Section 5.2.2, the analyses of data in this study are performed at the level of flow paths, rather than tracer tests or features. However, it may be interesting to examine the relationship between δ_m and T depending on the level of data, i.e. if it is analysed based on all tracer tests, flow paths or features. Figure 6-1 shows δ_m and T_S for tracer tests, flow paths and features as well as fits to the data. As seen in the figure, the differences between the fits to the different levels of data are very small, indicating that the results are rather insensitive for the chosen level of data.

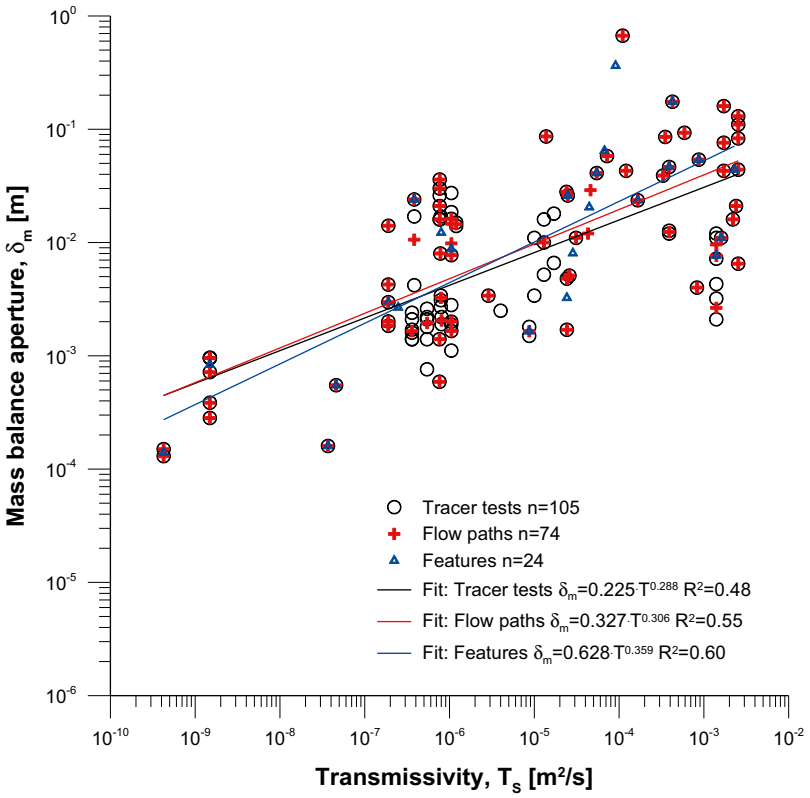

Figure 6-1. *Mass balance aperture vs. transmissivity for tracer tests, flow paths and features.*

6.2.2 Selection of transmissivity values

The method of selecting transmissivity values, as described in Section 5.2.3, has consequences for the result of the analyses. It is therefore important to establish a confidence that the selection method is suitable for the purposes of this study. Figure 6-2 to Figure 6-4 shows T versus δ_m for the flow paths included in the analysis but with different ways of selecting T from the three categories T_C, T_W and T_I. In Figure 6-2 the values are selected as given in Section 5.2.3, i.e. with T_C as the primary choice followed by T_W and finally T_I. This order of prioritizing is called T_S in this report. In Figure 6-3 and Figure 6-4, T_C is the least prioritized with T_W and T_I, respectively, as the primary choice. It is evident that that the fits and the data in Figure 6-2 and Figure 6-3 are quite similar. This suggests that the end result is not that dependent of the primary choice between T_C and T_W. The fit in Figure 6-4 deviates considerably from the other two. Also the data in Figure 6-4 are more scattered then in the other two plots. This shows that T_I deviates from the other and also that the relationship between δ_m and T_I is less clear.

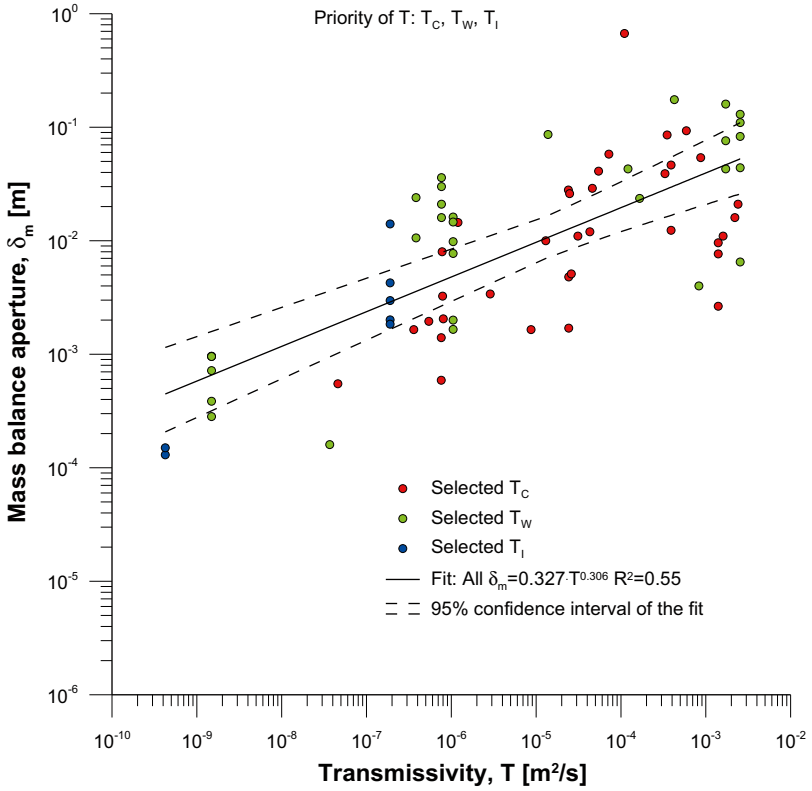

Figure 6-2. *Mass balance aperture vs. transmissivity for flow paths with transmissivity values selected primarily from T_C, secondly from T_W and finally from T_I.*

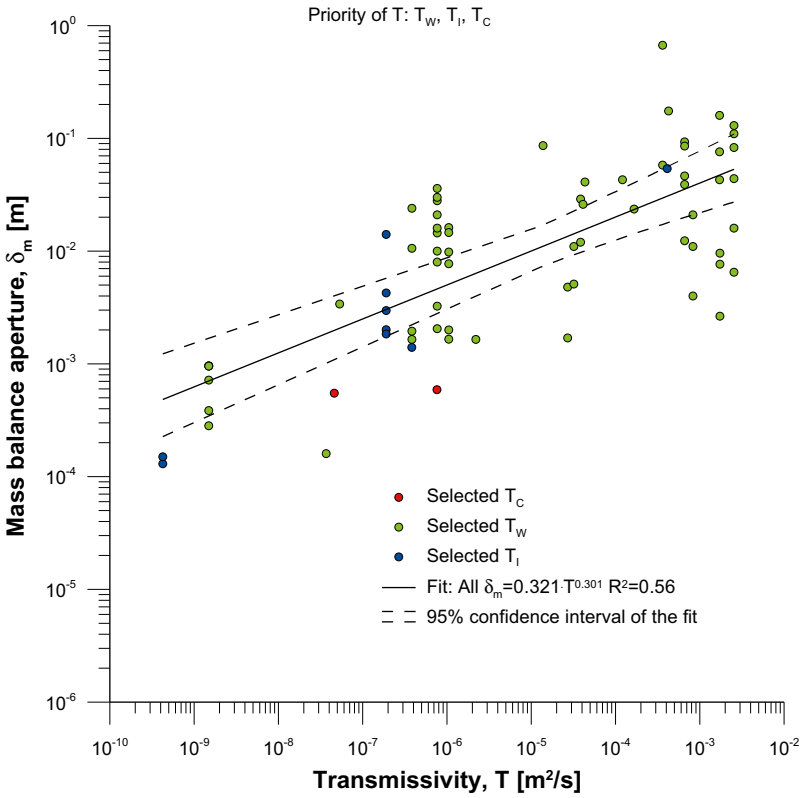

Figure 6-3. *Mass balance aperture vs. transmissivity for flow paths with transmissivity values selected primarily from T_W, secondly from T_I and finally from T_C.*

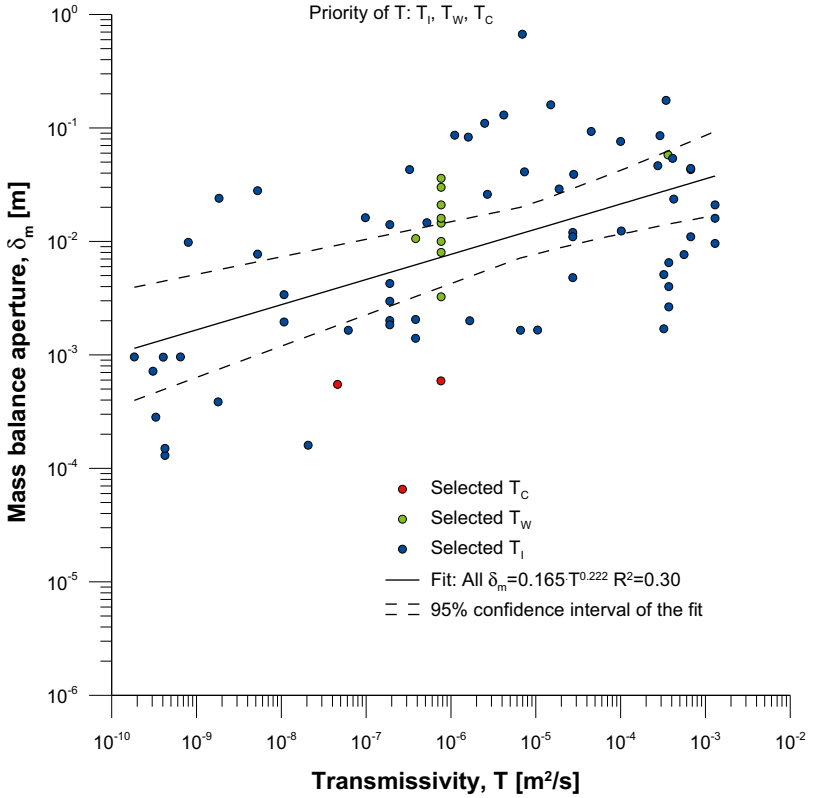

Figure 6-4. *Mass balance aperture vs. transmissivity for flow paths with transmissivity values selected primarily from T_I, secondly from T_W and finally from T_C.*

6.2.3 Effect of possible uncertain data

In general, no estimates of uncertainty in the data are presented in the reports from which values were collected. As identified in Section 4, some of the data may have larger uncertainties than other for various reasons. In the experiment "Migration in Single Fracture" (Section 4.3.1), an assumption of the collection length B was made and it is not clear what basis there is for this. In the small-scale tracer test at the SGAB tracer test drift (Section 4.3.2), the transmissivity of the system changed over time. Finally, at the tracer test with pumping in HLX35 (Section 4.6.2), the evaluation of mean residence time was identified as very uncertain due to a very low tracer recovery. Having stated this, other tests included in this study may also include great or even greater uncertainties. However, no such uncertainty evaluation could be found in the reports.

For most tracer tests included in this study the injection and pumping sections were often selected so that they would be in the same interpreted feature and have good hydraulic connection. This makes assumptions of radial flow and straight line distance between injection and pumping section in the evaluation reasonable. However, for a few tests this was not the case. The tests with pumping in HLX27 and HXL28, as described in Sections 4.6.4 and 4.6.5, were performed with pumping in a different feature than the injection, making the evaluated mass balance aperture possibly more uncertain.

Figure 6-5 shows a plot of δ_m versus T_S for all data with indications of the possible more uncertain data as described above. The figure also displays linear fits to all data (black line) and to data without the possibly more uncertain values (red line). As seen in the figure, the two fits are very similar indicating that the possibly more uncertain data do not significantly affect the overall evaluation. Preliminary results of the present study in terms of an aperture-transmissivity relationship have been used in the SR-site project. This preliminary result consists of a linear fit to all data excluding HLX28 (data from HLX28 was obtained at a late stage in the present compilation project). The result of this fit is also displayed in Figure 6-5 and it is seen that the fits with and without HLX28 data are very close to each other.

One might argue that estimates from equal dipole tracer tests should not be included in the data due to the lack of any simple equation to calculate mass balance for equal dipole tests, see Section 3.3.1. However, a closer examination of the few cases of equal dipole tests in Appendix 1, show that these tracer tests does not deviate from others in any major way. These equal dipole tests are therefore included in the analysis.

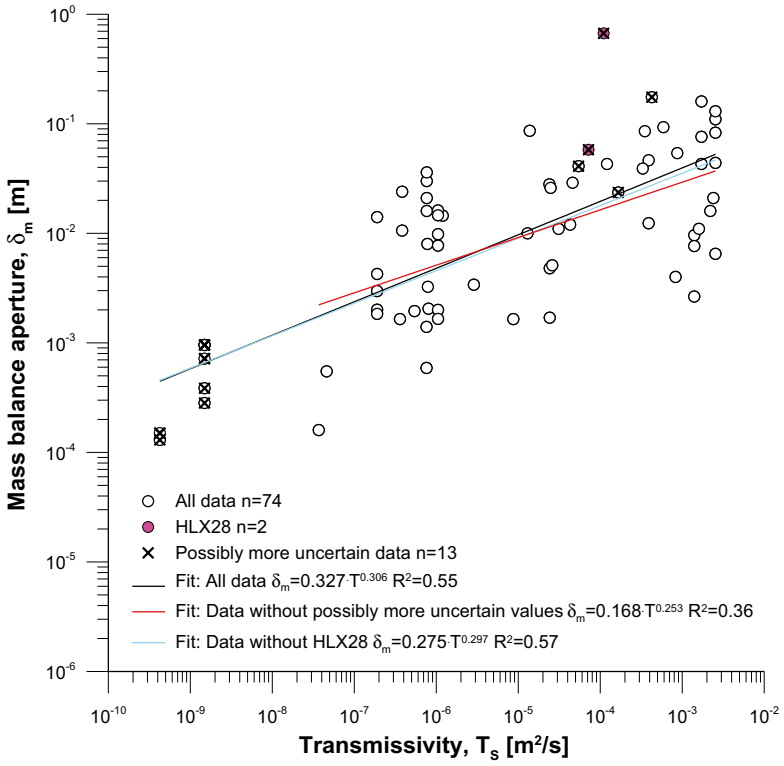

Figure 6-5. *Mass balance aperture vs. transmissivity for flow paths with indications of possibly more uncertain data.*

6.2.4 Tested formation

The data were categorised with respects to tested formation into three groups: fracture zone, single fracture and rock-soil aquifer. The latter includes two tests where both crystalline rock and quaternary deposits were involved in the tracer transport. For a majority of the tracer tests included in this study, it is mentioned in the reports if the feature tested is considered to be a fracture zone or a single fracture. In other cases, the classification was made based on the available description in the reports.

The definition of single fracture and fracture zone is ambiguous and may also have changed during the time period considered. Further, the term single fracture is not entirely accurate since some of the tests, for example at the TRUE Block Scale site in Äspö, are better described as a network of single fractures. However, these were still categorised as single fractures in this study.

In Figure 6-6, δ_m is plotted versus T_S and with data points categorised according to the type of test formation for the individual flow paths. The single fractures are generally displaying a lower T_S and δ_m than the fracture zones. This is not unexpected considering the differences in these two types of test formations. When fitting a straight line to the data it seems like the fit to the fracture zone data (red line) display a relationship similar to the fit to all data (black line). The fit to single fracture data (blue line) appears to have a slightly steeper slope than the other two.

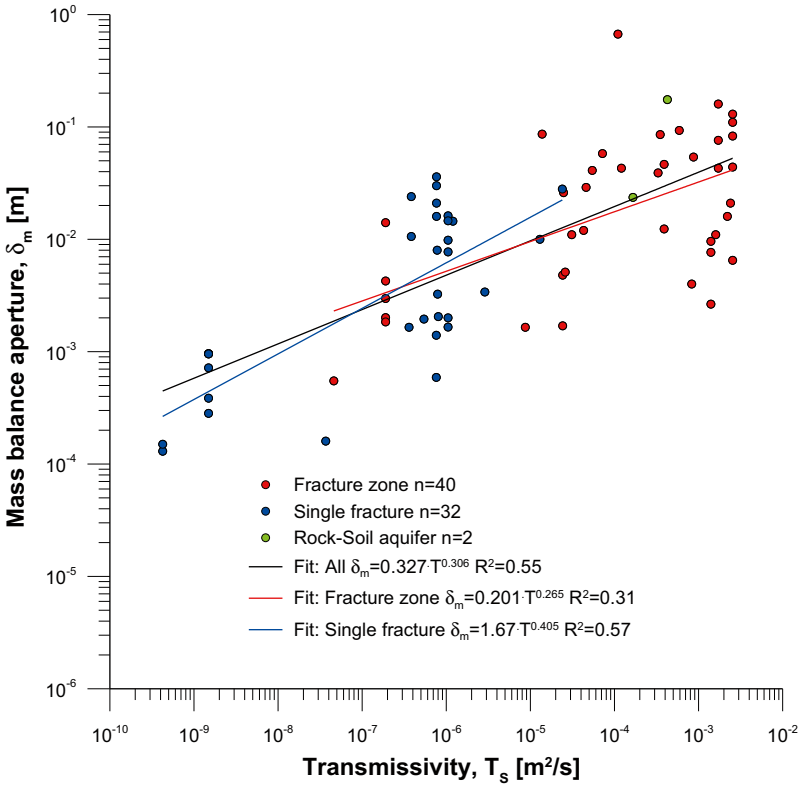

Figure 6-6. *Mass balance aperture vs. transmissivity for flow paths categorised based on the type of test formation.*

6.2.5 Test area and feature

Figure 6-7 shows the flow path data with indications of test area together with a power law fit. From the figure it is obvious that Finnsjön, Forsmark and Laxemar represent the upper end of the transmissivity range, while Äspö and Studsvik are in the middle and Stripa represents the lower end of the range.

Figure 6-8 shows the same data as Figure 6-7 but grouped by the tested feature instead of the test area. Some features are not given any specific names in the report, e.g. the tests in Laxemar. In these cases they are given names based on the boreholes or report name. In Figure 6-8 it is visible that the data for a specific feature generally has a rather limited range for T_S but more extended regarding δ_m. In some cases this is an effect of that only a single value of T_S is used for the entire feature. For example, for Feature #19 in TRUE Block Scale at Äspö, the same borehole section was used for pumping for all included tests and no values for T_C were found, making all flow paths for the feature in Figure 6-8 having the same T_S. In other cases, as for example Zone A2 in Forsmark with pumping in HFM14, individual values of T_C were available for all flow paths. However, in this case they were all rather similar making the range of T_S for that feature limited compared with the range of δ_m.

The difference ($\Delta\delta_m$) between δ_m from data and according to the presented fit was calculated according to Equation 6-1:

$$\Delta\delta_m = \log(\delta_{m,data}) - \log(\delta_{m,fit}) \qquad \text{Equation 6-1}$$

These differences are shown in Table 6-1 and may also be seen in Figure 6-7 and Figure 6-8 as the vertical distance from the data points to the fitting line. Additionally, $\Delta\delta_m$ is displayed in Figure 6-9. If it is assumed that the values of $\Delta\delta_m$ are normally distributed, it is possible to calculate the standard deviation which also is displayed in Figure 6-9.

In general, the data for the test areas are distributed rather evenly around the general fit. However, some interesting differences may be found in Figure 6-7 to Figure 6-9 and Table 6-1. For example, the data from Forsmark and Laxemar are generally situated above the fitting line, indicating that these areas have a rather large δ_m relative its T_S compared to the other data.

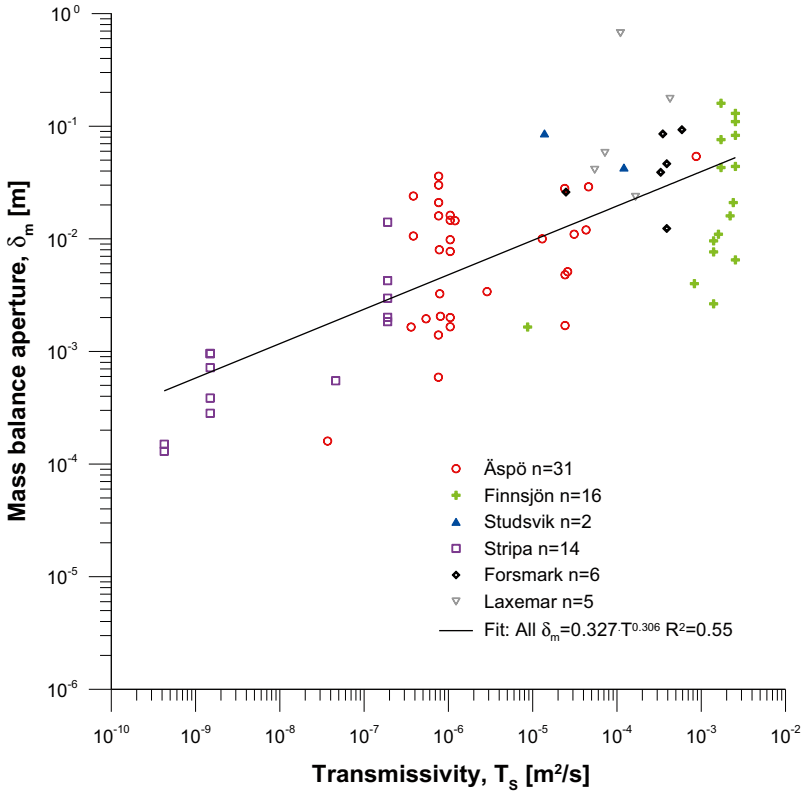

Figure 6-7. Mass balance aperture vs. transmissivity for flow paths with indications of test area.

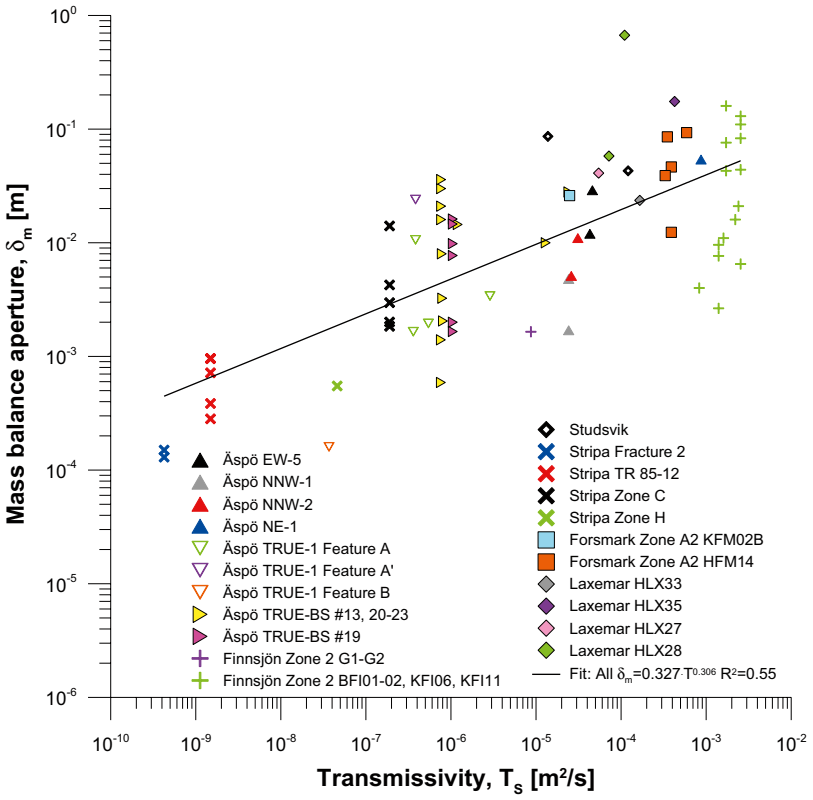

Figure 6-8. *Mass balance aperture vs. transmissivity for flow paths with indications of tested feature.*

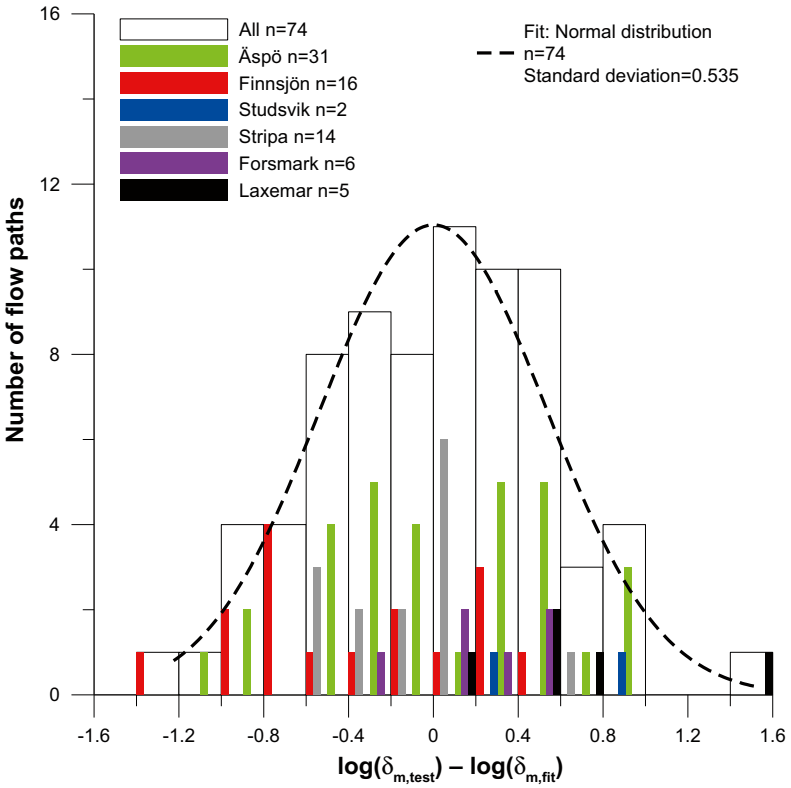

Figure 6-9. *Histogram of difference in mass balance aperture (δ_m) according to the fit in Figure 6-7 and evaluated for flow paths with indications of test area.*

Table 6-1. Statistics for the difference between δ_m from data and according to fit. Standard deviations are only presented for entire test areas.

			$\Delta\delta_m = \log(\delta_{m,data}) - \log(\delta_{m,fit})$				
Test area	**Feature**	**Number**	**Average**	**Median**	**Max**	**Min**	**stdev**
Äspö	EW-5	2	0.09	0.09	0.27	–0.10	
	NNW-1	2	–0.65	–0.65	–0.42	–0.87	
	NNW-2	2	–0.25	–0.25	–0.09	–0.41	
	NE-1	1	0.15	0.15	0.15	0.15	
	TRUE-1 Feature A	4	–0.11	–0.30	0.47	–0.33	
	TRUE-1 Feature A'	1	0.83	0.83	0.83	0.83	
	TRUE-1 Feature B	1	–1.04	–1.04	–1.04	–1.04	
	TRUE-BS #13, 20–23	12	0.18	0.30	0.91	–0.87	
	TRUE-BS #19	6	0.11	0.25	0.52	–0.47	
	Total	31	0.02	–0.02	0.91	–1.04	0.53
Finnsjön	Zone 2 G1–G2	1	–0.75	–0.75	–0.75	–0.75	
	Zone 2 BFI01–02, KFI06, KFI11	15	–0.30	–0.39	0.54	–1.22	
	Total	16	–0.33	–0.44	0.54	–1.22	0.55
Studsvik	Total	2	0.61	0.61	0.91	0.32	0.42
Stripa	Fracture 2	2	–0.50	–0.50	–0.47	–0.54	
	TR 85-12	6	–0.01	0.10	0.17	–0.37	
	Zone C	5	0.10	0.01	0.69	–0.20	
	Zone H	1	–0.53	–0.53	–0.53	–0.53	
	Total	14	–0.08	–0.07	0.69	–0.54	0.34
Forsmark	Zone A2 KFM02B	1	0.31	0.31	0.31	0.31	
	Zone A2 HFM14	5	0.17	0.20	0.47	–0.38	
	Total	6	0.20	0.25	0.47	–0.38	0.31
Laxemar	HLX33	1	0.01	0.01	0.01	0.01	
	HLX35	1	0.76	0.76	0.76	0.76	
	HLX27	1	0.40	0.40	0.40	0.40	
	HLX28	2	1.02	1.02	1.52	0.52	
	Total	5	0.64	0.52	1.52	0.01	0.56
Total		**74**	**0.00**	**0.03**	**1.52**	**–1.22**	**0.54**

6.3 Aperture – transmissivity

As mentioned earlier in this report, other types of apertures and relationships between aperture and transmissivity have been suggested earlier.

For 59 of the 74 flow paths selected for analyses, frictional loss aperture δ_l was possible to calculate. In Figure 6-10 these are plotted versus T_S together with the corresponding δ_m and fits to both data sets. Note that only the flow paths where δ_l was available are included in the figure. The same subset of flow paths are also used for δ_m in Figure 6-10, thus there are only 59 flow paths in the figure compared with 74 in, for example, Figure 6-7.

The fit in Figure 6-10 to data for δ_m is almost identical to the corresponding fit in previous figures, e.g. Figure 6-7. This indicates that the subset of flow paths used in Figure 6-10 does not significantly deviates from the total data set for all flow paths. Furthermore, it is evident that δ_l is much smaller than δ_m for all values of T_S.

In Figure 6-11 a number of suggested relationships between transmissivity and aperture are shown together with all available data for δ_m and δ_l for flow paths. Green and deep blue solid lines represents maximum values and green and deep blue dashed lines represents minimum values of δ_h and δ_t, respectively, from /Dershowitz et al. 2003/, /Dershowitz and Klise 2002/ and /Dershowitz et al. 2002/ according to Section 3.3.4.

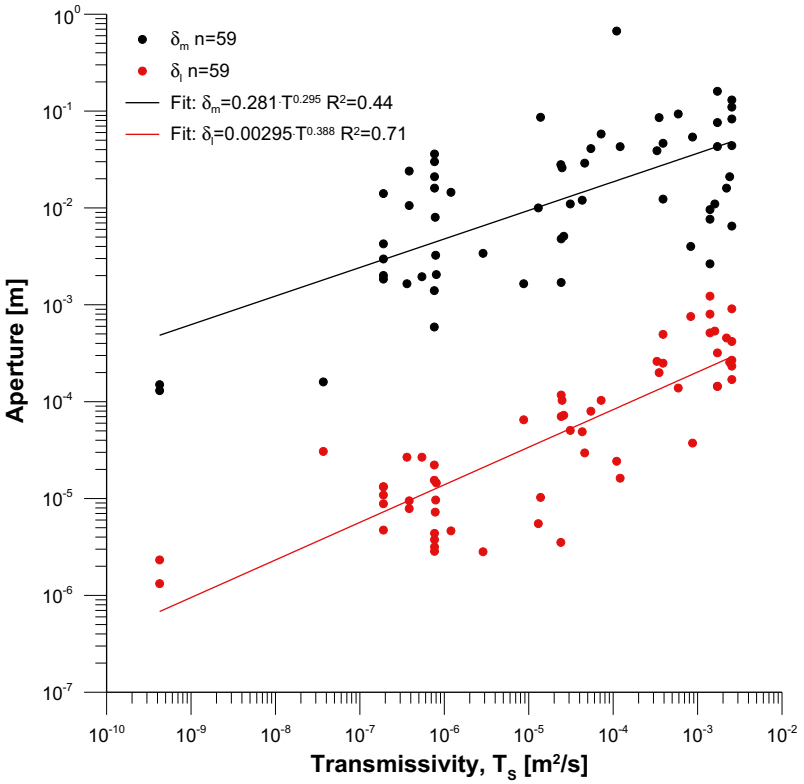

Figure 6-10. *Frictional loss aperture (δ_l) and mass balance aperture (δ_m) vs. transmissivity for flow paths where frictional loss aperture is available.*

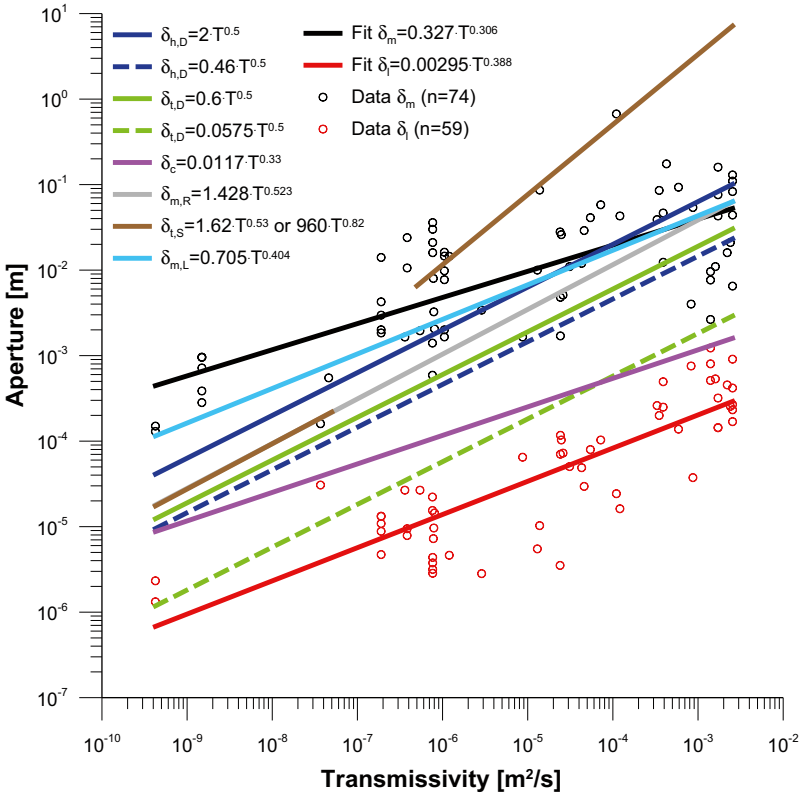

Figure 6-11. *Relationships between aperture and transmissivity for mass balance aperture (δ_m), frictional loss aperture (δ_l), hydraulic aperture (δ_h), transport aperture (δ_t) and cubic law aperture (δ_c) together with data for δ_m and δ_l.*

6.4 Mass balance aperture – hydraulic diffusivity

As mentioned in Section 3.2.2, hydraulic diffusivity, T_o/S_o, is related to the pressure response time, often considered to be the most reliable parameter evaluated from a hydraulic interference test. However, the relationship between hydraulic diffusivity and mass balance aperture is very poor as seen in Figure 6-12. Note that there are fewer data points in Figure 6-12 than in for example Figure 6-7 since hydraulic diffusivity data only were available for some of the flow paths. However, due to the poor relationship in Figure 6-12 it is not expected that any clear relationship between mass balance aperture and hydraulic diffusivity would be found even with more data available. In Figure 6-13, the two components of hydraulic diffusivity, apparent storativity and transmissivity, are plotted against each other. For most data in Figure 6-13, T_o equals T_S as used in e.g. Figure 6-8. The exceptions are T_o for the TRUE-1 data where the estimates of T_S also, besides the estimate of T_o, includes stationary estimates of T from interference tests.

Still, it may not be excluded that there exists some kind of relationship between hydraulic diffusivity and mass balance aperture. One alternative could be to look at pressure response time, dt_L (related to hydraulic diffusivity, see Section 3.2.2) and mean residence time, t_m (basis for mass balance aperture, see Section 3.3.1). However, pressure response time was only reported for a few of the tests included in this report. Besides, for most tests dt_L were given when a pressure response, dp, of 0.1 m was registered while other tests uses a dp of 0.02 m. Hence, the comparison of dt_L and t_m has to be regarded as more uncertain than others in this report. Still, the plot in Figure 6-14 shows that there might be a relationship between dt_L and t_m, suggesting that some kind of relationship also may exist between hydraulic diffusivity and mass balance aperture.

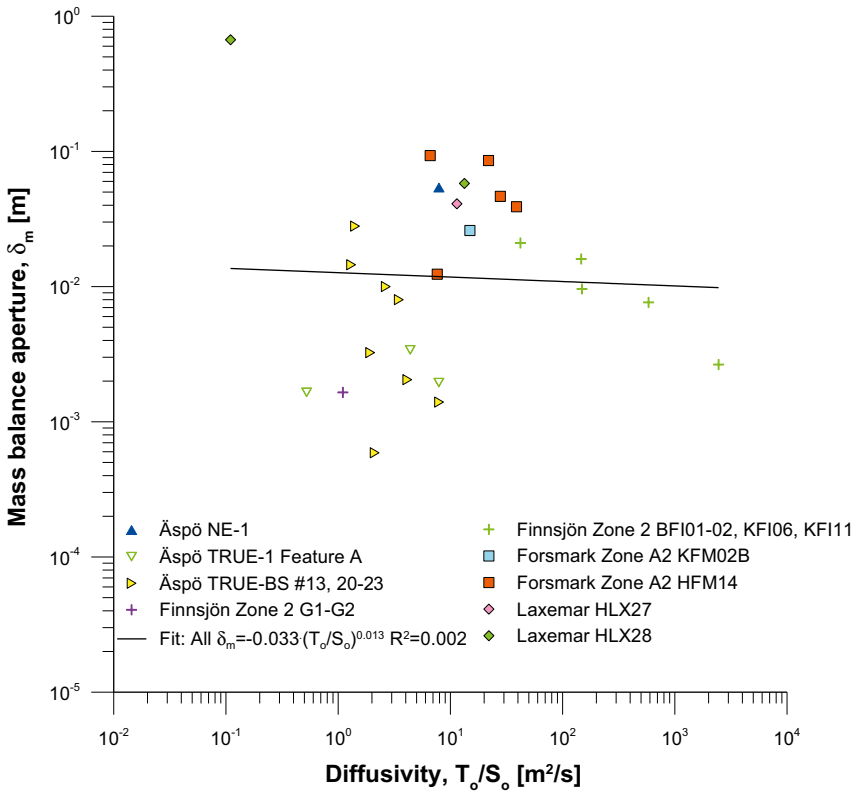

Figure 6-12. *Mass balance aperture vs. hydraulic diffusivity for flow paths with indications of tested feature.*

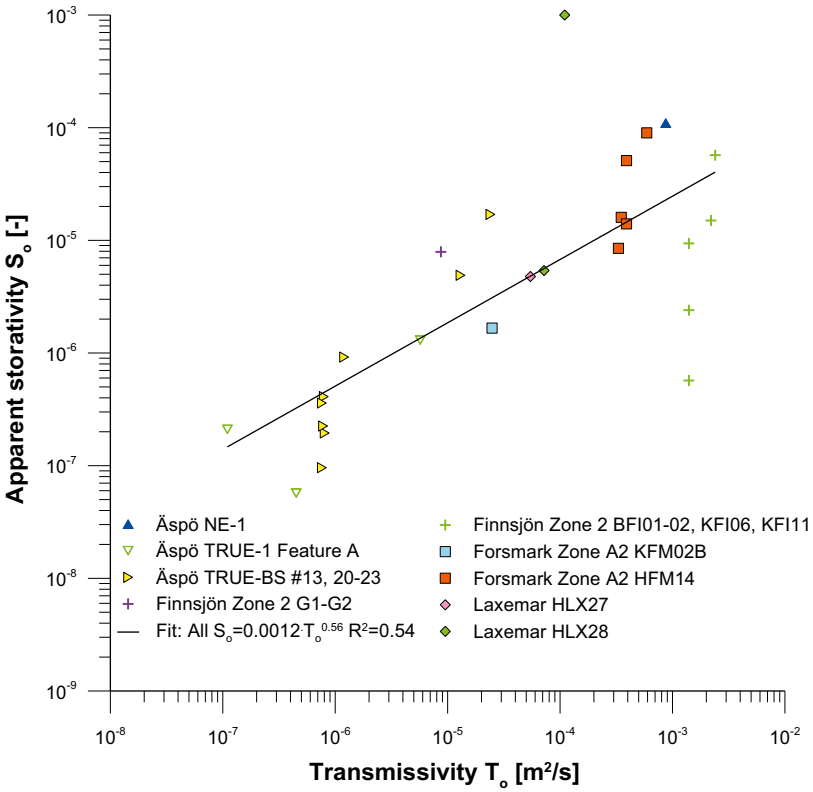

Figure 6-13. *Apparent storativity, S_o, vs transmissivity evaluated from interference test, T_o.*

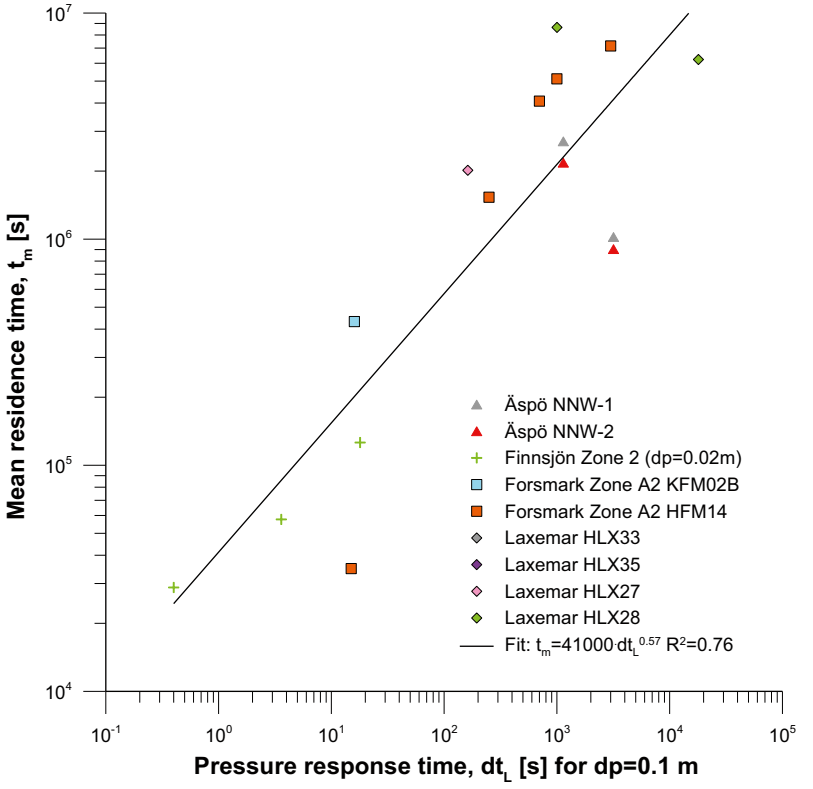

Figure 6-14. *Mean residence time vs. pressure response time. If nothing else given the pressure response time is given for dp=0.1 m.*

6.5 Mass balance aperture – apparent storativity

For 28 of the flow paths a value for storativity, S_o, was found during the collection of data. As discussed in Section 3.2.2, storativity evaluated from hydraulic interference tests may not be a good estimate of the true storativity of the system. Storativity evaluated from hydraulic interference tests, S_o, is therefore referred to as apparent storativity in this report. In Figure 6-15 the mass balance aperture is plotted versus apparent storativity along with a linear fit to the data. For comparison, Figure 6-16 show the transmissivity values for the same flow paths together with a fit to the data in the figure (black line) and, as a reference, the fit to all transmissivity data (red line) as for example shown in Figure 6-7. As seen in Figure 6-16, the fit to the data is rather close to the overall fit shown as reference in the figure. Hence, there are no indications that the subset of flow paths where values of S_o are available would deviate considerably from the entire data set of flow paths used in this study.

The data in Figure 6-15 is in general rather close to the linear fit in the figure. However, the data from Finnsjön zone 2 G2–G1 and Stripa zone H deviates considerably. Some interesting differences may be observed between Figure 6-15 and Figure 6-16. For the flow paths to HLX28 in Laxemar with a very large value of δ_m, the data point is rather close to the linear fit in Figure 6-15 while it deviates considerably in Figure 6-16. This is also one of the flow paths where the assumption of a straight line distance from the injection point to the pumping section is regarded to be far from true, see Section 6.2.3. For a specific feature it seems like the range of S_o is relatively large compare to the range of T. This is particularly noticeable for Finnsjön Zone 2 (BFI01–02, KFI06, KFI11), where S_o ranges from $5.7 \cdot 10^{-7}$ to $5.7 \cdot 10^{-5}$ while T_s ranges from $1.4 \cdot 10^{-3}$ to $2.4 \cdot 10^{-3}$ m^2/s, and Forsmark zone A2 (HFM14), where S_o ranges from $8.5 \cdot 10^{-6}$ to $9.0 \cdot 10^{-5}$ and T_s ranges from $3.3 \cdot 10^{-4}$ to $5.9 \cdot 10^{-4}$ m^2/s.. A conclusion may then be that apparent storativity responds better than transmissivity to the heterogeneity of the fracture system as indicated by mass balance aperture. However, as discussed in Section 3.2.2, the apparent storativity actually is transmissivity divided by diffusivity. Additionally, T_o tends to be relatively homogeneous for an individual interference test since the same pumping flow rate is used for all observation sections. Considering this, the observations above could then be viewed as an indication that there exists a correlation between hydraulic diffusivity and mass balance aperture, although not as straight-forward as in the case of transmissivity.

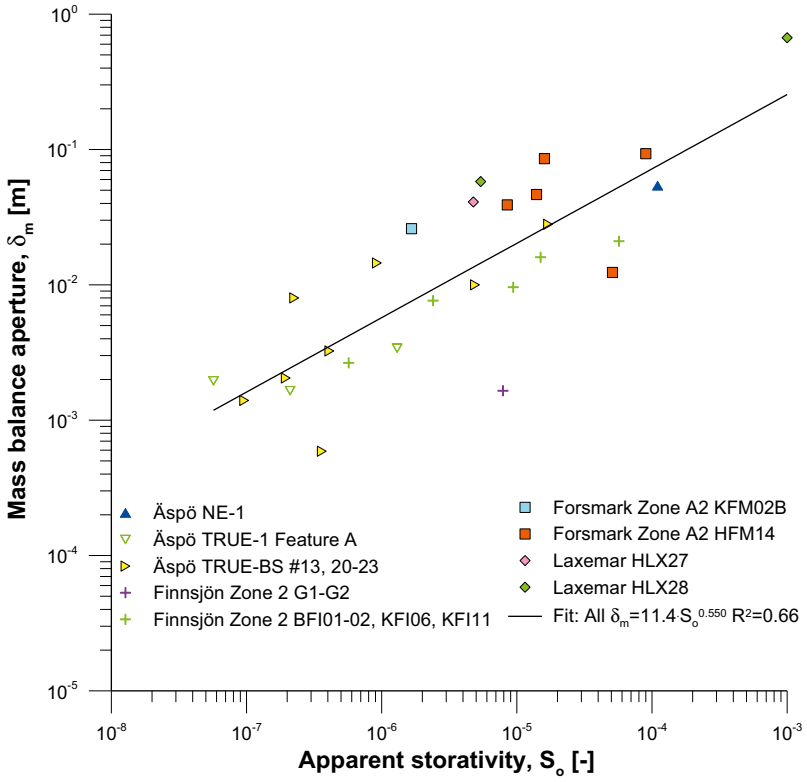

Figure 6-15. *Mass balance aperture vs. apparent storativity for flow paths with indications of tested feature.*

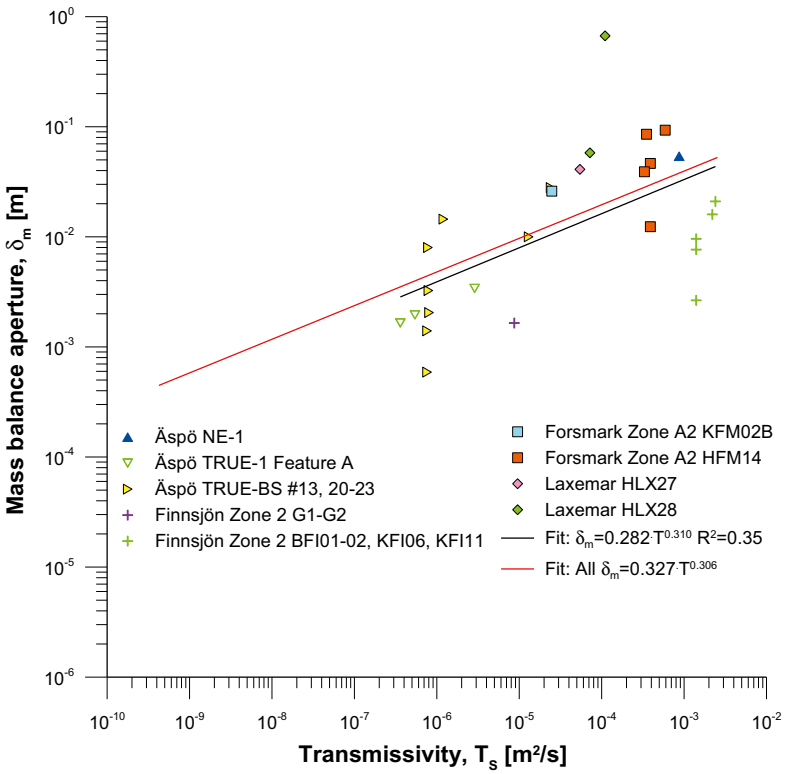

Figure 6-16. *Mass balance aperture vs. transmissivity for flow paths where also apparent storativity is available with indications of tested feature.*

6.6 Dispersivity

For 67 of the 74 flow paths at least one estimate of dispersivity is reported. Dispersivity is in this report only discussed in terms of Peclet number, Pe [–], according to Equation 3-23. As stated in Section 3.4.1, the use of a 1-D model in combination with high dispersivity, i.e low Pe, may introduce additional uncertainties about other evaluated transport parameters, such as mass balance aperture. However, mass balance aperture versus transmissivity including indication of Pe is shown in Figure 6-17 and from that plot it is very hard to detect any tendencies that flow paths with Pe within a certain interval would be clustered in any specific part of the plot. Instead, the position of the data relative the fitting line in the plot, i.e. above or below, does not seem to depend solely on the Peclet number.

Values of Pe are plotted against T, with indications of type of test formation, in Figure 6-18. The figure also includes a power law fit. As seen in the figure, there is a weak tendency for higher Pe with higher T. In Figure 6-19, Pe are plotted against travel distance, r_d. In both Figure 6-18 and Figure 6-19 the data points are rather scattered and the relationships are very weak. In Figure 6-20 longitudinal dispersivity are plotted against travel distance together with a power law fit to the data. Additionally, a fit to other data presented by /Neuman et al. 1990/ is also displayed in Figure 6-20.

Since the relationships in Figure 6-18 and Figure 6-19 are very weak, it is not particularly interesting to analyse the difference between the Pe data and respective fit. Instead, the overall distribution of Pe could be of interest as a basis for predictive transport modelling. As seen in Figure 6-21, a log-normal distribution of Pe seems rather reasonable, although the fit is not perfect. The fit displayed in Figure 6-21 corresponds to Pe with an average of 7.9 and a range from 2.5 to 25 for one standard deviation.

The difference ($\Delta\alpha_L$) between α_L from data and according to the presented fit in Figure 6-20 was calculated according to Equation 6-2:

$$\Delta\delta_m = \log(\delta_{m,data}) - \log(\delta_{m,fit}) \qquad \text{Equation 6-2}$$

These differences may be seen in Figure 6-20 as the vertical distance from the data points to the fitting line. Additionally, $\Delta\alpha_L$ is displayed in Figure 6-22. If it is assumed that the values of $\Delta\alpha_L$ are normally distributed, it is possible to calculate the standard deviation which also is displayed in Figure 6-22.

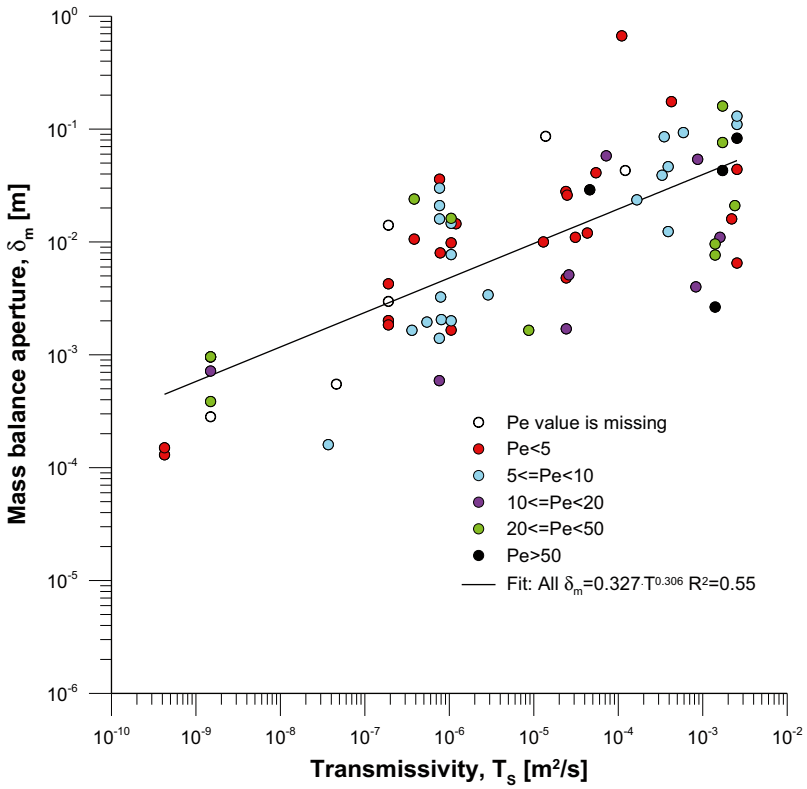

Figure 6-17. *Mass balance aperture vs. transmissivity for flow paths with indication of Peclet number, Pe.*

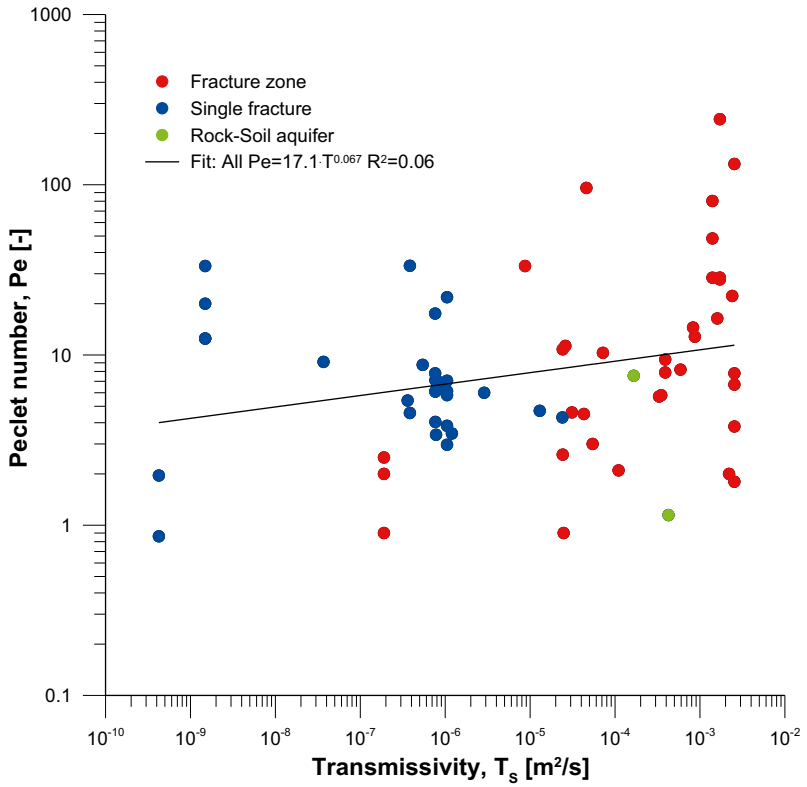

Figure 6-18*. Peclet number vs. transmissivity for flow paths with indications of type of test formation.*

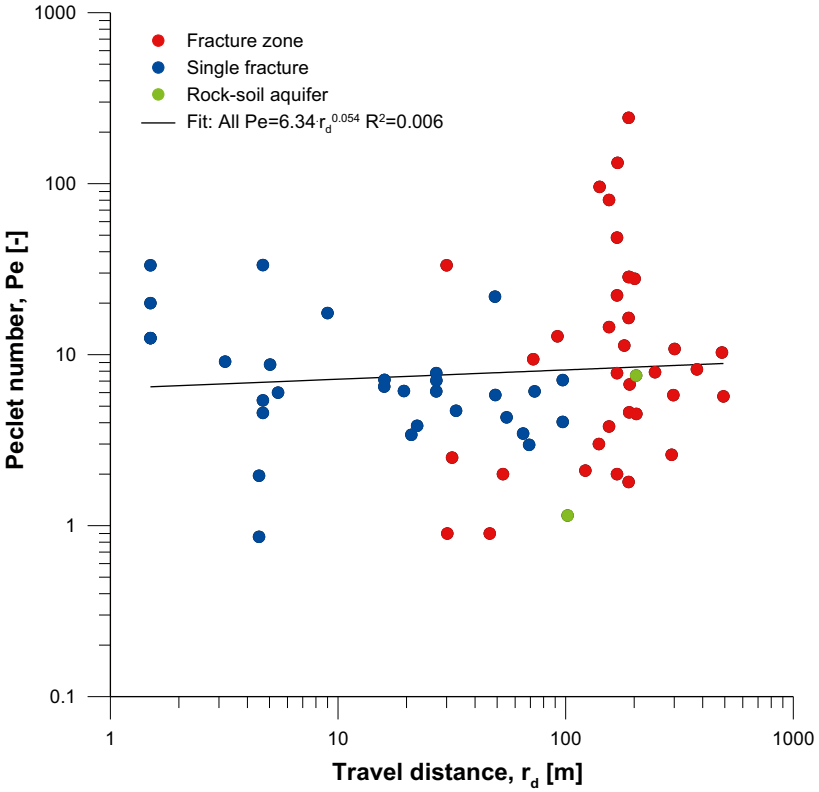

Figure 6-19. *Peclet number vs. travel distance for flow paths with indications of type of test formation.*

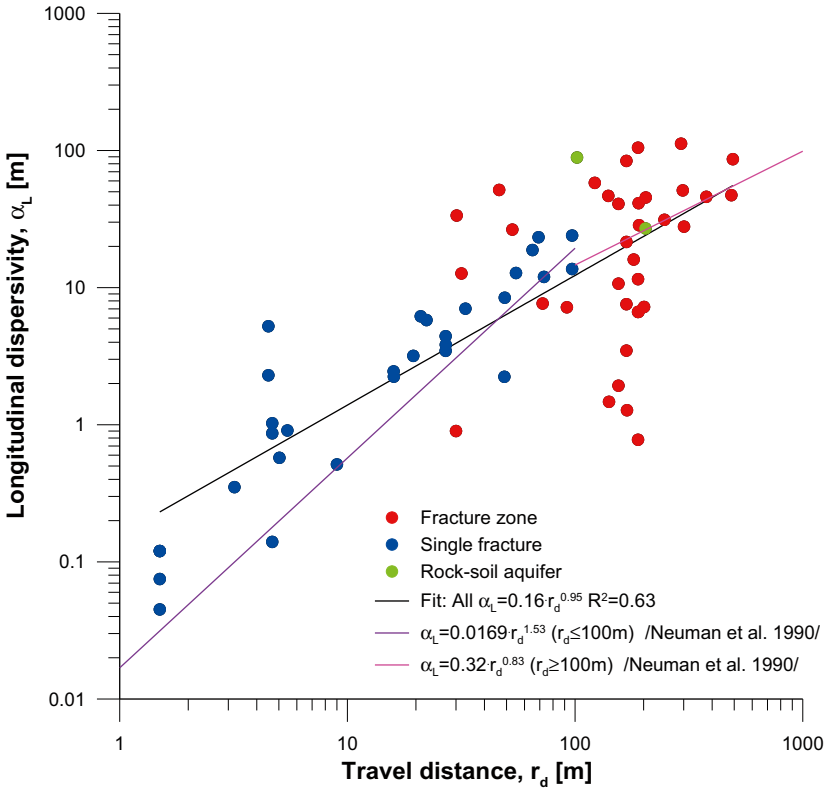

Figure 6-20. *Longitudinal dispersivity vs. travel distance for flow paths with indications of type of test formation.*

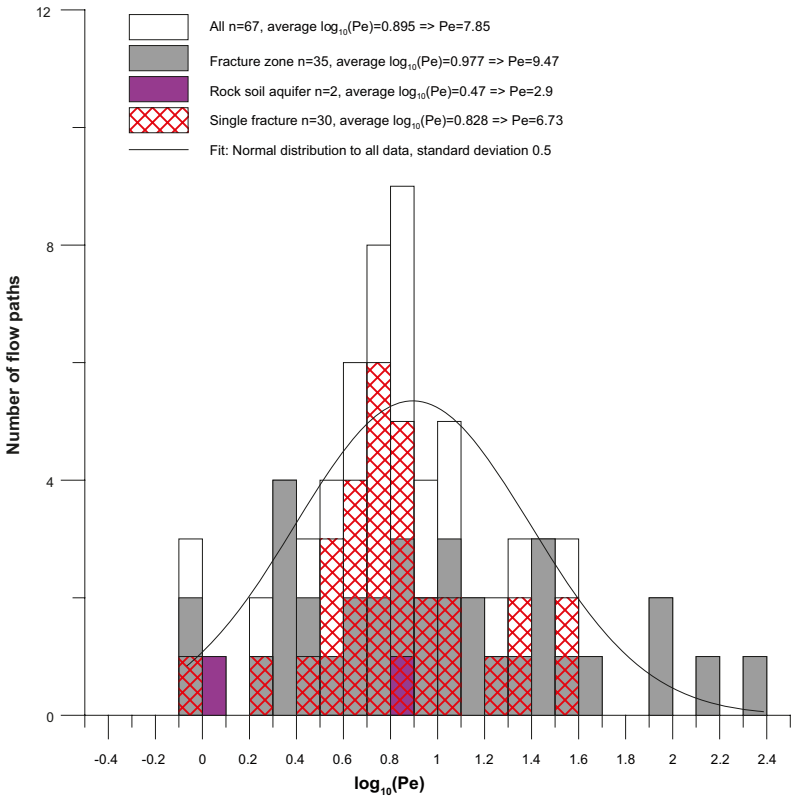

Figure 6-21. *Histogram over Peclet number for flow paths.*

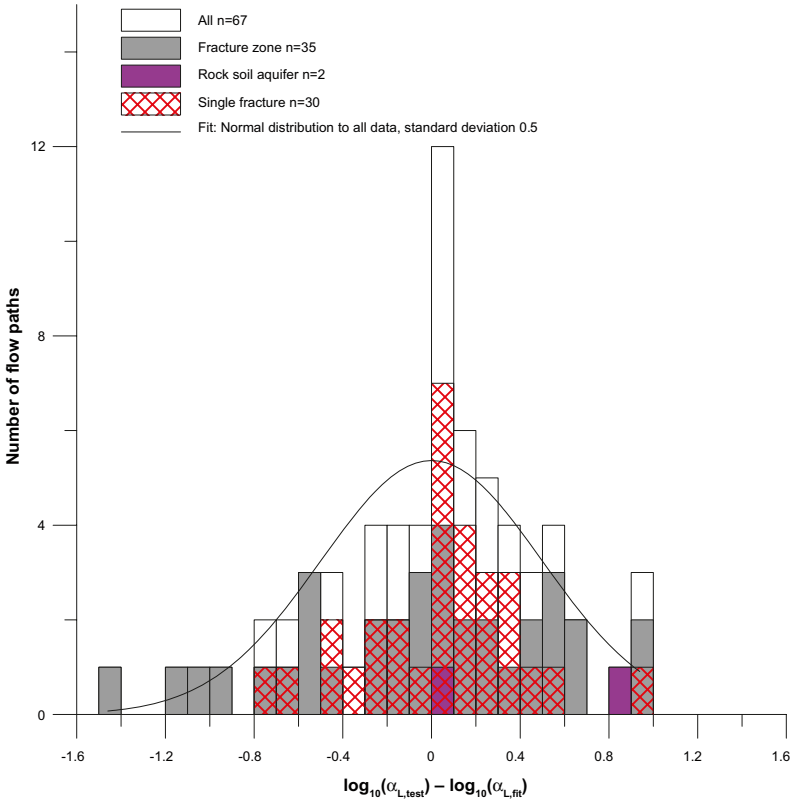

Figure 6-22. *Histogram of difference in longitudinal dispersivity (α_L) according to the fit in Figure 6-20 and evaluated for flow paths.*

7 Discussion and conclusions

7.1 Discussion

First of all, when discussing the results of this study, it is important to keep in mind that the flow paths used for tracer tests are not randomly chosen. On the contrary, in many cases the selection process prior to the tracer test has been rigorous in forms of hydraulic testing, dilution measurements and geological characterisation in order to choose flow paths where it is likely to observe tracer breakthrough within a reasonable time span.

Additionally, tracer tests where no tracer breakthrough was observed were not included in this study for the simple reason that no estimates of mass balance aperture are reported. In some cases, a tracer breakthrough may have been possible if only the test time would have been longer. In such cases, further on referred to as *absent tests*, when the mean residence time was unexpectedly long, it is likely that the actual value of δ_m would be larger than the average considering the transmissivity, i.e. be present above the fitting line in for example Figure 6-7. Hence, there is probably a built in bias that is impossible to avoid in the analysis of tracer test results towards lower values of δ_m. It is difficult to establish what effect this probable bias would have on the fit in for example Figure 6-7 depending on if the absent tests are concentrated to one part of the range of spread over the entire range. If the absent test results are concentrated to high transmissivity tests, the slope of the fit would probably be steeper without the probable bias so that there would be a higher estimate for mass balance aperture for high transmissivity feature while it would be more or less unchanged for low transmissivity features. If the absent test results would be evenly distributed over the entire range of transmissivity, higher value of the aperture over the entire transmissivity range would be expected compared with data shown in this study.

Another uncertainty and possible bias in the data is due to the assumption that mean residence time for 2-D radial case is approximately the same as the mean residence time from the 1-D model used for evaluation of the tracer breakthrough curves. However, as discussed in Section 3.4.1, the evaluated mean residence time with 1-D models may be both shorter and longer than the true mean residence time in a 2-D case depending on several factors. It is therefore not likely that the use of 1-D evaluation models causes any systematic bias towards smaller or larger mass balance apertures.

An additional source of systematic bias when comparing the evaluated mass balance aperture with a true mean aperture of the flow path is the assumption of the straight line distance between the injection and withdrawal point as discussed in Section 4. The travel distance may be significantly longer than the straight line distance for a number of reasons, e.g. if the injection is made in some other fracture plane than the pumping takes place, if the flow in the fracture mainly takes place in winding channels or if a low transmissivity region is present in between the injection and pumping points. Regardless of reason why the travel distance is significantly longer than the straight line distance, the evaluated mass balance aperture would be larger than the true mean aperture of the flow path.

Due to the unavoidable bias and uncertainty in the data it is difficult to establish that the conclusions of this study is valid generally for fractured rock within the geographical area study or even the sites used for tracer tests.

7.1.1 Mass balance aperture – transmissivity

The selection of transmissivity values may of course also affect the overall analysis results. This is most evident when considering Figure 5-1 where median of the transmissivity values for the different categories are displayed. An alternative to selecting the median value would be to actively select representative values for each flow path. However, due to the many different hydraulic test and evaluation methods used it would require a large effort.

Furthermore, transmissivity values from hydraulic interference tests, T_C, were prioritised in the analysis. The second choice was transmissivity values from single-hole tests in the tracer withdrawal section, T_W. Values from single-hole tests in the tracer injection section, T_I, were only used if the two other were missing. The basic reason for prioritizing T_C is that T_C is the only transmissivity value evaluated

where effects of both the pumping (flow rate) and observation hole (pressure response) are taken into account. One may argue that T_C could be a very uncertain estimate for the flow path if the connection between the two holes and the flow path considered to be tested is poor. However, in the cases considered in this report, where a relatively good tracer recovery has been achieved between the observations and pumping boreholes, the risk of a poor connection between the tested borehole sections has to be considered as low. The prioritizing of T_W over T_I was strictly based on that previous experiences and Figure 5-1 show that T_C often is more closely correlated to T_W than T_I.

One may argue that the correlation analysis involving transmissivity values should be carried out with transmissivity data from one type of evaluation at a time and not grouped together as done in this study. These analyses would then include a smaller data set than used in this study, which would reduce the possibility of indentifying potential dependence of aperture and transmissivity. Besides, Figure 6-2 and Figure 6-3 indicates that the overall correlation between δ_m and T was not significantly different if carried out with T_C or T_W as the prioritized transmissivity category, making it rather reasonable to group all tests together.

In general, the data was analysed on the level of flow paths. An alternative could be to make the analyses on the level of tracer tests or features. The reasons for choosing the level of flow paths is that analyses based on tracer tests includes a bias for flow paths tested multiple times and analyses based on features does not account for heterogeneity in the features. Besides, Figure 6-1 do not display any significant differences in the correlation analysis of δ_m and T, making this choice probably not so crucial for the overall results in this study. The chosen level of data for analysis, flow paths, seems rather reasonable.

It is difficult to calculate the uncertainty of a single value of δ_m from evaluation of tracer tests. This is due to uncertainty in the many parts involved in the evaluation such as chemical tracer analysis, model fit to the data, approximation of radial flow field etc. This is probably why estimates of uncertainty in δ_m rarely are reported. Still, some reports included in this study have pointed to some factors making the tracer test evaluation possibly more uncertain than usual. Besides, for some tests, it was known that the injection and withdrawal points were located in different features, making the assumption of radial flow and straight line transport distance rather unreasonable. However, exclusion of these data has a very small effect on the overall correlation between δ_m and T as seen in Figure 6-5. Due to this, and since other data also include varying degrees of uncertainty, it was decided to not exclude the flow paths where the data was identified as possibly more uncertain.

The relationship between δ_m and T was analysed on the basis of type of test formation, i.e. single fracture, fracture zone and rock-soil aquifer. The latter only included two data points. Figure 6-6 indicates a slightly different relationship between δ_m and T for fracture zones compared to single fractures. However, the single fracture data is concentrated to the centre of the data range with a few data close to the range end points. This makes the fit sensitive to the data points with low and high values. Due to the sensitivity of the fit to the single fracture data and some uncertainties about the classifications of the data into fracture zone and single fracture, it is difficult to establish whether there exists any difference between fracture zones and single fractures regarding the relationship between δ_m and T.

Correlation between δ_m and T was also analysed regarding test site and feature. Some observations may be made, for example that data for Forsmark and Laxemar generally displays larger δ_m relative their reported values of T than the overall correlation between δ_m and T. However, the number of values for each test site and feature is rather limited making any definite conclusions about specific test area or feature difficult. Instead, these observations may be regarded as tendencies.

The distribution of logarithmic residuals between data and the general fit to the data of δ_m versus T, $\Delta\delta_m$, may be regarded as approximately normally distributed as seen on Figure 6-8. The standard deviation of $\Delta\delta_m$ (based on log10 δ_m) is then close to 0.5.

7.1.2 Aperture – transmissivity

The correlation between δ_m and T may be compared with other suggested relationships between aperture and T. In Figure 6-10 it is clear that δ_m is larger than the frictional loss aperture, δ_l. Furthermore, the cubic law aperture, δ_c, is larger than δ_l but smaller than δ_m as seen in Figure 6-11. This is consistent with /Tsang 1992/.

In Figure 6-11 it is evident that the relationship between δ_m and T is quite different from most other relationships between δ and T. In general, they differ both in slope and offset, constant b_x and a_x, respectively in Equation 3-15.

Regarding δ_m contra $\delta_{t,D}$, δ_m is larger than δ_t for the same value of T except for the highest values of T. The difference in slope is not unexpected since the constant b_m (0.3) is evaluated empirically based on tracer and hydraulic tests while the constant b_t (0.5) is based on a theoretical derivation of the relationship between transmissivity and storage based on a pipe flow according to /Uchida et al. 1994/: When considering pipe flow, the conductance changes by the fourth power of radius while the storage of the pipe changes by a second power of radius. Hence, the storage, i.e. aperture in a channel, should vary with the square root of transmissivity.

The evaluation of the relationship between $\delta_{t,D}$ and T as reported in this study was based on tracer test data from TRUE-BS as performed by /Dershowitz and Klise 2002/, /Dershowitz et al. 2002/ and /Dershowitz et al. 2003/. The transmissivities of TRUE-BS are c 10^{-6}, see Figure 6-8. In this interval of transmissivity the value of δ_m is significantly larger than $\delta_{t,D}$. This indicates that the differences in methods and geometrical assumption when evaluating δ_m and $\delta_{t,D}$ has a significant effect on the results.

Also the relationships $\delta_{t,S}$, $\delta_{m,R}$ and $\delta_{m,L}$ versus T display a higher slope than the relationship between δ_m and T. Regarding $\delta_{m,R}$ and $\delta_{m,L}$ contra T, which basically have been estimated in the same manner as δ_m contra T, this may be a result of the differences in data. For $\delta_{m,R}$ the data are partly not the same and only 11 data points were used, which is much less than the 74 data points used for δ_m. The same applies for $\delta_{m,L}$ where 9 data points were used. Still, $\delta_{m,R}$ and $\delta_{m,L}$ are rather close to δ_m in comparison with other estimates of δ, especially for high values of T. The lower section of $\delta_{t,S}$ ($T < 5 \cdot 10^{-8}$ m^2/s) was based on the relationship from /Rhén et al. 1997/ according to /Vidstrand P 2009, pers. comm./ so it is very close to $\delta_{m,R}$.

The upper section of $\delta_{t,S}$ ($T > 5 \cdot 10^{-7}$ m^2/s) deviates considerably from δ_m. The relationship was also evaluated by using a general relationship between structure length and width as well as transmissisivity and by assigning what was thought to be reasonable values of porosity according to /Svensson U et al. 2008/ and / Vidstrand P 2009, pers. comm./.

It is not the intention to determine which of the different aperture concepts that is best and should be used for calculations. This may not even be possible, as it in some situations may be preferable to use δ_m and in other to use $\delta_{t,D}$ or $\delta_{t,S}$, depending on the specific situation and available information about the system. However, δ_m, as presented in this report has a rather good support in the data compared to the other, although uncertainty exists for some of the data.

The differences between δ_m and $\delta_{t,D}$ may to a large extent be explained by differences in the assumed geometry in the evaluation. As stated in Section 3.3.1, δ_m assumes a homogenous radial flow field, which of course is a major simplification. Furthermore, in most cases, the travel distance for the tracer is assumed to be equal to the straight line distance between the tracer injection and the withdrawal point. This simplification may in some cases, e.g. Feature A in TRUE-1, be rather good while it in other cases may be far from true and will in these cases result in an evaluated mass balance aperture larger than the true mean aperture of the flow path, as discussed above. On the other hand, evaluation of δ_m is rather simple and robust as it does not require any extensive information about the site.

The evaluation of $\delta_{t,D}$ is briefly explained in Section 3.3.5. This type of modelling does not assume homogenous conditions and straight line tracer transport, so it may be considered a more realistic evaluation. However, the complexity of the modelling introduces other types of assumptions and uncertainties that may affect the evaluation of $\delta_{t,D}$. For example, the channels are assigned a width, based on the length of the fracture intersections, which together with $\delta_{t,D}$ makes up the transport volume in a channel. So a different assumption about the correlation between channel width and the length of the fracture intersections changes $\delta_{t,D}$. Additionally, assumptions about the fracture network made in the modelling may also have a profound effect on the simulated flow field and thereby also affect the evaluation of $\delta_{t,D}$. One may conclude that δ_m and $\delta_{t,D}$ are very different regarding several aspects and it is therefore of limited use to compare the two other than briefly.

7.1.3 Mass balance aperture – hydraulic diffusivity – apparent storativity

The number of available estimates of hydraulic diffusivity was much lower than transmissivity values for the tests considered in this report. Still, the data available was considered enough to establish that no direct and simple correlation between mass balance aperture and hydraulic diffusivity is visible as displayed in Figure 6-12. This said, it may not be excluded that some alteration and/or normalisation of the data using other parameter such as distance etc, may provide a good indirect relationship between mass balance aperture and hydraulic diffusivity. One example of this may be Figure 6-14, where indications of a relationship between mean residence time (included in calculation of δ_m) and pressure response time (related to hydraulic diffusivity) may be found. However, it should be pointed out that the amount of data in this comparison is rather low.

Apparent storativity, S_o, may also be viewed as a variable dependent of hydraulic diffusivity, since it actually is transmissivity, T_o, divided by hydraulic diffusivity. As shown in Section 6.5, S_o seems to, in a better way then T_o, reflect the heterogeneity of the mass balance aperture in a tested system and also in general display a relatively good relationship with mass balance aperture. Hence, this may also be considered as an indication that there exists a correlation between hydraulic diffusivity and mass balance aperture, although not as straight-forward as in the case of transmissivity.

7.1.4 Dispersivity

No well established correlation between dispersivity in term of Peclet number, Pe, and transmissivity or travel distance could be found. In addition, no obvious correlation between Pe and deviation from the mass balance aperture and transmissivity correlation was found.

A log normal distribution of Pe seems to be quite reasonable when considering Figure 6-21, with $\log_{10}$(Pe) average of 0.895 and one standard deviation of 0.5. This corresponds to a Pe average of 8 and a range from 2.5 to 25, which could be quite reasonable to use for scoping calculation purposes. The fracture zones are much more frequent when considering large values of Pe than single fractures. This may, however, depend on a few tracer test evaluations with poor fit to the data or in other ways deviating from the majority of the test.

When plotting longitudinal dispersivity against travel distance a positive correlation was found. A power law fit to the data is quite close to a similar fit to other data as presented by /Neuman et al. 1990/. The distribution of logarithmic residuals between the data and fit in Figure 6-20 may be regarded as approximately normally distributed as seen in Figure 6-22 with a standard deviation of 0.5.

7.1.5 Suggestions for future tracer tests

During this study it was found that some aspects of reporting and evaluation of tracer test may be improved to facilitate the overall interpretation of tracer tests and to improve the usefulness of tracer test results for predictive modelling:

- The conceptual model of the geometry of the features tested should be clearly described.
- Evaluate and report hydraulic parameters from tracer test, e.g. transmissivity, diffusivity, storativity and time lag etc in a comprehensive manner.
- In order to compare tracer test parameter with hydraulic parameters it is important that they reflect the same feature. For example, if the tracer test is evaluated assuming three pathways for a breakthrough curve it may not be relevant to compare an individual pathway with hydraulic parameters for the whole section since they do not reflect the same feature. Ideally, the tracer test should be evaluated using one flow path or the evaluation should include a summation of multiple pathways which then could be compared to hydraulic parameters for the entire feature.
- For tests where no tracer breakthrough is observed it would be valuable for future compilations and evaluations like this to estimate a minimum value of δ_m.
- Report hydraulic parameters available from earlier tests for the tested feature, both injection and withdrawal borehole sections, or give clear references to such reports.
- In the SKB data base Sicada there is a column for evaluated flow path. However, as pointed out above, pathways are important especially when compared with hydraulic information. Therefore it would be preferable to give pathways in the data base out of total number of pathways. For example pathway 1 of 3, 2 of 3, 3 of 3, 1of 1.

- In the Sicada data base, there is column for the project name for identification purposes. However, in some projects, e.g. TRUE-1 and TRUE-BS, multiple tracer tests have been performed in identical flow paths. In reports, the tracer tests are often given common names, e.g. STT-2 in TRUE-1. For identification purposes in Sicada it would therefore be convenient with an additional column for the common name of the tracer test.

7.1.6 Suggested complementary study

The differences between δ_m and $\delta_{t,D}$ are discussed in Section 7.1.2 above. The conclusion is that a major part of the differences may depend on different geometrical configurations and assumptions when evaluating the two definitions of aperture. In order to further investigate this and to evaluate the effect of the assumptions of a radially homogenous flow field for calculating δ_m a complementary study is suggested.

This study should initially be carried out as a literature search in order to find any previous work that investigates this issue. If no previous studies are found that fully explain the effect of the assumptions of a radial homogenous flow field for calculating δ_m, it is suggested that the study continues with simulations of tracer transport in simple generic fracture systems. For example, simulation of tracer transport in a 2-D fracture where one half has a lower transmissivity than the other half in order to investigate the assumption of homogeneity. Another example may be tracer transport in a 2-D homogenous fracture intersected in the transport path by another homogenous fracture with similar transmissivity with the purpose of investigate the assumption of a radial flow field. A third example could be simulation of tracer transport where the injection point and withdrawal point is not located in the same fracture. It is beneficial in this suggested study to initially keep the complexity in the model to a minimum in order to facilitate conclusions. A natural second step in the simulations is to use stochastic heterogeneity and/or assumptions of a channel width in order to make the models more realistic than in the examples above. The simulation results should then be compared to the calculation of δ_m according to Equation 3-6.

A possible expansion of the study could be to simulate real tracer tests where it may be suspected that the assumption of homogenous converging radial flow field is unrealistic. One example is the tracer test in Zone A2 in Forsmark between KFM02A and KFM02B as reported by /Lindquist et al. 2008a/. This is interesting since the borehole section in KFM02B displayed a significantly higher transmissivity than in KFM02A. This tracer test was performed as a weak dipole which also may have affected the evaluated parameters. A second interesting example is the tracer test carried out between KLX15A and HLX27 in Laxemar /Lindquist et al. 2008b/. In this case, the fracture model of the site did not suggest any fracture directly connecting the two borehole sections. Instead, it is likely that the tracer transport occurred in two or more fracture planes.

7.2 Conclusions

The following conclusions are made:

- An empirical relationship between mass balance aperture, δ_m, and transmissivity, T, was found although some deviations and uncertainties for individual data exist. The best-fit for the relationship by using 74 data was quantified to $\delta_m = 0.33 \cdot T^{0.31}$. The logarithmic residuals between data and the fit may be regarded as approximately normally distributed with a standard deviation of 0.5.
- No difference in the relationship between δ_m and T could be firmly established for single fractures and fracture zones.
- Some tendencies could be found regarding deviations from the overall relationship between δ_m and T for some test sites and features. However, these differences were not firmly established.
- The empirical relationship between δ_m and T deviates considerably from cubic law aperture, δ_c. δ_m changes with approximately the cubic root of T as also δ_c do. But δ_m is according to the relationship to T at least one order of magnitude larger than δ_c. Hence, usage of cubic law aperture for transport predictions is unsuitable since the advective transport time will be considerably underestimated.

- The empirical relationship between δ_m and T evaluated in this study agrees rather well with the empirical relationship presented in /Rhén et al. 1997/, especially for higher values of T. However, the slope of the two fits are somewhat different as this study suggests that δ_m changes with approximately the cubic root of T while $\delta_{m,R}$ changes with approximately the square root of T.
- The empirical relationship between δ_m and T as presented in this study agrees rather well with the lower section of the relationship between $\delta_{t,S}$ and T as presented by /Svensson U et al. 2008/. However, the upper section of the relationship between $\delta_{t,S}$ and T results in significantly higher values of δ for the same value of T compared with the empirical relationship suggested in this study.
- The relationship between transport aperture, $\delta_{t,D}$ and T as suggested earlier by /Dershowitz and Klise 2002/, /Dershowitz et al. 2002/ and /Dershowitz et al. 2003/ deviates considerably from the empirical relationship between δ_m and T as presented in this study. δ_m is larger than $\delta_{t,D}$ for the same value of T except for high values of T. The empirical relationship between δ_m and T indicates that δ_m changes with approximately the cubic root of T while $\delta_{t,D}$ was assumed to change with the square root of T. The differences regarding the relationships of δ_m and $\delta_{t,D}$ to T are probably due to differences in methods and geometrical assumptions.
- There was no direct relationship found between hydraulic diffusivity and mass balance aperture. However, there are indications of a relationship between mass balance aperture and apparent storativity from hydraulic interference tests evaluations as well as between mean residence time and pressure response time, indicating that there may exist an indirect relationship between hydraulic diffusivity and mass balance aperture.
- No correlation between dispersivity in terms of Peclet number, Pe, and transmissivity or travel distance could be found.
- The distribution of Pe values seems to approximately follow a log normal distribution with an average of 8 and a range from 2.5 to 25 for one standard deviation.
- A positive correlation between longitudinal dispersivity, αL, and travel distance, rd, was found and was quantified to $\alpha_L = 0.16 . r_d^{0.95}$. The distribution of logarithmic residuals between the data and fit may be regarded as approximately normally distributed with a standard deviation of 0.5.

8 Acknowledgements

The authors like to thanks Ingvar Rhén, Sven Follin, Thomas Doe and Vladimir Cvetkovic for a careful review and many insightful points which have greatly improved this report.

References

SKB's (Svensk Kärnbränslehantering AB) publications can be found at www.skb.se/publications.

Abelin H, Birgersson L, 1987. 3-D migration experiment – Report 1. Site preparation and documentation. SKB Stripa Project Technical Report 87-19, Svensk Kärnbränslehantering AB.

Abelin H, Neretniks I, Tunbrant S, Moreno L, 1985. Final report of the migration in a single fracture – Experimental results and evaluation. SKB Stripa Project Technical Report 85-03, Svensk Kärnbränslehantering AB.

Abelin H, Birgersson L, Gidlund J, 1987a. 3-D migration experiment – Report 2. Instrumentation and tracers. SKB Stripa Project Technical Report 87-20, Svensk Kärnbränslehantering AB.

Abelin H, Birgersson L, Gidlund J, Moreno L, Neretniks I, Widén H, Ågren T, 1987b. 3-D migration experiment- Report 3, part I. Performed experiments, results and evaluation. SKB Stripa Project Technical Report 87-21, Svensk Kärnbränslehantering AB.

Abelin H, Birgersson L, Gidlund J, Moreno L, Neretniks I, Widén H, Ågren T, 1987c. 3-D migration experiment- Report 3, part II. Performed experiments, results and evaluation. Appendices 15, 16 and 17. SKB Stripa Project Technical Report 87-21, Svensk Kärnbränslehantering AB.

Abelin H, Birgersson L, Widén H, Ågren T, Moreno L, Neretniks I, 1990. Channelling experiment. SKB Stripa Project Technical Report 90-13, Svensk Kärnbränslehantering AB.

Andersson J-E, Ekman L, Gustafsson E, Nordquist R, Tirén S, 1989. Hydraulic interference tests and tracer tests within the Brändan area, Finnsjön study site. The fracture zone projekt – phase 3. SKB TR 89-12, Svensk Kärnbränslehantering AB.

Andersson P, Klockars C-E, 1985. Hydrogeological investigations and tracer tests in a well-defined rock mass in the Stripa mine. SKB TR 85-12, Svensk Kärnbränslehantering AB.

Andersson Per, Andersson Peter, Gustavsson E, Olsson O, 1989. Investigation of flow distribution in a fracture zone at the Stripa mine, using the radar method, results and interpretation. SKB TR 89-33, Svensk Kärnbränslehantering AB.

Andersson P, Nordqvist R, Persson T, Eriksson C-O, Gustafsson E, Ittner T, 1993. Dipole tracer experiment in a low-angle fracture zone at Finnsjön – results and interpretation. The Fracture Zone Project – Phase 3. SKB TR 93-26, Svensk Kärnbränslehantering AB.

Andersson P, Byegård J, Winberg A, 2002a. Final report of the TRUE Block Scale project. 2. Tracer tests in the block scale. SKB TR-02-14, Svensk Kärnbränslehantering AB.

Andersson P, Wass E, Gröhn S, Holmqvist M, 2002b. Äspö Hard Rock Laboratory. TRUE-1 Continuation Project. Complementary investigations at the TRUE-1 site – Crosshole interference, dilution and tracer tests, CX-1–CX-5. SKB IPR-02-47, Svensk Kärnbränslehantering AB.

Andersson P, Gröhn S, Nordqvist R, Wass E, 2004. Äspö Hard Rock Laboratory. TRUE Block Scale continuation project. BS2B pretests. Crosshole interference, dilution and tracer tests, CPT-1–CPT-4. SKB IPR-04-25, Svensk Kärnbränslehantering AB.

Andersson P, Byegård J, Billaux D, Cvetkovic V, Dershowitz W, Doe T, Hermanson J, Poteri A, Tullborg E-L, Winberg A (ed), 2007. TRUE Block Scale Continuation Project. Final report. SKB TR-06-42, Svensk Kärnbränslehantering AB.

Birgersson L, Widén H, Ågren T, Neretniks I, Moreno L, 1992. Site characterization and validation – tracer migration experiment in the validation drift, report 2, part 1: Performed experiments, results and evaluation. SKB Stripa Project Technical Report 92-03, Svensk Kärnbränslehantering AB.

Byegård J, Widestrand H, Nilsson K, Gustafsson E, Kronberg M, 2010. Long-term Sorption Diffusion Experiment (LTDE-SD). Performance of main in situ experiment and results from water phase measurements. SKB IPR-10-10, Svensk Kärnbränslehantering AB.

Dershowitz W, Klise K, 2002. Äspö Hard Rock Laboratory. TRUE Block Scale project. Evaluation of fracture network transport pathways and processes using the Channel Network approach. SKB IPR-02-34, Svensk Kärnbränslehantering AB.

Dershowitz W, Klise K, Fox A, Takeuchi S, Uchida M, 2002. Äspö Hard Rock Laboratory. TRUE Block Scale project. Channel network and discrete fracture network analysis of hydraulic interference and transport experiments and prediction of Phase C experiments. SKB IPR-02-29, Svensk Kärnbränslehantering AB.

Dershowitz W, Winberg A, Hermanson J, Byegård J, Tullborg E-L, Andersson P, Mazurek M, 2003. Äspö Hard Rock Laboratory. Äspö Task Force on modelling of groundwater flow and transport of solutes. Task 6c. A semi-synthetic model of block scale conductive structures at the Äspö HRL. SKB IPR-03-13, Svensk Kärnbränslehantering AB.

Dickson S E, Thomson N R, 2003. Dissolution of entrapped DNAPLs in variable aperture fractures: Experimental data and empirical model. Environmental Science & Technology, 37, pp 4128–4137.

Gustafsson E, Klockars C-E, 1981. Studies on groundwater transport in fractured crystalline rock under controlled conditions using nonradioactive tracers. SKBF/KBS TR 81-07, Svensk Kärnbränsleförsörjning AB.

Gustafsson E, Klockars C-E, 1984. Study of strontium and cesium migration in fractured crystalline rock. SKBF/KBS TR 84-07, Svensk Kärnbränslehantering AB.

Gustafsson E, Ludvigson J-E, 2005. Oskarshamn site investigation. Combined interference test and tracer test between KLX02 and HLX10. SKB P-05-20, Svensk Kärnbränslehantering AB.

Gustafsson E, Nordqvist R, 1993. Radially converging tracer test in a low-angle fracture zone at the Finnsjön site, central Sweden. The Fracture Zone Project – Phase 3. SKB TR 93-25, Svensk Kärnbränslehantering AB.

Javandel I, Doughty C, Tsang C-F, 1984. Groundwater transport: handbook of mathematical models. Washington D.C.: American Geophysical Union.

Klockars C-E, Persson O, Landström O, 1982. The hydraulic properties of fracture zones and tracer tests with non-reactive elements in Studsvik. SKBF/KBS TR 82-10, Svensk Kärnbränsleförsörjning AB.

Landström O, Klockars C-E, Holmberg K-E, Westerberg S, 1978. In situ experiments on nuclide migration in fractured crystalline rocks. KBS TR 110, Kärnbränslesäkerhet.

Landström O, Klockars C-E, Persson O, Tullborg E-L, Larson S-Å, Andersson K, Allard B, Torstenfelt B, 1983. Migration experiment in Studsvik. SKBF/KBS TR 83-18, Svensk Kärnbränsleförsörjning AB.

Lindquist A, Hjerne C, Nordqvist R, Byegård J, Walger E, Ludvigson J-E, Wass E, 2008a. Forsmark site investigation. Confirmatory hydraulic interference test and tracer test at drill site 2. SKB P-08-13, Svensk Kärnbränslehantering AB.

Lindquist A, Hjerne C, Nordqvist R, Ludvigson J-E, Harrström J, Carlsten S, 2008b. Oskarshamn site investigation. Confirmatory hydraulic interference test and tracer test in Laxemar. SKB P-08-96, Svensk Kärnbränslehantering AB.

Lindquist A, Hjerne C, Nordqvist R, Wass E, 2008c. Forsmark site investigation. Large-scale confirmatory multiple-hole tracer test. SKB P-08-59, Svensk Kärnbränslehantering AB.

Ludvigson J-E, Hjerne C, Thur P, 2010. Synthesis of results from hydraulic interference tests at Forsmark and Laxemar – review of new analysis methods in heterogeneous media. SKB R-10-73, Svensk Kärnbränslehantering AB.

Löfgren M, Crawford J, Elert M, 2007. Tracer test – possibilities and limitations. Experiences from SKB fieldwork 1977–2007. SKB R-07-39, Svensk Kärnbränslehantering AB.

Morosini M, Wass E, 2007. Oskarshamn site investigation. Hydraulic interference and tracer testing of a rock-soil aquifer between HLX35 and HLX34, SSM000037, SSM000222 and SSM000223. SKB P-06-151, Svensk Kärnbränslehantering AB.

Neuman S P, 1990. Universal scaling of hydraulic conductivities and dispersivities in geologic media. Water Research, 26, no 8, pp 1749–1758.

Nordqvist R, 2008. Evaluation and modelling of SWIW tests performed within the SKB site characterisation programme. SKB R-08-104, Svensk Kärnbränslehantering AB.

Nordqvist R, Gustafsson E, Andersson P, Thur P, 2008. Groundwater flow and hydraulic gradients in fractures and fracture zones at Forsmark and Oskarsham. SKB R-08-103, Svensk Kärnbränslehantering AB.

Olsson O, Andersson P, Gustafsson E, 1991. Site characterization and validation – monitoring of saline tracer transport by borehole radar measurement, final report. SKB Stripa Project Technical Report 91-18, Svensk Kärnbränslehantering AB.

Rhén I, Svensson U, Andersson J-E, Andersson P, Eriksson C-O, Gustafsson E, Ittner T, Nordqvist R, 1992. Äspö hard rock laboratory: Evaluation of the combined longterm pumping and tracer test (LPT2) in borehole KAS06. SKB TR 92-32, Svensk Kärnbränslehantering AB.

Rhén I (ed), Gustafsson G, Stanfors R, Wikberg P, 1997. Äspö HRL – Geoscientific evaluation 1997/5. Models based on site characterization 1986–1995. SKB TR 97-06, Svensk Kärnbränslehantering AB.

Rhén I, Forsmark T, Hartley L, Jackson P, Roberts D, Swan D, Gylling B, 2008. Hydrogeological conceptualisation and parameterisation. Site descriptive modelling. SDM-Site Laxemar. SKB R-08-78, Svensk Kärnbränslehantering AB.

Rhén I, Forsmark T, Hartley L, Joyce S, Roberts D, Gylling B, Marsic N, 2009. Bedrock hydrogeology. Model testing and synthesis. Site descriptive modelling, SDM-Site Laxemar. SKB R-08-91, Svensk Kärnbränslehantering AB.

Rouhiainen P, Heikkinen P, 1998. Äspö hard rock laboratory. TRUE Block Scale project. Difference flow logging measurements in boreholes KI0025F02 at the Äspö HRL. SKB IPR-01-46, Svensk Kärnbränslehantering AB.

Rouhiainen P, Heikkinen P, 1999a. Äspö hard rock laboratory. TRUE Block Scale project. Difference flow logging measurements in boreholes KA2563A and KA2511A at the Äspö HRL. SKB IPR-01-48, Svensk Kärnbränslehantering AB.

Rouhiainen P, Heikkinen P, 1999b. Äspö hard rock laboratory. TRUE Block Scale project. Difference flow logging measurements in boreholes KI0025F03 at the Äspö HRL. SKB IPR-01-55, Svensk Kärnbränslehantering AB.

Sauty J-P, 1980. An analysis of hydrodispersive transfer in aquifers. Water Resources Research, 16, pp 145–148.

SKB, 1992. Passage through water-bearing fracture zones. Compilation of technical notes. Passage through fracture zone NE-1. Hydrogeology and groundwater chemistry. SKB HRL Progress Report 25-92-18c, Svensk Kärnbränslehantering AB.

SKB, 2009. Site description of Laxemar at completion of the site investigation phase. SDM-Site Laxemar. SKB TR-09-01, Svensk Kärnbränslehantering AB.

Streltsova T D, 1988. Well testing in heterogeneous formations. New York: Wiley.

Svensson T, Ludvigson J-E, Walger E, Thur P, Gokall-Norman K, Wass E, Morosini M, 2008. Oskarshamn site investigation. Combined hydraulic interference- and tracer test in HLX33, SSM000228 and SSM000229. SKB P-07-187, Svensk Kärnbränslehantering AB.

Svensson U (ed), Vidstrand P, Neretnieks I, Wallin B, 2008. Towards a new generation of flow and transport models for the Äspö Hard Rock Laboratory. Main results from the project Äspömodels 2005. SKB R-08-74, Svensk Kärnbränslehantering AB.

Thur P, Hjerne C, Ludvigson J-E, Svensson T, Nordqvist R, 2010. Oskarshamn site investigation. HLX28 large-scale confirmatory multiple-hole tracer test and hydraulic interference test. SKB P-09-62, Svensk Kärnbränslehantering AB.

Tsang Y W, 1992. Usage of "equivalent apertures" for rock fractures as derived from hydraulic and tracer tests. Water Resources Research, 28, pp 1451–1455.

Uchida M, Doe T, Dershowitz W, Thomas A, Wallmann P, Sawada A, 1994. Discrete-fracture modelling of the Äspo LPT-2, large-scale pumping and tracer test. SKB ICR 94-09, Svensk Kärnbränslehantering AB.

van Genuchten M T, Alves W J, 1982. Analytical solutions of one-dimensional convective-dispersive solute transport equation. Washington D.C.: U.S. Department of Agriculture. (Technical bulletin 1661).

Wass E, Andersson P, 2006. Forsmark site investigation. Groundwater flow measurements and tracer tests at drill site 1. SKB P-06-125, Svensk Kärnbränslehantering AB.

Winberg A, Andersson P, Hermanson J, Byegård J, Cvetkovic V, Birgersson L, 2000. Äspö Hard Rock Laboratory. Final report of the first stage of the tracer retention understanding experiments. SKB TR-00-07, Svensk Kärnbränslehantering AB.

Zheng Q, Dickson S E, Guo Y, 2008. On the appropriate "equivalent aperture" for the description of solute transport in single fractures: Laboratory-scale experiments. Water Resources Research, 44, W04502, doi:10.1029/2007WR005970.

Appendix 1

Compiled data from tracer and hydraulic tests

Table A1-1. Results from tracer test included in study.

Site	Test name and/or report	Type of test [1]	Test formation [2]	Formation name	Withdrawal borehole	Secup [m]	Seclow [m]	Injection borehole	Secup [m]	Seclow [m]	Mass balance aperture, δ_m [m]	Kinematic porosity ε_f [–]	Fracture conductivtiy, K_{fr} [m/s]	Peclet number, Pe [–]	Travel distance, r [m]	Frictional loss aperture δ_l [m]
Äspö	LPT-2, TR-92-32	RC	FZ	EW-5	KAS06	353	353	KAS05:E3	320	380	1.1E-02		5.3E-04	106.9	141	2.9E-05
Äspö	LPT-2, TR-92-32	RC	FZ	EW-5	KAS06	399	399	KAS05:E3	320	380	1.8E-02		5.6E-04	84.8	141	3.0E-05
Äspö	LPT-2, TR-92-32	RC	FZ	EW-5	KAS06	353	353	KAS12:DB	279	330	3.4E-03		1.7E-03	6.1	200	5.2E-05
Äspö	LPT-2, TR-92-32	RC	FZ	EW-5	KAS06	364	364	KAS12:DB	279	330	2.5E-03		1.2E-03	4.5	213	4.4E-05
Äspö	LPT-2, TR-92-32	RC	FZ	EW-5	KAS06	399	399	KAS12:DB	279	330	6.6E-03		1.6E-03	3.3	200	5.0E-05
Äspö	LPT-2, TR-92-32	RC	FZ	NNW-1	KAS06	217	217	KAS08:M1	503	601	1.7E-03	2.5E-03	8.6E-03	10.8	301	1.2E-04
Äspö	LPT-2, TR-92-32	RC	FZ	NNW-1	KAS06	217	217	KAS12:DB	279	330	4.8E-03	6.9E-03	3.1E-03	2.6	292	7.0E-05
Äspö	LPT-2, TR-92-32	RC	FZ	NNW-2	KAS06	448	448	KAS08:M1	503	601	5.1E-03	6.8E-03	3.3E-03	11.3	181	7.2E-05
Äspö	LPT-2, TR-92-32	RC	FZ	NNW-2	KAS06	448	448	KAS12:DB	279	330	1.1E-02	1.4E-02	1.6E-03	4.6	190	5.0E-05
Äspö [3]	PR 25-92-18	RC	FZ	NE-1	KA1131B	92.05	203.1	KAS14	147	175	5.4E-02	7.2E-03	1.1E-03	12.8	92	3.7E-05
Äspö	TRUE-1 PTT-1	RC	SF	Feature A	KXTT3:P2	10.92	14.42	KXTT1:P2	15	16	1.4E-03	1.8E-04	3.5E-04	8.4	5	2.4E-05
Äspö	TRUE-1 RC-1	RC	SF	Feature A	KXTT3:R2	10.92	14.42	KXTT1:R2	15.5	16	2.2E-03	1.2E-04	5.0E-04	21.0	5	2.8E-05
Äspö	TRUE-1 STT1b	RC	SF	Feature A	KXTT3:R2	10.92	14.42	KXTT1:R2	15.5	16	1.8E-03	1.1E-03	1.8E-04	9.1	5	1.7E-05
Äspö	TRUE-1 PDT-1	RC	SF	Feature A	KXTT3:R2	10.92	14.42	KXTT1:R2	15.5	16	2.1E-03	4.0E-04	1.1E-03	3.9	5	4.2E-05
Äspö	TRUE-1 PDT-2	RC	SF	Feature A	KXTT3:R2	10.92	14.42	KXTT1:R2	15.5	16	2.6E-03	7.0E-04	5.6E-04	5.0	5	3.0E-05
Äspö	TRUE-1 CX-5	RC	SF	Feature A	KXTT3:R2	10.92	14.42	KXTT1:R2	15.5	16	7.6E-04	2.6E-04	4.0E-04	29.6	5	2.5E-05
Äspö	TRUE-1 DP-5	DP	SF	Feature A	KXTT3:R2	10.92	14.42	KXTT4:R3	11.92	13.92	1.6E-03	5.0E-04	2.0E-04	13.8	5	1.8E-05
Äspö	TRUE-1 DP-6	DP	SF	Feature A	KXTT3:R2	10.92	14.42	KXTT4:P3	11.92	13.92	2.4E-03	4.4E-04	4.0E-04	9.8	5	2.5E-05
Äspö	TRUE-1 RC-1	RC	SF	Feature A	KXTT3:R2	10.92	14.42	KXTT4:R3	11.92	13.92	1.4E-03	9.0E-05	7.1E-04	3.0	5	3.4E-05
Äspö	TRUE-1 STT1	RC	SF	Feature A	KXTT3:R2	10.92	14.42	KXTT4:R3	11.92	13.92	1.4E-03	8.0E-04	4.2E-04	2.3	5	2.6E-05
Äspö	TRUE-1 PDT-1	RC	SF	Feature A	KXTT3:R2	10.92	14.42	KXTT4:R3	11.92	13.92	2.1E-03	5.0E-04	6.4E-04	7.8	5	3.2E-05
Äspö	TRUE-1 PDT-3	RC	SF	Feature A	KXTT3:R2	10.92	14.42	KXTT4:R3	11.92	13.92	1.7E-03	7.0E-04	4.8E-04	2.8	5	2.8E-05
Äspö	TRUE-1 CX-4	RC	SF	Feature A'	KXTT3:R2	10.92	14.42	KXTT4:S2	12.92	13.92	2.4E-02	3.5E-03	3.9E-05	33.4	5	7.9E-06

Site	Test name and/or report	Type of test [1)]	Test formation [2)]	Formation name	Withdrawal borehole	Secup [m]	Seclow [m]	Injection borehole	Secup [m]	Seclow [m]	Mass balance aperture, δ_m [m]	Kinematic porosity ε_f [–]	Fracture conductivtiy, K_{fr} [m/s]	Peclet number, Pe [–]	Travel distance, r [m]	Frictional loss aperture δ_l [m]
Äspö	TRUE-1 CX-4	RC	SF	Feature A	KXTT3:R2	10.92	14.42	KXTT4:S3	11.92	12.42	1.7E-02	2.8E-03	4.9E-05	4.0	5	8.8E-06
Äspö	TRUE-1 CX-5	RC	SF	Feature A	KXTT3:R2	10.92	14.42	KXTT4:S3	11.92	12.42	4.2E-03	1.6E-03	6.4E-05	5.1	5	1.0E-05
Äspö	TRUE-1 RC-2	RC	SF	Feature A	KXTT4:R3	11.92	13.92	KXTT1:R2	15.5	16	3.4E-03	4.6E-03	5.0E-06	6.0	5	2.8E-06
Äspö	TRUE-1 PTT-1	RC	SF	Feature B	KXTT4:P4	8.42	10.42	KXTT3:P3	8.92	9.92	1.6E-04	2.3E-05	5.9E-04	9.1	3	3.1E-05
Äspö	TRUE-BS B-2	RC	SF	#19,13,21	KI0023B:P6	70.95	71.95	KA2563A:S1	242	246	2.8E-02	1.5E-02	7.8E-06	4.3	55	3.5E-06
Äspö	TRUE-BS PT-4	RC	SF	#20,21	KI0023B:P6	70.95	71.95	KA2563A:S4	187	190	2.2E-03	1.1E-03	9.8E-05	3.0	16	1.2E-05
Äspö	TRUE-BS ESV-1c	RC	SF	#20,21	KI0023B:P6	70.95	71.95	KA2563A:S4	187	190	1.9E-03	2.3E-03	1.7E-04	10.0	16	1.6E-05
Äspö	TRUE-BS B-2	DPw	SF	#21	KI0023B:P6	70.95	71.95	KI0025F03:P3	89	92.5	3.0E-02	1.7E-02	6.3E-06	6.1	27	3.2E-06
Äspö	TRUE-BS A-4	RC	SF	#20,21	KI0023B:P6	70.95	71.95	KI0025F03:P5	66.58	74.08	1.7E-02	9.4E-03	1.2E-05	4.5	16	4.4E-06
Äspö	TRUE-BS C1	DPw	SF	#20,21	KI0023B:P6	70.95	71.95	KI0025F03:P5	66.58	74.08	3.4E-03	1.8E-03	5.6E-05	7.0	16	9.4E-06
Äspö	TRUE-BS B-2	DPw	SF	#20,21	KI0023B:P6	70.95	71.95	KI0025F03:P5	66.5	74	2.7E-03	1.5E-03	7.2E-05	7.3	16	1.1E-05
Äspö	TRUE-BS C4	DPw	SF	#20,21	KI0023B:P6	70.95	71.95	KI0025F03:P5	66.58	74.08	3.1E-03	1.7E-03	6.1E-05	7.6	16	9.9E-06
Äspö	TRUE-BS A-4	RC	SF	#22,20,21	KI0023B:P6	70.95	71.95	KI0025F03:P6	59.58	65.58	2.1E-02	1.2E-02	8.9E-06	12.6	73	3.8E-06
Äspö	TRUE-BS B-1	DPw	SF	#22,20,21	KI0023B:P6	70.95	71.95	KI0025F03:P6	59.5	65.5	1.6E-02	9.9E-03	1.3E-05	6.1	73	4.5E-06
Äspö	TRUE-BS B-2	DPw	SF	#22,20,21	KI0023B:P6	70.95	71.95	KI0025F03:P6	59.5	65.5	2.6E-02	1.5E-02	7.0E-06	5.6	73	3.3E-06
Äspö	TRUE-BS C2	DPw	SF	#23,21	KI0023B:P6	70.95	71.95	KI0025F03:P7	55.08	58.58	3.6E-02	2.0E-02	5.1E-06	4.0	97	2.8E-06
Äspö	TRUE-BS PT-4	RC	SF	#13,21,#22	KI0023B:P6	70.95	71.95	KI0025F02:P3	93.35	99.25	5.2E-03	2.7E-03	4.1E-05	11.4	33	8.1E-06
Äspö	TRUE-BS B-2	RC	SF	#13,21,#22	KI0023B:P6	70.95	71.95	KI0025F02:P3	93.4	99.25	1.0E-02	5.0E-03	1.9E-05	4.7	33	5.5E-06
Äspö	TRUE-BS C3	RC	SF	#13,21,#22	KI0023B:P6	70.95	71.95	KI0025F02:P3	93.35	99.25	1.6E-02	8.1E-03	1.2E-05	3.4	33	4.4E-06
Äspö	TRUE-BS B-1	DPw	SF	#20,21	KI0023B:P6	70.95	71.95	KI0025F02:P5	73.3	77.25	8.0E-03	3.9E-03	3.3E-05	3.4	21	7.2E-06
Äspö	TRUE-BS PT-4	RC	SF	#22,20,21	KI0023B:P6	70.95	71.95	KI0025F02:P6	64	72.3	1.4E-02	8.0E-03	1.4E-05	3.6	65	4.7E-06
Äspö	TRUE-BS B-2	RC	SF	#22,20,21	KI0023B:P6	70.95	71.95	KI0025F02:P6	64	72.3	1.5E-02	8.2E-03	1.3E-05	3.3	65	4.5E-06
Äspö	TRUE-BS B-2	DPw	SF	#23,20,21	KI0023B:P6	70.95	71.95	KI0025F03:P7	55	58.5	1.6E-02	9.1E-03	1.2E-05	7.1	97	4.4E-06
Äspö	TRUE-BS A-5	RC	SF	#20	KI0025F03:P5	66.58	74.08	KI0025F02:P5	73.3	77.25	5.9E-04	6.9E-05	3.1E-04	17.5	9	2.2E-05
Äspö	TRUE-BS A-5	RC	SF	#20	KI0025F03:P5	66.58	74.08	KA2563A:S4	187	190	1.4E-03	1.5E-04	1.5E-04	7.8	27	1.5E-05
Äspö	TRUE-BS CPT-4b	DPw	SF	#19	KI0025F03:R3	123.03	128.03	KA2563A:S1	242	246	7.7E-03			5.8	49	
Äspö	TRUE-BS CPT-4b	DPw	SF	#19	KI0025F03:R3	123.03	128.03	KA2563A:S2	236	241	1.6E-02			21.8	49	
Äspö	TRUE-BS CPT-4a	RC	SF	#19	KI0025F03:R3	123.03	128.03	KI0023B:P2	111.25	112.7	2.8E-03			7.2	27	
Äspö	TRUE-BS CPT-4c	DPw	SF	#19	KI0025F03:R3	123.03	128.03	KI0023B:P2	111.25	112.7	2.0E-03			7.1	27	
Äspö	TRUE-BS CPT-4a	RC	SF	#19	KI0025F03:R3	123.03	128.03	KI0025F:R2	165.5	169.5	1.7E-03			3.0	69	

Site	Test name and/or report	Type of test [1]	Test formation [2]	Formation name	Withdrawal borehole	Secup [m]	Seclow [m]	Injection borehole	Secup [m]	Seclow [m]	Mass balance aperture, δ_m [m]	Kinematic porosity ε_f [–]	Fracture conductivtiy, K_{fr} [m/s]	Peclet number, Pe [–]	Travel distance, r [m]	Frictional loss aperture δ_l [m]
Äspö	TRUE-BS CPT-4b	DPw	SF	#19, BG1	KI0025F03:R3	123.03	128.03	KI0025F02:R2	135.1	139.05	1.9E-02			3.5	22	
Äspö	TRUE-BS CPT-4c	DPw	SF	#19, BG1	KI0025F03:R3	123.03	128.03	KI0025F02:R2	135.1	139.05	1.1E-03			4.2	22	
Äspö	TRUE-BS CPT-4a	RC	SF	#19	KI0025F03:R3	123.03	128.03	KI0025F02:R3	129.2	134.1	1.9E-03			1.5	19	
Äspö	TRUE-BS CPT-4c	DPw	SF	#19	KI0025F03:R3	123.03	128.03	KI0025F02:R3	129.2	134.1	2.7E-02			10.8	19	
Finnsjön	Test 2, TR-81-07	RC	FZ		G1	100	102	G2	91	93	1.8E-03	8.8E-04	2.5E-03		30	6.3E-05
Finnsjön	Test 5, TR-81-07	RC	FZ		G1	100	102	G2	91	93	1.5E-03	7.9E-04	2.8E-03	33.3	30	6.7E-05
Finnsjön	TR-89-12	RC	FZ	Zone 2	BFI02 U	193	217	BFI01:4 U	239	250	1.2E-02		1.6E-01	70.0	168	5.0E-04
Finnsjön	TR-93-25, Test 1-1	RC	FZ	Zone 2	BFI02 U	193	288.7	BFI01 U	241.5	246.5	7.2E-03	1.0E-02	1.7E-01	26.8	168	5.2E-04
Finnsjön	TR-93-25, Test 1-1	RC	FZ	Zone 2	BFI02 L	193	288.7	BFI01 U	241.5	246.5	2.1E-02	7.5E-03	4.1E-02	22.2	168	2.6E-04
Finnsjön	TR-93-25, Test 1-1	RC	FZ	Zone 2	BFI02 U and L	193	288.7	BFI01 U	241.5	246.5	1.6E-02		1.3E-01	2.0	168	4.5E-04
Finnsjön	TR-93-25, Test 1-2	RC	FZ	Zone 2	BFI02 E	193	288.7	BFI01 M	263.5	266.5	1.1E-01		1.8E-02	7.8	168	1.7E-04
Finnsjön	TR-93-25, Test 1-3	RC	FZ	Zone 2	BFI02 U	193	288.7	BFI01 L	351.5	356.5	7.6E-02		1.3E-02	27.8	201	1.4E-04
Finnsjön	TR-89-12	RC	FZ	Zone 2	BFI02 U	193	217	KFI06:4 U	202	227	4.3E-03		6.1E-01	49.0	189	9.9E-04
Finnsjön	TR-93-25, Test 2-1	RC	FZ	Zone 2	BFI02 U	193	288.7	KFI06 U	212	217	1.1E-02	7.5E-03	2.4E-01	7.9	189	6.2E-04
Finnsjön	TR-93-25, Test 2-2	RC	FZ	Zone 2	BFI02 U and L	193	288.7	KFI06 M	236.5	239.5	1.3E-01		3.4E-02	6.7	191	2.3E-04
Finnsjön	TR-93-25, Test 2-3	RC	FZ	Zone 2	BFI02 L	193	288.7	KFI06 L	252.5	271.5	1.1E-02	1.1E-02	1.8E-01	16.4	189	5.4E-04
Finnsjön	TR-93-25, Test 2-3	RC	FZ	Zone 2	BFI02 U	193	288.7	KFI06 L	252.5	271.5	4.3E-02		6.4E-02	243.0	189	3.2E-04
Finnsjön	TR-93-25, Test 2-3	RC	FZ	Zone 2	BFI02 U and L	193	288.7	KFI06 L	252.5	271.5	4.4E-02		1.1E-01	1.8	189	4.2E-04
Finnsjön	TR-89-12	RC	FZ	Zone 2	BFI02 U	193	217	KFI11:4 U	217	240	3.2E-03		9.7E-01	118.0	155	1.2E-03
Finnsjön	TR-93-25, Test 3-1	RC	FZ	Zone 2	BFI02 U	193	288.7	KFI11 U	221.5	226.5	2.1E-03	1.9E-03	9.3E-01	42.7	155	1.2E-03
Finnsjön	TR-93-25, Test 3-1	RC	FZ	Zone 2	BFI02 L	193	288.7	KFI11 U	221.5	226.5	4.0E-03		3.6E-01	14.5	155	7.6E-04
Finnsjön	TR-93-25, Test 3-1	RC	FZ	Zone 2	BFI02 U and L	193	288.7	KFI11 U	221.5	226.5	6.5E-03		5.2E-01	3.8	155	9.1E-04
Finnsjön	TR-93-25, Test 3-2	RC	FZ	Zone 2	BFI02 U and L	193	288.7	KFI11 M	287.5	294.5	8.3E-02		4.5E-02	132.4	169	2.7E-04
Finnsjön	TR-93-25, Test 3-3	RC	FZ	Zone 2	BFI02 U	193	288.7	KFI11 L	329.5	338.5	1.6E-01		1.3E-02	28.5	190	1.4E-04
Studsvik [3]	TR 82-10	DPw	FZ		B6N	94	102	B1N	91	92.3	8.6E-02	2.6E-02	6.6E-05		12	1.0E-05
Studsvik [3]	TR 82-10	DPw	FZ		B6N	64	66	B5N	78.8	80.1	4.3E-02	3.7E-01	1.7E-04		15	1.6E-05
Stripa	Stripa Project 85-03	RC	SF	Fracture 2	Sampling hole 2-6			H2	15.77	15.77	1.3E-04		1.1E-06	2.0	5	1.3E-06
Stripa	Stripa Project 85-03	RC	SF	Fracture 2	Sampling hole 2-8			H2	15.77	15.77	1.5E-04		3.4E-06	0.9	5	2.3E-06

Site	Test name and/or report	Type of test [1]	Test formation [2]	Formation name	Withdrawal borehole	Secup [m]	Seclow [m]	Injection borehole	Secup [m]	Seclow [m]	Mass balance aperture, δ_m [m]	Kinematic porosity ε_f [–]	Fracture conductivtiy, K_{fr} [m/s]	Peclet number, Pe [–]	Travel distance, r [m]	Frictional loss aperture δ_l [m]
Stripa	TR85-12	RD	SF	Short range	3 L	15.8	20	Central borehole	11	20.1	2.8E-04				2	
Stripa	TR85-12	RD	SF	Short range	9 L	15.8	20	Central borehole	11	20.1	9.6E-04				2	
Stripa	TR85-12	RD	SF	Short range	11 L	15.8	20	Central borehole	11	20.1	9.6E-04			33.3	2	
Stripa	TR85-12	RD	SF	Short range	13 U	11	15.5	Central borehole	11	20.1	3.9E-04			20.0	2	
Stripa	TR85-12	RD	SF	Short range	13 L	15.8	20	Central borehole	11	20.1	9.5E-04			12.5	2	
Stripa	TR85-12	RD	SF	Short range	15 L	15.8	20	Central borehole	11	20.1	7.2E-04			12.5	2	
Stripa	TR89-33	MP	FZ	Zone C	E1	145	146	F3	103	117.5	2.0E-03	1.4E-04	1.1E-04	2.0	53	1.3E-05
Stripa	TR89-33	MP	FZ	Zone C	F1	108	136	F3	103	117.5	1.4E-02	9.7E-04	1.4E-05		23	4.7E-06
Stripa	TR89-33	MP	FZ	Zone C	F2	120	121	F3	103	117.5	1.8E-03	1.3E-04	1.1E-04	0.9	30	1.3E-05
Stripa	TR89-33	MP	FZ	Zone C	F4	90	140	F3	103	117.5	3.0E-03	2.1E-04	7.4E-05		43	1.1E-05
Stripa	TR89-33	MP	FZ	Zone C	F5	94	95	F3	103	117.5	4.3E-03	2.9E-04	4.9E-05	2.5	32	8.8E-06
Stripa	Stripa project 91-28	DP	FZ	Zone H	overall zone H			C2			5.5E-04	1.1E-04				
Forsmark	SKB P-08-13	DPw	FZ	Zone A2	KFM02B	408.5	434	KFM02A	411	442	2.6E-02	2.5E-04	6.7E-03	0.9	46	1.0E-04
Forsmark	SKB P-08-59	RC	FZ	Zone A2	HFM14	6	150.5	HFM01	33.5	45.5	9.3E-02		1.2E-02	8.2	377	1.4E-04
Forsmark	SKB P-08-59	RC	FZ	Zone A2	HFM14	6	150.5	HFM13	159	173	8.6E-02		2.5E-02	5.8	297	2.0E-04
Forsmark	SKB P-08-59	RC	FZ	Zone A2	HFM14	6	150.5	HFM15_Gd	85	95	1.2E-02		1.6E-01	14.1	72	5.0E-04
Forsmark	SKB P-08-59	DPw	FZ	Zone A2	HFM14	6	150.5	HFM15_Uranine	85	95	1.3E-02		1.5E-01	4.7	72	4.9E-04
Forsmark	SKB P-08-59	RC	FZ	Zone A2	HFM14	6	150.5	HFM19	168	182	4.7E-02		3.9E-02	7.9	247	2.5E-04
Forsmark	SKB P-08-59	RC	FZ	Zone A2	HFM14	6	150.5	KFM10A	430	440	3.9E-02		4.3E-02	5.7	493	2.6E-04
Laxemar	SKB P-07-187	RC	RS		HLX33	9	202.1	SSM000228	6	7	2.4E-02			7.6	204	
Laxemar	SKB P-06-151	RC	RS		HLX35	3	151.8	SSM000223		12	1.7E-01			1.1	102	
Laxemar	SKB P-08-96	DPw	FZ		HLX27	6.03	164.7	KLX15A	260	272	4.1E-02	3.6E-03	4.0E-03	3.0	140	8.0E-05
Laxemar	in prep	RC	FZ		HLX28	6	154	HLX32	20	30	6.7E-01	3.2E-03	3.7E-04	2.1	122	2.4E-05
Laxemar	in prep	RC	FZ		HLX28	6	154	HLX37	150	199.8	5.8E-02	1.8E-04	6.7E-03	10.3	486	1.0E-04

[1] Type of test: RC = Radially converging, RD = Radially diverging, DP = Dipole, DPw = Weak dipole, MP = Multipolar.
[2] Test formation: FZ = Fracture zone, SF = Single fracture, RS= Rock soil aquifer.
[3] Some values recalculated are not in agreement with original report due to uncertainties or errors found in the original calculations.

Table A1-2. Compilation of transmissivity for flow paths included in study.

		T_C [m²/s]				T_W [m²/s]				T_I [m²/s]			
Site	Flow path (boreholes)	Number of values	Median	Min	Max	Number of values	Median	Min	Max	Number of values	Median	Min	Max
Äspö	EW-5 (KAS05:E3-KAS06)	1	4.60E-05			2	3.85E-05	3.10E-05	4.60E-05	2	1.88E-05	2.43E-06	3.52E-05
Äspö	EW-5 (KAS12:DB-KAS06)	1	4.30E-05			2	3.85E-05	3.10E-05	4.60E-05	1	2.73E-05		
Äspö	NNW-1 (KAS08:M1-KAS06)	1	2.42E-05			2	2.70E-05	2.50E-05	2.90E-05	2	3.23E-04	1.25E-04	5.22E-04
Äspö	NNW-1 (KAS12:DB-KAS06)	1	2.42E-05			2	2.70E-05	2.50E-05	2.90E-05	1	2.73E-05		
Äspö	NNW-2 (KAS08:M1-KAS06)	1	2.60E-05			2	3.20E-05	2.80E-05	3.60E-05	2	3.23E-04	1.25E-04	5.22E-04
Äspö	NNW-2 (KAS12:DB-KAS06)	1	3.10E-05			2	3.20E-05	2.80E-05	3.60E-05	1	2.73E-05		
Äspö	NE-1 (KAS14-KA1131B)	1	8.70E-04							1	4.10E-04		
Äspö	Feature A (KXTT1-KXTT3)	2	5.44E-07	4.50E-07	6.37E-07	4	3.83E-07	3.20E-07	1.00E-06	4	1.08E-08	1.00E-08	3.00E-08
Äspö	Feature A (KXTT4-KXTT3)	2	3.61E-07	1.10E-07	6.12E-07	4	3.83E-07	3.20E-07	1.00E-06	4	6.15E-08	2.88E-08	1.90E-07
Äspö	Feature A (KXTT4-KXTT3)					4	3.83E-07	3.20E-07	1.00E-06				
Äspö	Feature A (KXTT1-KXTT4)	2	2.87E-06	4.67E-08	5.70E-06	4	5.33E-08	2.88E-08	1.90E-07	4	1.08E-08	1.00E-08	3.00E-08
Äspö	Feature A' (KXTT4-KXTT3)					4	3.83E-07	3.20E-07	1.00E-06	1	1.84E-09		
Äspö	Feature B (KXTT3-KXTT4)					1	3.68E-08			1	2.07E-08		
Äspö	#19,13,21 (KA2563A:S1-KI0023B:P6)	1	2.40E-05			3	7.65E-07	1.30E-07	8.10E-07	1	5.25E-09		
Äspö	#20,21 (KA2563A:S4-KI0023B:P6)	1	8.05E-07			3	7.65E-07	1.30E-07	8.10E-07	1	3.82E-07		
Äspö	#21 (KI0025F03:P3-KI0023B:P6)					3	7.65E-07	1.30E-07	8.10E-07				
Äspö	#20,21 (KI0025F03:P5-KI0023B:P6)	1	7.90E-07			3	7.65E-07	1.30E-07	8.10E-07				
Äspö	#22,20,21 (KI0025F03:P6-KI0023B:P6)					3	7.65E-07	1.30E-07	8.10E-07				
Äspö	#23,21 (KI0025F03:P7-KI0023B:P6)					3	7.65E-07	1.30E-07	8.10E-07				
Äspö	#13,21,#22 (KI0025F02:P3-KI0023B:P6)	1	1.30E-05			3	7.65E-07	1.30E-07	8.10E-07				
Äspö	#20,21 (KI0025F02:P5-KI0023B:P6)	1	7.80E-07			3	7.65E-07	1.30E-07	8.10E-07				
Äspö	#22,20,21 (KI0025F02:P6-KI0023B:P6)	1	1.20E-06			3	7.65E-07	1.30E-07	8.10E-07				
Äspö	#23,20,21 (KI0025F03:P7-KI0023B:P6)					3	7.65E-07	1.30E-07	8.10E-07				
Äspö	#20 (KI0025F02:P5-KI0025F03:P5)	1	7.60E-07										
Äspö	#20 (KA2563A:S4-KI0025F03:P5)	1	7.60E-07							1	3.82E-07		
Äspö	#19 (KA2563A:S1-KI0025F03:R3)					1	1.05E-06			1	5.25E-09		
Äspö	#19 (KA2563A:S2-KI0025F03:R3)					1	1.05E-06			1	9.80E-08		
Äspö	#19 (KI0023B:P2-KI0025F03:R3)					1	1.05E-06			3	1.67E-06	9.90E-08	7.94E-06
Äspö	#19 (KI0025F:R2-KI0025F03:R3)					1	1.05E-06			2	1.05E-05	7.30E-07	2.03E-05
Äspö	#19, BG1 (KI0025F02:R2-KI0025F03:R3)					1	1.05E-06			1	8.00E-10		
Äspö	#19 (KI0025F02:R3-KI0025F03:R3)					1	1.05E-06			1	5.20E-07		
Finnsjön	(G2-G1)	1	8.70E-06			1	2.20E-06			1	6.60E-06		
Finnsjön	Zone 2 (BFI01 U-BFI02 U)	1	1.40E-03			1	1.73E-03			1	1.30E-03		
Finnsjön	Zone 2 (BFI01 U-BFI02 L)	1	2.40E-03			1	8.29E-04			1	1.30E-03		
Finnsjön	Zone 2 (BFI01 U-BFI02 U and L)	1	2.20E-03			1	2.55E-03			1	1.30E-03		

Site	Flow path (boreholes)	T_C [m²/s]				T_W [m²/s]				T_I [m²/s]			
		Number of values	Median	Min	Max	Number of values	Median	Min	Max	Number of values	Median	Min	Max
Finnsjön	Zone 2 (BFI01 M-BFI02 E)					1	2.55E-03			1	2.50E-06		
Finnsjön	Zone 2 (BFI01 L-BFI02 U)					1	1.72E-03			1	1.00E-04		
Finnsjön	Zone 2 (KFI06 U-BFI02 U)	1	1.40E-03			1	1.73E-03			1	5.60E-04		
Finnsjön	Zone 2 (KFI06 M-BFI02 U and L)					1	2.55E-03			1	4.20E-06		
Finnsjön	Zone 2 (KFI06 L-BFI02 L)	1	1.60E-03			1	8.29E-04			1	6.70E-04		
Finnsjön	Zone 2 (KFI06 L-BFI02 U)					1	1.72E-03			1	6.70E-04		
Finnsjön	Zone 2 (KFI06 L-BFI02 U and L)					1	2.55E-03			1	6.70E-04		
Finnsjön	Zone 2 (KFI11 U-BFI02 U)	1	1.40E-03			1	1.73E-03			1	3.70E-04		
Finnsjön	Zone 2 (KFI11 U-BFI02 L)					1	8.29E-04			1	3.70E-04		
Finnsjön	Zone 2 (KFI11 U-BFI02 U and L)					1	2.55E-03			1	3.70E-04		
Finnsjön	Zone 2 (KFI11 M-BFI02 U and L)					1	2.55E-03			1	1.60E-06		
Finnsjön	Zone 2 (KFI11 L-BFI02 U)					1	1.72E-03			1	1.50E-05		
Studsvik	(B1N-B6N)					1	1.38E-05			1	1.11E-06		
Studsvik	(B5N-B6N)					1	1.21E-04			1	3.25E-07		
Stripa	Fracture 2 (H2-Sampling hole 2–6)									1	4.25E-10		
Stripa	Fracture 2 (H2-Sampling hole 2–8)									1	4.25E-10		
Stripa	Short range (Central borehole-3 L)					2	1.49E-09	1.45E-09	1.53E-09	1	3.31E-10		
Stripa	Short range (Central borehole-9 L)					2	1.49E-09	1.45E-09	1.53E-09	1	6.46E-10		
Stripa	Short range (Central borehole-11 L)					2	1.49E-09	1.45E-09	1.53E-09	1	1.85E-10		
Stripa	Short range (Central borehole-13 U)					2	1.49E-09	1.45E-09	1.53E-09	1	1.80E-09		
Stripa	Short range (Central borehole-13 L)					2	1.49E-09	1.45E-09	1.53E-09	1	4.05E-10		
Stripa	Short range (Central borehole-15 L)					2	1.49E-09	1.45E-09	1.53E-09	1	3.07E-10		
Stripa	Zone C (F3–E1)									1	1.90E-07		
Stripa	Zone C (F3–F1)									1	1.90E-07		
Stripa	Zone C (F3–F2)									1	1.90E-07		
Stripa	Zone C (F3–F4)									1	1.90E-07		
Stripa	Zone C (F3–F5)									1	1.90E-07		
Stripa	Zone H (C2-overall zone H)	1	4.60E-08										
Forsmark	Zone A2 (KFM02A–KFM02B)	1	2.48E-05			4	4.12E-05	2.98E-05	4.45E-05	4	2.69E-06	2.08E-06	3.14E-06
Forsmark	Zone A2 (HFM01–HFM14)	1	5.90E-04			2	6.61E-04	4.78E-04	8.45E-04	1	4.50E-05		
Forsmark	Zone A2 (HFM13–HFM14)	1	3.50E-04			2	6.61E-04	4.78E-04	8.45E-04	1	2.91E-04		
Forsmark	Zone A2 (HFM15–HFM14)	1	3.90E-04			2	6.61E-04	4.78E-04	8.45E-04	1	1.02E-04		
Forsmark	Zone A2 (HFM19–HFM14)	1	3.90E-04			2	6.61E-04	4.78E-04	8.45E-04	1	2.75E-04		
Forsmark	Zone A2 (KFM10A–HFM14)	1	3.30E-04			2	6.61E-04	4.78E-04	8.45E-04	4	2.79E-05	2.17E-05	3.03E-05
Laxemar	(SSM000228-HLX33)					2	1.66E-04	1.36E-04	1.96E-04	2	4.23E-04	4.69E-05	8.00E-04
Laxemar	(SSM000223-HLX35)					2	4.26E-04	3.70E-04	4.82E-04	1	3.44E-04		
Laxemar	(KLX15A–HLX27)	1	5.45E-05			2	4.34E-05	3.87E-05	4.81E-05	2	7.35E-06	3.70E-06	1.10E-05
Laxemar	(HLX32–HLX28)	1	1.10E-04			1	3.62E-04			1	6.94E-06		
Laxemar	(HLX37–HLX28)	1	7.20E-05			1	3.62E-04						

Table A1-3. Compilation of parameters tracer test parameters, transmissivity and storativity for flow paths included in study.

Site	Type of test [1)]	Test formation [2)]	Flow path (boreholes)	Mass balance aperture δ_m [m]	Kinematic porosity ε_f [–]	Fracture conducitivity K_{fr} [m/s]	Peclet number Pe [–]	Travel distancer [m]	Frictional loss aperture δ_l [m]	Cubic law aperture δ_c [m]	T_S [m^2/s]	S_o [–]	T_o/S_o [m^2/s]
Äspö	RC	FZ	EW-5 (KAS05:E3-KAS06)	2.9E-02	8.0E-04	5.5E-04	95.9	141	3.0E-05	4.2E-04	4.60E-05		
Äspö	RC	FZ	EW-5 (KAS12:DB-KAS06)	1.2E-02	3.0E-04	1.5E-03	4.5	204	4.9E-05	4.1E-04	4.30E-05		
Äspö	RC	FZ	NNW-1 (KAS08:M1-KAS06)	1.7E-03	2.5E-03	8.6E-03	10.8	301	1.2E-04	3.4E-04	2.42E-05		
Äspö	RC	FZ	NNW-1 (KAS12:DB-KAS06)	4.8E-03	6.9E-03	3.1E-03	2.6	292	7.0E-05	3.4E-04	2.42E-05		
Äspö	RC	FZ	NNW-2 (KAS08:M1-KAS06)	5.1E-03	6.8E-03	3.3E-03	11.3	181	7.2E-05	3.5E-04	2.60E-05		
Äspö	RC	FZ	NNW-2 (KAS12:DB-KAS06)	1.1E-02	1.4E-02	1.6E-03	4.6	190	5.0E-05	3.7E-04	3.10E-05		
Äspö	RC	FZ	NE-1 (KAS14-KA1131B)	5.4E-02	7.2E-03	1.1E-03	12.8	92	3.7E-05	1.1E-03	8.70E-04	1.10E-04	7.91E+00
Äspö	RC	SF	Feature A (KXTT1–KXTT3)	2.0E-03	3.3E-04	4.5E-04	8.8	5	2.7E-05	9.5E-05	5.44E-07	5.70E-08	7.89E+00
Äspö	RC/DP	SF	Feature A (KXTT4–KXTT3)	1.7E-03	5.0E-04	4.5E-04	5.4	5	2.7E-05	8.3E-05	3.61E-07	2.10E-07	5.24E-01
Äspö	RC	SF	Feature A (KXTT4–KXTT3)	1.1E-02	2.2E-03	5.7E-05	4.6	5	9.5E-06	8.5E-05	3.83E-07		
Äspö	RC	SF	Feature A (KXTT1–KXTT4)	3.4E-03	4.6E-03	5.0E-06	6.0	5	2.8E-06	1.7E-04	2.87E-06	1.30E-06	4.38E+00
Äspö	RC	SF	Feature A' (KXTT4–KXTT3)	2.4E-02	3.5E-03	3.9E-05	33.4	5	7.9E-06	8.5E-05	3.83E-07		
Äspö	RC	SF	Feature B (KXTT3–KXTT4)	1.6E-04	2.3E-05	5.9E-04	9.1	3	3.1E-05	3.9E-05	3.68E-08		
Äspö	RC	SF	#19,13,21 (KA2563A:S1-KI0023B:P6)	2.8E-02	1.5E-02	7.8E-06	4.3	55	3.5E-06	3.4E-04	2.40E-05	1.70E-05	1.41E+00
Äspö	RC	SF	#20,21 (KA2563A:S4-KI0023B:P6)	2.1E-03	1.7E-03	1.3E-04	6.5	16	1.4E-05	1.1E-04	8.05E-07	1.95E-07	4.13E+00
Äspö	DPw	SF	#21 (KI0025F03:P3-KI0023B:P6)	3.0E-02	1.7E-02	6.3E-06	6.1	27	3.2E-06	1.1E-04	7.65E-07		
Äspö	RC	SF	#20,21 (KI0025F03:P5-KI0023B:P6)	3.3E-03	1.8E-03	5.9E-05	7.1	16	9.6E-06	1.1E-04	7.90E-07	4.10E-07	1.93E+00
Äspö	RC	SF	#22,20,21 (KI0025F03:P6-KI0023B:P6)	2.1E-02	1.2E-02	8.9E-06	6.1	73	3.8E-06	1.1E-04	7.65E-07		
Äspö	DPw	SF	#23,21 (KI0025F03:P7-KI0023B:P6)	3.6E-02	2.0E-02	5.1E-06	4.0	97	2.8E-06	1.1E-04	7.65E-07		
Äspö	RC	SF	#13,21,#22 (KI0025F02:P3-KI0023B:P6)	1.0E-02	5.0E-03	1.9E-05	4.7	33	5.5E-06	2.8E-04	1.30E-05	4.90E-06	2.65E+00
Äspö	DPw	SF	#20,21 (KI0025F02:P5-KI0023B:P6)	8.0E-03	3.9E-03	3.3E-05	3.4	21	7.2E-06	1.1E-04	7.80E-07	2.25E-07	3.47E+00
Äspö	RC	SF	#22,20,21 (KI0025F02:P6-KI0023B:P6)	1.5E-02	8.1E-03	1.4E-05	3.5	65	4.6E-06	1.2E-04	1.20E-06	9.20E-07	1.30E+00
Äspö	DPw	SF	#23,20,21 (KI0025F03:P7-KI0023B:P6)	1.6E-02	9.1E-03	1.2E-05	7.1	97	4.4E-06	1.1E-04	7.65E-07		
Äspö	RC	SF	#20 (KI0025F02:P5-KI0025F03:P5)	5.9E-04	6.9E-05	3.1E-04	17.5	9	2.2E-05	1.1E-04	7.60E-07	3.60E-07	2.11E+00
Äspö	RC	SF	#20 (KA2563A:S4-KI0025F03:P5)	1.4E-03	1.5E-04	1.5E-04	7.8	27	1.5E-05	1.1E-04	7.60E-07	9.60E-08	7.92E+00
Äspö	DPw	SF	#19 (KA2563A:S1-KI0025F03:R3)	7.7E-03			5.8	49		1.2E-04	1.05E-06		
Äspö	DPw	SF	#19 (KA2563A:S2-KI0025F03:R3)	1.6E-02			21.8	49		1.2E-04	1.05E-06		
Äspö	RC	SF	#19 (KI0023B:P2-KI0025F03:R3)	2.0E-03			7.1	27		1.2E-04	1.05E-06		
Äspö	RC	SF	#19 (KI0025F:R2-KI0025F03:R3)	1.7E-03			3.0	69		1.2E-04	1.05E-06		

Site	Type of test [1)]	Test formation [2)]	Flow path (boreholes)	Mass balance aperture δ_m [m]	Kinematic porosity ε_f [–]	Fracture conducitivity K_{fr} [m/s]	Peclet number Pe [–]	Travel distancer [m]	Frictional loss aperture δ_l [m]	Cubic law aperture δ_c [m]	T_S [m²/s]	S_o [–]	T_o/S_o [m²/s]
Äspö	DPw	SF	#19, BG1 (KI0025F02:R2-KI0025F03:R3)	9.8E-03			3.8	22		1.2E-04	1.05E-06		
Äspö	RC	SF	#19 (KI0025F02:R3-KI0025F03:R3)	1.5E-02			6.1	19		1.2E-04	1.05E-06		
Finnsjön	RC	FZ	(G2–G1)	1.7E-03	8.4E-04	2.7E-03	33.3	30	6.5E-05	2.4E-04	8.70E-06	7.90E-06	1.10E+00
Finnsjön	RC	FZ	Zone 2 (BFI01 U–BFI02 U)	9.6E-03	1.0E-02	1.7E-01	48.4	168	5.1E-04	1.3E-03	1.40E-03	9.40E-06	1.49E+02
Finnsjön	RC	FZ	Zone 2 (BFI01 U–BFI02 L)	2.1E-02	7.5E-03	4.1E-02	22.2	168	2.6E-04	1.6E-03	2.40E-03	5.70E-05	4.21E+01
Finnsjön	RC	FZ	Zone 2 (BFI01 U–BFI02 U and L)	1.6E-02		1.3E-01	2.0	168	4.5E-04	1.5E-03	2.20E-03	1.50E-05	1.47E+02
Finnsjön	RC	FZ	Zone 2 (BFI01 M–BFI02 E)	1.1E-01		1.8E-02	7.8	168	1.7E-04	1.6E-03	2.55E-03		
Finnsjön	RC	FZ	Zone 2 (BFI01 L–BFI02 U)	7.6E-02		1.3E-02	27.8	201	1.4E-04	1.4E-03	1.72E-03		
Finnsjön	RC	FZ	Zone 2 (KFI06 U–BFI02 U)	7.7E-03	7.5E-03	4.3E-01	28.5	189	8.0E-04	1.3E-03	1.40E-03	2.40E-06	5.83E+02
Finnsjön	RC	FZ	Zone 2 (KFI06 M–BFI02 U and L)	1.3E-01		3.4E-02	6.7	191	2.3E-04	1.6E-03	2.55E-03		
Finnsjön	RC	FZ	Zone 2 (KFI06 L–BFI02 L)	1.1E-02	1.1E-02	1.8E-01	16.4	189	5.4E-04	1.4E-03	1.60E-03		
Finnsjön	RC	FZ	Zone 2 (KFI06 L–BFI02 U)	4.3E-02		6.4E-02	243.0	189	3.2E-04	1.4E-03	1.72E-03		
Finnsjön	RC	FZ	Zone 2 (KFI06 L–BFI02 U and L)	4.4E-02		1.1E-01	1.8	189	4.2E-04	1.6E-03	2.55E-03		
Finnsjön	RC	FZ	Zone 2 (KFI11 U–BFI02 U)	2.7E-03	1.9E-03	9.5E-01	80.4	155	1.2E-03	1.3E-03	1.40E-03	5.70E-07	2.46E+03
Finnsjön	RC	FZ	Zone 2 (KFI11 U–BFI02 L)	4.0E-03		3.6E-01	14.5	155	7.6E-04	1.1E-03	8.29E-04		
Finnsjön	RC	FZ	Zone 2 (KFI11 U–BFI02 U and L)	6.5E-03		5.2E-01	3.8	155	9.1E-04	1.6E-03	2.55E-03		
Finnsjön	RC	FZ	Zone 2 (KFI11 M–BFI02 U and L)	8.3E-02		4.5E-02	132.4	169	2.7E-04	1.6E-03	2.55E-03		
Finnsjön	RC	FZ	Zone 2 (KFI11 L–BFI02 U)	1.6E-01		1.3E-02	28.5	190	1.4E-04	1.4E-03	1.72E-03		
Studsvik	DPw	FZ	(B1N–B6N)	8.6E-02	2.6E-02	6.6E-05		12	1.0E-05	2.8E-04	1.38E-05		
Studsvik	DPw	FZ	(B5N–B6N)	4.3E-02	3.7E-01	1.7E-04		15	1.6E-05	5.8E-04	1.21E-04		
Stripa	RC	SF	Fracture 2 (H2-Sampling hole 2–6)	1.3E-04		1.1E-06	2.0	5	1.3E-06	8.8E-06	4.25E-10		
Stripa	RC	SF	Fracture 2 (H2-Sampling hole 2–8)	1.5E-04		3.4E-06	0.9	5	2.3E-06	8.8E-06	4.25E-10		
Stripa	RD	SF	Short range (Central borehole-3 L)	2.8E-04				2		1.3E-05	1.49E-09		
Stripa	RD	SF	Short range (Central borehole-9 L)	9.6E-04				2		1.3E-05	1.49E-09		
Stripa	RD	SF	Short range (Central borehole-11 L)	9.6E-04			33.3	2		1.3E-05	1.49E-09		
Stripa	RD	SF	Short range (Central borehole-13 U)	3.9E-04			20.0	2		1.3E-05	1.49E-09		
Stripa	RD	SF	Short range (Central borehole-13 L)	9.5E-04			12.5	2		1.3E-05	1.49E-09		
Stripa	RD	SF	Short range (Central borehole-15 L)	7.2E-04			12.5	2		1.3E-05	1.49E-09		
Stripa	MP	FZ	Zone C (F3–E1)	2.0E-03	1.4E-04	1.1E-04	2.0	53	1.3E-05	6.7E-05	1.90E-07		
Stripa	MP	FZ	Zone C (F3–F1)	1.4E-02	9.7E-04	1.4E-05		23	4.7E-06	6.7E-05	1.90E-07		
Stripa	MP	FZ	Zone C (F3–F2)	1.8E-03	1.3E-04	1.1E-04	0.9	30	1.3E-05	6.7E-05	1.90E-07		

Site	Type of test [1)]	Test formation [2)]	Flow path (boreholes)	Mass balance aperture δ_m [m]	Kinematic porosity ε_f [–]	Fracture conducitivity K_{fr} [m/s]	Peclet number Pe [–]	Travel distancer [m]	Frictional loss aperture δ_l [m]	Cubic law aperture δ_c [m]	T_S [m^2/s]	S_o [–]	T_o/S_o [m^2/s]
Stripa	MP	FZ	Zone C (F3–F4)	3.0E-03	2.1E-04	7.4E-05		43	1.1E-05	6.7E-05	1.90E-07		
Stripa	MP	FZ	Zone C (F3–F5)	4.3E-03	2.9E-04	4.9E-05	2.5	32	8.8E-06	6.7E-05	1.90E-07		
Stripa	DP	FZ	Zone H (C2-overall zone H)	5.5E-04	1.1E-04					4.2E-05	4.60E-08		
Forsmark	DPw	FZ	Zone A2 (KFM02A–KFM02B)	2.6E-02	2.5E-04	6.7E-03	0.9	46	1.0E-04	3.4E-04	2.48E-05	1.66E-06	1.49E+01
Forsmark	RC	FZ	Zone A2 (HFM01–HFM14)	9.3E-02		1.2E-02	8.2	377	1.4E-04	9.8E-04	5.90E-04	9.00E-05	6.60E+00
Forsmark	RC	FZ	Zone A2 (HFM13–HFM14)	8.6E-02		2.5E-02	5.8	297	2.0E-04	8.2E-04	3.50E-04	1.60E-05	2.19E+01
Forsmark	RC	FZ	Zone A2 (HFM15–HFM14)	1.2E-02		1.5E-01	9.4	72	4.9E-04	8.5E-04	3.90E-04	5.10E-05	7.65E+00
Forsmark	RC	FZ	Zone A2 (HFM19–HFM14)	4.7E-02		3.9E-02	7.9	247	2.5E-04	8.5E-04	3.90E-04	1.40E-05	2.79E+01
Forsmark	RC	FZ	Zone A2 (KFM10A–HFM14)	3.9E-02		4.3E-02	5.7	493	2.6E-04	8.1E-04	3.30E-04	8.50E-06	3.88E+01
Laxemar	RC	RS	(SSM000228-HLX33)	2.4E-02			7.6	204		6.4E-04	1.66E-04		
Laxemar	RC	RS	(SSM000223-HLX35)	1.7E-01			1.1	102		8.8E-04	4.26E-04		
Laxemar	DPw	FZ	(KLX15A–HLX27)	4.1E-02	3.6E-03	4.0E-03	3.0	140	8.0E-05	4.4E-04	5.45E-05	4.77E-06	1.14E+01
Laxemar	RC	FZ	(HLX32–HLX28)	6.7E-01	3.2E-03	3.7E-04	2.1	122	2.4E-05	5.6E-04	1.10E-04	1.00E-03	1.10E-01
Laxemar	RC	FZ	(HLX37–HLX28)	5.8E-02	1.8E-04	6.7E-03	10.3	486	1.0E-04	4.9E-04	7.20E-05	5.40E-06	1.33E+01
Summation, number of values													
	RC=60	FZ=40		74	43	59	67	73	59	74	74	27	27
	RD=6	SF=32											
	DP=1	RS=2											
	RC/DP=1												
	DPw=11												
	MP=5												

[1)] Type of test: RC = Radially converging, RD = Radially diverging, DP = Dipole, DPw = Weak dipole, MP = Multiple poles.

[2)] Test formation: FZ = Fracture zone, SF = Single fracture, RS= Rock soil aquifer.